COO-1407-6

THE UNIVERSITY OF MICHIGAN

COLLEGE OF ENGINEERING
Department of Meteorology and Oceanography

Scientific Report No. 1

DEPOSITION OF ATMOSPHERIC PARTICULATE MATTER BY CONVECTIVE STORMS: THE ROLE OF THE CONVECTIVE UPDRAFT AS AN INPUT MECHANISM

Donald F. Gatz

A. Nelson Dingle
Project Director

ORA Project 06867

under contract with:

ATOMIC ENERGY COMMISSION
CONTRACT NO. AT(11-1)-1407
ARGONNE, ILLINOIS

administered through:

OFFICE OF RESEARCH ADMINISTRATION ANN ARBOR

March 1966

This report was also a dissertation submitted in partial fulfillment of the requirements for the degree of Doctor of Philosophy in The University of Michigan, 1966.

ACKNOWLEDGMENTS

I am deeply grateful for the assistance of all who contributed to this study in large and small ways. Special thanks to to Professor A. Nelson Dingle, Chairman of the Doctoral Committee. His competent guidance instilled a spirit of enthusiasm for the problem, and his precise command of language and the structuring of ideas contributed much to this dissertation. The Committee, composed of Professors Edward S. Epstein, G. Hoyt Whipple, and Aksel C. Wiin-Nielsen gave valuable advice and reviewed the manuscript.

Much credit is due those individuals and groups who assisted in the collection of the data and made their own data available to this study. Dr. Edwin Kessler, III, Director of the National Severe Storms Laboratory, and his staff provided storm warnings and other assistance during the field operations and freely contributed data and advice. Mr. Kenneth E. Wilk gave helpful advice concerning the analysis of the radar data, and discussions with Mr. L. D. Sanders and Mr. James C. Fankhauser contributed much to the surface analyses and mass-budget study, respectively. Mr. Monroe A. Hartman and Mr. Arlin D. Nicks of the Agricultural Research Service provided data from the rain-gauge network. Mr. Samuel J. Hall of the University of Oklahoma provided data from the network of automatic rain samplers. Mr. Cecil W. Neville made available the site for the field station.

Professor William S. Benninghoff, Dr. Margaret B. Davis, and Mrs. Darlene E. Southworth provided advice, assistance, and facilities for the pollen analyses. Professor Richard D. Remington provided useful discussions concerning the statistical analysis of the pollen data.

Professor Waldo R. Tobler made available the computer program used to plot the rainfall rate data.

The help of Mr. Dirk Herkhof, Mr. Reinhardt Mittelstaedt, Mr. Cyril Peat, and Mr. Robert Trueman, who assisted with the data collection and reduction is sincerely appreciated.

Support of the research was provided by the U. S. Atomic Energy Commission under Contracts AT(11-1)-739, AT(11-1)-1370, and AT(11-1)-1407, and by Michigan—Memorial Phoenix Project 245.

TABLE OF CONTENTS

TABLE OF CONTENTS (Continued)

TABLE OF CONTENTS (Concluded)

LIST OF TABLES

LIST OF FIGURES

LIST OF FIGURES (Continued)

ABSTRACT

It is the purpose of this study to provide quantitative evidence regarding the mechanism by which airborne particulate matter enters convective storms, and to clarify the relationships among (1) time profiles of contaminant concentrations, (2) time profiles of rainfall rate, (3) input mechanism, and (4) mechanism of particle capture, each with respect to two dissimilar contaminants.

To this end a field observation program was established near Chickasha, Oklahoma, during May, 1964, to obtain rain scavenging data of high resolution from convective storms. The field site was chosen to take advantage of the data collection facilities of the National Severe Storms Laboratory at Norman, Oklahoma, the Agricultural Research Service raingauge network centered at Chickasha, and the University of Oklahoma network of automatic rain samplers, also centered at Chickasha.

At the field site, sequential samples of rain were collected at frequent intervals for later analysis of their content of artificial radioactivity, plant pollens, and gross residue. Observations were also made of raindrop-size spectra, rainfall, wind and concentrations of pollen in air. From these data were prepared time profiles of concentrations of the three contaminants, rainfall rate, and deposition rates of radioactivity and pollens, for the storms of May 9 and 10, 1964.

Data obtained from the Severe Storms Laboratory and the Agricultural Research Service are used to reconstruct the storms in terms of time sequences of radar echo distributions, rainfall rate distributions, and mesoscale pressure and wind distributions.

Conventional synoptic weather data are used to depict large scale flow conditions aloft and at the surface, and to prepare vertical cross-sections of the atmosphere for the time of the storm.

Quantitative investigations of the contaminant input mechanism are carried out. A mass-budget analysis of the severe storm of May 10 is undertaken to test the hypothesis that low-altitude input of radioactivity could account for that deposited by the storm. Results show that the total low-altitude input and total deposition are nearly equal. A simplified analysis, using the concept of proportional mixing ratios of contaminants and water, both in air and rain, is used to extend the results of the mass-budget study. Results indicate that many other convective storms behave in the same manner as the May 10 storm.

Computations to evaluate causes for observed variation of radioactivity concentrations are carried out. Raindrop evaporation, dilution of contaminants by condensation of excess water, and first precipitation of highly contaminated condensed water all contribute to the observed variations.

It is concluded (1) that contaminants deposited in rain from most convective storms are drawn into the storms from low levels of the atmosphere, along with the water vapor, and (2) that temporal variations of contaminant concentration in rain at the ground are generated both within and below the cloud. The interacting mechanisms which cause these variations include evaporation, dilution, first precipitation of condensed water, and, for large particles, impaction.

CHAPTER 1

INTRODUCTION

The use of our atmosphere as a receptacle for the disposal of wastes is without question the object of much current concern. The atmosphere is clearly able to perform this function; nevertheless it is essential that such uses of the atmosphere be properly controlled, so as not to interfere with its aesthetic values or to render it harmful to public health. Principles of prudent control must be grounded in knowledge of the physical processes which affect the budget, i.e., input, storage, and removal of particulate and gaseous matter in the atmosphere. Because contaminants of all kinds are systematically removed from the atmosphere by various natural processes, it is becoming imperative that these processes be clearly understood and quantified.

Atmospheric contaminants may be divided into two classes: gases and particles. Gases are removed from the atmosphere by adsorption or reaction at the surface, by conversion to solid particles, by escape to space, and by sorption upon or reaction with precipitation elements which eventually reach the ground (Junge, 1963). Particles, on the other hand, are removed by sedimentation, by turbulent impaction at or near the earth's surface, and by a group of processes which may be described collectively as "wet." Deposition of a particle by a "wet" process means that the particle comes to earth attached to a precipita-

tion particle, e.g., a raindrop, snowflake, or hailstone. Interaction of these processes is to be expected. For example, a particle may be brought close to the earth's surface attached to a raindrop which evaporates before reaching the ground. From this point the particle may settle gravitationally for some distance and eventually be impacted on a surface obstruction by atmospheric turbulence.

This dissertation is concerned with several aspects of the deposition of particulate matter by rain, one of the group of "wet" processes. It has been estimated (Junge, 1963; Small, 1960) that 80% to 90% of artificial radioactivity comes to the earth's surface via the wet processes. Rain is of particular importance because it can quickly deposit large amounts of radioactivity (List, et al., 1964). In this regard, convective storms are of interest because of their ability to deposit large amounts of rain and radioactivity in local areas.

Observations of atmospheric contaminants in rain have shown that concentrations exhibit large variations, both within and between individual rains. Variations during individual rains and their relationship to rainfall rate variations have been the object of much interest. Most attempts to explain recurrent patterns have been made in terms of the source of the contaminant with respect to the rain system, i.e., the method and location of the input. This aspect is of considerable

significance, but one should not neglect the relevant scavenging* mechanisms. Proposed hypotheses must be consistent with the physics of these mechanisms. Thus far, our knowledge in this area has derived mainly from theoretical investigations and laboratory verification. Field verification has necessarily been limited to well controlled situations (e.g., May, 1958). Descriptions of the most important scavenging mechanisms and the particle-size ranges at which they are effective, based on theoretical considerations, are given in the next section.

1.1 MECHANISMS OF PARTICLE ATTACHMENT

That particles must first become attached to cloud or rain elements is an obvious prerequisite to their eventual deposition. The physical mechanisms of particle attachment may be crucial to the explanation of certain observed phenomena, for example, concentration variations, and should be examined in some detail. Of particular interest are systematic variations of attachment mechanism with particle size.

Goldsmith, et al. (1963), listed five main mechanisms by which particles may become attached to cloud or rain elements. These are:

1. Diffusiophoresis, in which aerosol particles are moved toward a condensing droplet by the inward flux of water vapor;

*The general term scavenging will be used to denote the removal of particles from the atmosphere by precipitation processes, without specification of a particular physical mechanism.

2. Brownian diffusive capture, in which particles in random motion collide with and adhere to cloud particles; this is merely a special case of the process of agglomeration between small particles in the atmosphere;

3. Turbulent diffusive capture, in which eddy diffusion in the vicinity of cloud droplets causes collision between particles and droplets;

4. Nucleation, in which the particles serve as condensation nuclei for the cloud droplets; and

5. Impaction, in which falling droplets collide with and capture airborne particles.

Diffusiophoresis has been shown (Goldsmith, et al., 1963) to make a negligible contribution to total precipitation scavenging in water clouds. It was also shown that cloud droplets of 20μ diameter will not remove significant numbers of particles larger than 0.1μ diameter by Brownian diffusion in less than 10 hours. Below 0.1μ, attachment efficiency increases rapidly as particle size decreases. These conclusions have been reached by other workers also (Greenfield, 1957; Junge, 1963).

Greenfield (1957) considered turbulent diffusive capture of particles by cloud droplets. The theoretical foundations of this process are rather weak and appear to be inconsistent with most treatments of airflow around droplets. Greenfield found that the scavenging effective-

ness of the turbulent process exceeded that of the Brownian process for particles larger than about 0.1μ diameter, but was still a negligible contributor to the total scavenging effect.

Nucleation of cloud droplets is a subject of central interest and importance to cloud physicists, but seldom is it viewed from the standpoint of its function as a scavenging mechanism. Yet, all soluble particles having diameters larger than about 0.1μ (Mordy, 1959) have the capacity to serve as condensation nuclei. The largest of these, i.e., those which contribute most to total particle mass, are nucleated most easily. Insoluble particles may also be utilized as nuclei, depending upon their degree of wettability. Wettability is described in terms of the contact angle, θ, between liquid water and the particle at equilibrium. The value of θ, and hence wettability, varies with the chemical nature of the particle. If a particle is completely wettable, $\theta = 0°$; if non-wettable $\theta = 180°$. In the usual case, $0° < \theta < 180°$, and the particle is described as partially wettable. McDonald (1964) showed theoretically that nucleation is possible for small θ. Under the most favorable conditions, nucleation is possible only for particles having $\theta < 12°$. In more common situations, the permissible value of θ is even more restricted.

Impaction has been a recognized mechanism for the growth of cloud droplets since the pioneering work of Langmuir (1948). This mechanism applies equally well to collection of solid particles by falling drops.

It is important to note that collection of a particle by a falling drop implies not only that the two collided, but that the particle remained attached to the drop after the collision. The former consideration is expressed quantitatively by an impaction efficiency, defined as the fraction of randomly distributed particles in the volume swept out by a falling drop which collide with the drop. The latter consideration is expressed by a retention efficiency, defined as the fraction of the colliding particles that adhere to the drop. The product of these two efficiencies is called the collection efficiency.

According to Langmuir's theory, impaction efficiency is primarily a function of the size of the target particle, and is zero for particles smaller than about 3μ diameter (Vaughn and Perkins, 1961). The impaction efficiency increases rapidly with particle size, reaching about 0.5 at 10μ diameter and 1.0 by 20μ diameter. Such a variation is representative of a broad range of raindrop sizes. Experimental results of Engelmann (1963) indicate that collection efficiencies exceeded 1.0 for all drop sizes for particles larger than 13μ diameter. This is a positive deviation from theory, which predicts a maximum collection efficiency of 1.0. Engelmann explained his results as being caused primarily by the turbulent wake behind a falling drop, which draws in particles from above the falling drop and causes them to impact on its trailing surface.

The particles used in Engelmann's study were all larger than the theoretical lower limit for collection by impaction; thus it was not

possible to check whether particles smaller than the theoretical limit can actually be collected.

The retention efficiency of a particle is again a function of θ. McDonald (1963) showed that retention efficiencies of less than 1.0 result only for $\theta > 90°$.

Effects of electrostatic forces appear to be small (Greenfield, 1957; Junge, 1963).

The ranges of particle size affected by the potentially important scavenging mechanisms are shown graphically in Figure 3.23 and will be discussed later with respect to particles of interest in this study.

Concentration variations are likely to be influenced partly by scavenging mechanisms and partly by the method and place of the input of the contaminants to the rain system. The next section is a review of work in the latter area.

1.2 INPUT OF CONTAMINANTS: PERTINENT LITERATURE

The subject of trace constitutents of rain water has been of interest for over a century. Most of this interest has been derived from analyses of rain water for agriculturally valuable minerals and nutrients. Quite naturally, much attention has been devoted to the identification of the original source of the material. For example, nitrates in precipitation have been attributed at one time or another to lightning, soil emanations, and sea surface phenomena (Viemeister, 1960). Other chemical constitutents are derived from cosmic ray inter-

actions with air molecules, forests and forest fires, meteoric dust, and volcanic gases (Rigby and Sinha, 1961).

While the ultimate source of rain water constituents has been of interest for many years, it has been only recently that such materials have been used for tracers to determine where and how the materials enter individual rain systems. The remainder of this chapter is devoted to a review of current literature on the subject of the mode of entry of artifical radionuclides and other particles into convective rain systems.

1.2.1 High Level Source—Evidence and Opinions

The idea that radioactive contaminants may enter convective clouds at high levels is a logical one, considering the vertical distribution of radioactivity. It is well established that the stratosphere, being essentially free of precipitation processes, serves as a reservoir for radioactive particles too small to have a significant settling velocity. With such a source aloft, one expects the mean vertical distribution of radioactivity concentration in air to increase upward from the earth's surface. Such has been observed to be the case. (Holland, 1959; Junge, 1963). With such a vertical distribution of radioactivity, and the knowledge that approximately 80% of fallout deposition on the earth occurs in precipitation (Junge, 1958; Small, 1960), it was logical to speculate upon the effect of storms which penetrate to the high troposphere and especially those which penetrate into the stratosphere.

Kruger and Hosler (1963) suggested that debris would enter convective clouds at high levels by entrainment of drier air through mixing processes with the environment. Once inside the cloud the particles would serve as condensation nuclei. These authors further suggested that concentrations of strontium-90 in precipitation would be governed by the height at which the precipitation was formed, that forming at higher levels having the greater activity because of the higher concentrations of radioactivity in the environment at such levels. Thus it was expected that concentrations of strontium-90 in convective rains would vary with the life cycle of the convective system. The first rain to fall would presumably contain a low concentration of radionuclides, having used as condensation nuclei particles from the lower atmosphere, where radionuclide concentrations are relatively low. Rain falling from the mature convective storm was expected to contain higher concentrations, having been formed at greater altitudes. Kruger and Hosler (1963) presented data on seven individual convective showers. In an attempt to relate strontium-90 concentrations in rain to mean locations of high concentrations of airborne strontium-90, the maximum radar echo top observed over the rain collector during the shower was paired with the maximum strontium-90 concentration. These data were plotted on a cross-section (Giles, 1961) showing the mean distribution of strontium-90 radioactivity with respect to tropopauses and jet streams. The results are shown in Figure 1.1. Based on this figure and the temporal variations

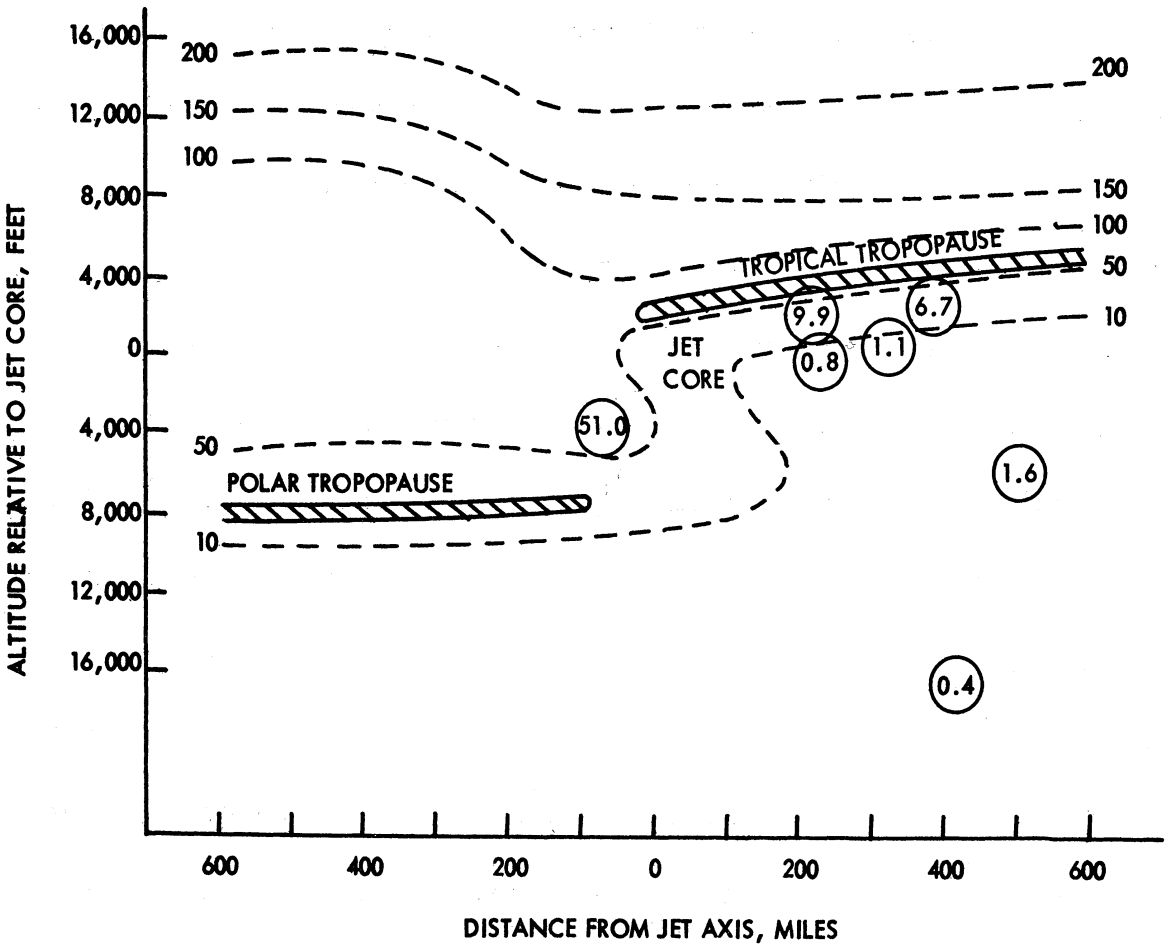

Figure 1.1. Maximum concentrations of strontium-90 during seven convective showers sampled in Pennsylvania during March-September, 1961. The concentrations are plotted at the position of the maximum (3 cm) radar echo top over the collector during the shower. The figure is from Kruger and Hosler (1962) who used a mean cross-section of strontium-90 radioactivity from Giles (1961).

of strontium-90 concentrations in rain, Kruger and Hosler concluded, "...we have been able to relate the peak strontium-90 concentration to the highest development of the precipitating cloud and to its position relative to the tropopause and the jet axis."

Results of sampling 1962 and 1963 convective storms in Pennsylvania were reported by Kruger, et al. (1963) and Kruger, et al. (1964), in which a vertically-pointing radar was used to observe echo tops over the collector. Based on the observations summarized in Table 1.1, Kruger, et al. (1964) concluded, "The peak concentration has been shown to occur during the period of peak cloud development as revealed by radar echo tops."

During May, 1963, this group sampled two severe storms in central Oklahoma, to investigate further the relationship between radionuclide concentrations in rain and the extent of upward development of the convective cloud. The results have been reported by Booker, et al. (1964). Maximum radar echo tops of 55,000 and 60,000 ft (MSL), respectively, were reported for the storms of May 4 and 26, 1963. Although both of these storms penetrated the tropopause, observed concentrations of strontium-90 in collected rain were in general slightly lower than those observed in Pennsylvania during the same period. Atmospheric cross-sections and isentropic trajectory analyses by E. F. Danielsen indicate that for the cases investigated "only tropospheric air was present in the vicinity of Oklahoma City up to quite high altitudes." Booker,

TABLE 1.1

DATA ON STRONTIUM-90 CONCENTRATIONS IN CONVECTIVE RAINS IN PENNSYLVANIA

[From Kruger, et al. (1963) and Kruger, et al. (1964)]

	1962			1963			
	6/24	8/20	9/10	4/19-20	4/22-23	5/10	5/21
Maximum Strontium-90 Concentration (dpm/liter)	45.5	38.8[1]	12.0	155	420	249[1]	126
Time of Maximum (EST)	1300-1302	1737-1744	1241-1246	2035-2120	2300-2317	1927-1933	2034-2045
Maximum Radar Echo Tops (ft, MSL)	41,000	46,000[3]	30,000	26,000	36,000	40,000	17,000
Time of Maximum (EST)	1255	1732	1238	2040	2305	1940	2040
Jet Stream Position (miles)	200 NW	160 N	250 NW	180 S	180 N	200 N	80 NW
Tropopause Height (ft, MSL)	43,000	47,000	49,300	39,600	40,000	45,000	39,500
Rainfall Rate Maximum[2] (mm/hr)	220	75	40	14	6.6	29	14
Time of Maximum (EST)	1302-1303	1759-1759.5[4]	1251-1253	0035-0045[4]	2322-2326	1920-1922	2045-2048

[1]Excluding first sample collected during period.
[2]Averaged over collection of each sample.
[3]Radar at collection site suffered power failure. These values estimated from notes taken at the site and teletype data.
[4]Maximum occurred in different shower from strontium-90 concentration peak.

et al. conclude that "...the precipitation reaching the ground from the severe storms (was) of about the same altitude-origin as the convective showers and may be indicative of the role of entrainment as a function of convective severity."

The occurrence of high concentrations of iodine-131 in milk a few days after the occurrence of rain from severe thunderstorms over several midwest milksheds led List, et al., (1964), following Machta (1963), to infer "...a cause-and-effect relationship between the penetration of thunderstorms into high concentrations of nuclear debris in the lower stratosphere and the subsequent amount of iodine-131 in milk." Aircraft sampling of the atmosphere over the United States on approximately north-south tracks at about longitude 105W showed the presence of high concentrations of fresh fission products between 50,000 and 60,000 ft on May 8, 10, 17, 18, 22, 24 and 31, 1962. High concentrations were absent on all samples below 40,000 ft. The first 10 atmospheric detonations of nuclear weapons in the U.S. 1962 Christmas Island tests, all with yields in the intermediate (20 to 1000 kilotons) to low megaton range, were made between April 25 and May 14 (List, et al., 1964). The Christmas Island origin of the debris sampled over the U.S. was confirmed by radiochemical dating techniques. Table 1.2 summarizes the iodine-131 and severe storm data used as the basis for the conclusion stated earlier. It is to be noted that no physical mechanism for the inclusion of the debris in cloud or precipitation elements was offered;

TABLE 1.2

SUMMARY OF DATA FROM LIST, ET AL. (1964) ON IODINE-131 CONCENTRATIONS IN MILK FROM MILKSHEDS AFFECTED BY SEVERE STORMS

Date (1962)	Location	Iodine-131 Concentration in Milk (pc/liter)	Data on Associated Severe Storms Over Milkshed	
			Date (1962)	Observed Radar Echo Tops
May 13	Wichita, Kansas	670	May 8-9	10 echo tops of 50,000 ft or higher were observed between 1900/8th and 0200/9th (CST).
May 29	Wichita, Kansas	340	May 24-25	"Numerous" thunderstorms extending to 50,000 ft or higher during night.
May 18	Kansas City, Missouri	600	May 8-9 (?)	Highest observed top over milkshed was at 47,000 ft.
June 1	Kansas City, Missouri	780	May 25-26	"Several" echo tops above 60,000 ft.
May 17	Des Moines, Iowa	300		
May 18	Minneapolis, Minnesota	290		All associated with echo tops of 50,000 ft or greater and heavy rain over the milkshed.
May 29	Oklahoma City, Oklahoma	460		
June 1	Omaha, Nebraska	340		

nevertheless the implication that the debris entered at high levels is clear, no fresh debris having been sampled below 40,000 ft. Although no large increases were observed in the activity of surface air the "apparent age" of low level debris decreased markedly in several areas of the midwest, indicating the presence of fresh debris (U.S. Weather Bureau and Public Health Service, 1963).

The stratospheric tapping proposal of Machta (1963), extended by List, et al., has been criticized by Martell (1965) who claims that "neither adequate observational evidence nor a sound theoretical basis" has been provided in its support. Martell further suggested that escaping debris from the underground tests in Nevada on May 7, 12, and 19, 1962, cannot be discounted as a source for the iodine-131 fallout in the midwest during May and early June, 1962. He states that the absence of mixed fission products in ground level air may be explained by "selective release of iodine-131 and a few other gaseous products," analogous to the high concentrations of iodine-131 released during the accident at Windscale, England on October 10, 1957 (Chamberlain, 1959). Gaseous iodine-131 would not be detected from filter sampling.

Dingle (1965) has suggested a possible mechanism whereby stratospheric debris may be drawn into very severe convective storms in such a way as to be efficiently collected and deposited by rain. The mechanism is based on photographs taken by a high-flying U-2 aircraft (Fitzgerald and Valovcin, 1964) of a hurricane-like vortex at the top of a tornado-

producing storm cloud. As in the case of a hurricane, down-currents in the vortex could transport debris particles from the lower stratosphere to the lower parts of convective systems. At such levels particles would have a better chance to become attached to cloud or rain elements than if they entered at high levels, owing to a longer lifetime in the cloud and more intimate association with large amounts of water vapor.

In this same vein, it has been suggested (Penn and Martell, 1963; Dingle, 1965; Malkowski, 1965) that ordinary thunderstorm downdrafts, such as those discussed by Squires (1958) could transport high-level debris to the surface, where it could then be drawn into following storms. Such an occurrence seems possible during the rain of May 19, 1962, sampled at Ypsilanti, Michigan (Dingle and Gatz, 1963). Figure 1.2 shows the observed temporal variations of radionuclide concentrations and rainfall rate on this day. Rain was sampled from two distinct lines of echoes; the first with maximum echo tops of 36,000 ft crossed the sampling station at about 0745 EST. The second line passed at about 1000 EST and had maximum echo tops of 32,000 ft. If one keeps in mind that high concentrations of fresh fallout from Christmas Island were observed over the U.S. at about longitude 105W several times during May 1962 (List, et al., 1964), Figure 1.2 shows an interesting pattern of concentration change in the case of barium-lanthanum-140. Barium-140, having a 12.8-day half-life, is indicative of fresh fallout. Between

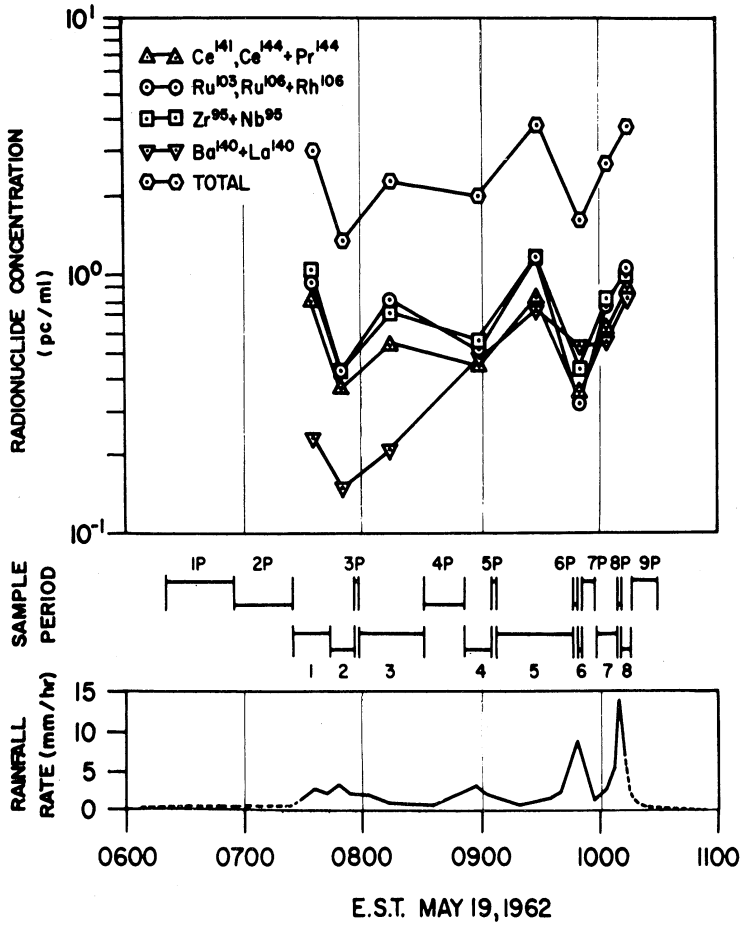

Figure 1.2. Temporal variations of rainfall rate and radionuclide concentrations in the rain of May 19, 1962.

May 18-25, concentrations of barium-140 in ground level air at Ann Arbor showed no significant changes from the low environmental levels still present from the Russian tests of autumn, 1961. Evidently the source of the fresh fallout was aloft. It is shown in Figure 1.2 that concentrations of barium-lanthanum-140 increased by a factor of 2 to 3 after the passage of the first line of convective echoes, which incidentally, had higher echo tops than any observed in the later line. Such a concentration increase was not observed in the case of the more abundant, longer-lived radionuclides shown. These events are consistent with the suggestion that high-level debris may be transported downward by downdrafts in convective rain systems and subsequently be drawn into following storms. Because of the limited areas affected by such downdrafts, it is not surprising that the fresh debris was not detected at ground level.

Huff and Stout (1964), using data from a network of automatic samplers capable of collecting 12 sequential samples, found four main types of temporal variation of beta concentration. Individual sample concentrations were normalized with respect to the mean concentration of all samples collected from each storm. Figure 1.3 shows the four major distribution types, averaged over all cases in each category and plotted as a function of cumulative percent of total storm rainfall. Also shown are the mean temporal variations of rainfall rate for each type, similarly normalized.

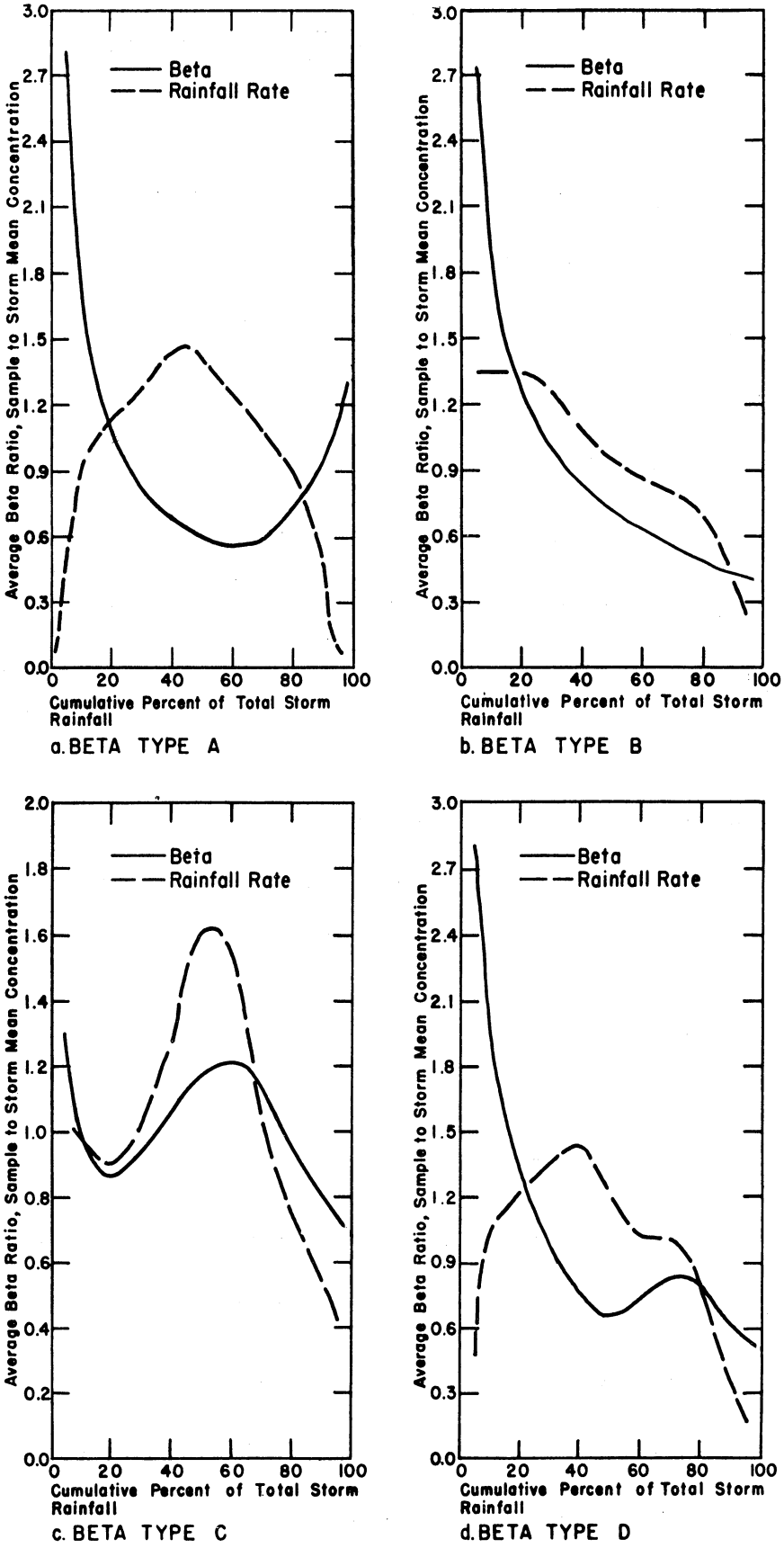

Figure 1.3. Average relations for the four major distribution patterns of beta radioactivity concentration; data from 1963. (From Huff and Stout, 1964.)

It was noted that concentration minima in most individual cases of Type A as well as the average relations (Figure 1.3) were associated with a major peak in the rainfall rate distribution. On the assumption that rain which fell during the rate peak was likely to have originated in the region of maximum cloud development, it followed that higher concentrations should be found if the cloud tower penetrated the stratosphere; Huff and Stout therefore concluded that, "Type A distributions appear to be representative of distributions in mature convective systems in which any high-level source of radioactivity has been diluted somewhat by earlier penetrations of convective storms." Type C distributions, having concentration maxima associated with rainfall rate maxima, were interpreted as arising from initial penetrations of high concentrations of radioactivity, such as the stratosphere or a stratospheric intrusion into the troposphere (Danielsen, 1964).

Hall (1965) and Hall and Nelson (1964) using data collected in central Oklahoma by a network of automatic rain samplers patterned after those of Huff (1963), found indications that beta radioactivity concentration minima occur with rainfall rate maxima for cells which do not penetrate the stratosphere. Coincidence of concentration maxima and rainfall rate maxima tended to occur when the convective cells were dissipating. This is directly opposed to the interpretation of Huff and Stout for their Type C distributions, which have the same relationship between concentration and rate maxima.

1.2.2 Low Level Source—Evidence and Opinions

Small (1960), interpreting data on concentrations of fallout radionuclides in air and precipitation, recognized that "...precipitation processes involve an upward movement of air from near the surface..." He considered low-level air to be the major source of radionuclides in precipitation, compared with amounts mixed into the cloud at higher levels. High level entrainment was expected to be a greater factor in convective clouds than layer clouds, but still not the dominant factor.

Huff (1964) noted a tendency toward high concentrations of both beta radioactivity and insoluble matter in first samples collected from individual convective rains. He interpreted this as evidence that, "...rainwater in this part of the storm may be contaminated by surface or low-level particulates brought in by strong convergence into the advancing storm."

Concentrations of radionuclides and plant pollens in rain from convective storms were presented by Gatz and Dingle (1965). Several cases in which concentrations of both contaminants decreased rapidly during rainfall rate maxima were interpreted as evidence that both contaminants were removed from the same air. Because pollens have their source at or near the earth's surface they serve as tracers for low-level air. Therefore it was concluded that the source of both radioactivity and pollens was the convective updraft of warm moist air.

Huff (1965) provided additional evidence in the form of temporal variations of the ratio of cerium-144 to strontium-90 during individual

convective storms. His results, shown in Figure 1.4, indicate a systematic change in the ratio as a storm progresses. This is indicative of a variation in apparent age of the fallout, proceeding from "younger" to "older" debris as the storm progresses. Huff was unable to find a consistent relation between this phenomenon and rainfall rate or duration, or type of storm. While a satisfactory explanation for this phenomenon is lacking, Huff offers the following as a possibility. Strontium-90, having a greater tendency to leach into the soil than cerium-144, would be relatively deficient in surface soil compared to cerium-144. If surface dirt were blown into the air and subsequently drawn into the leading edge of storms, the rain in this forward zone would show a relatively high cerium-144/strontium-90 ratio, as was observed.

Observations by Shleien, Oakes, et al. (1965) are pertinent here. They identified radium-226, a solid phase natural radionuclide found in the earth's crust, in rain samples. Limited data showed a tendency for concentrations of radium-226 in rain to increase with surface wind speed. If it could be shown conclusively that contamination of the sampler (3 ft above ground level) were not a factor, and a reliable value were available for the concentration of radium-226 in surface dirt, one could use observations such as these to compute how much surface dirt was redeposited in rain.

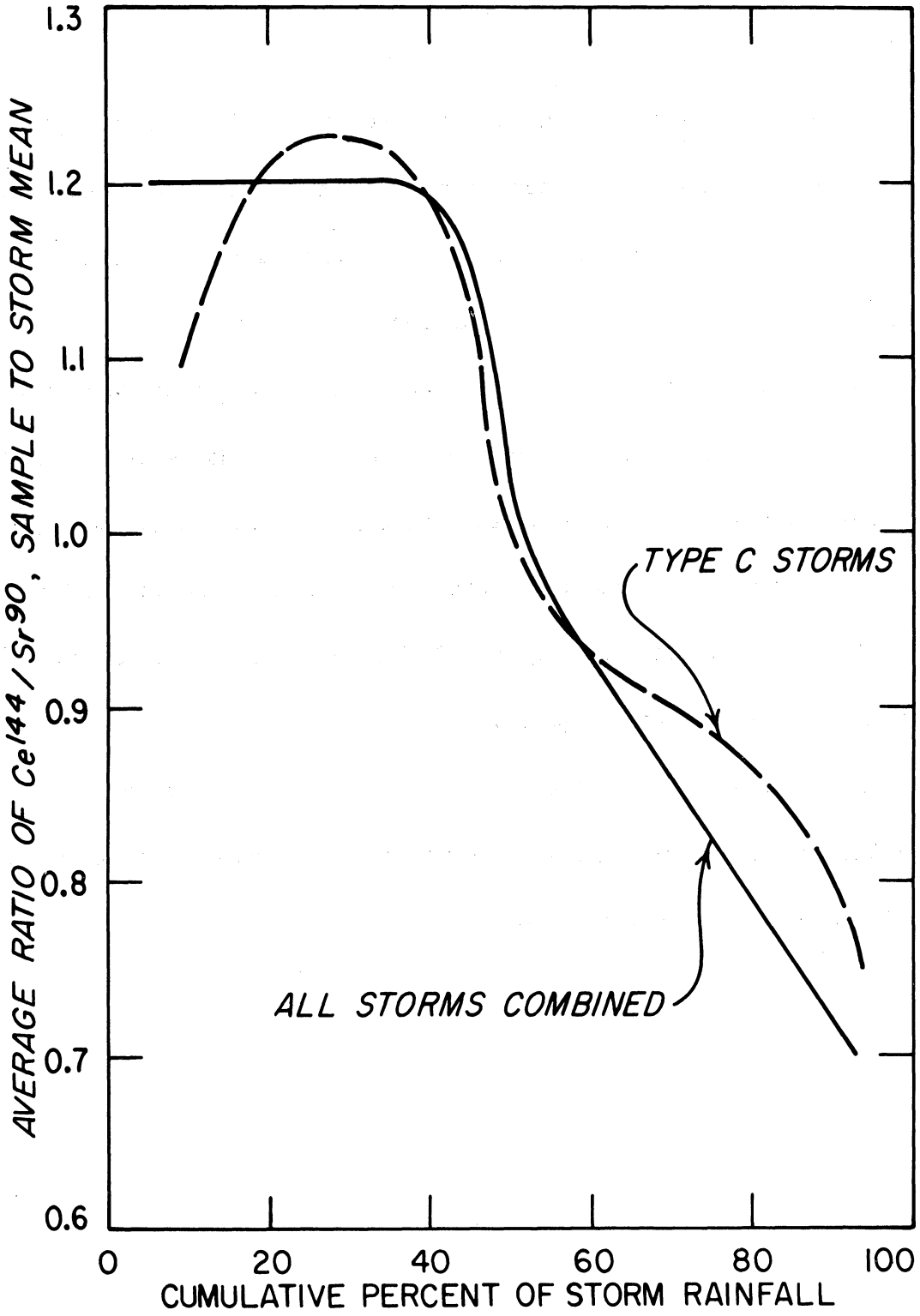

Figure 1.4. Distribution of the ratio cerium-144/strontium-90 in 1963 storms. (From Huff, 1965.)

1.2.3 Summary

It is rather obvious that a divergence of opinion exists regarding the place and mechanism whereby eventually-deposited contaminants enter convective storms. This is perhaps to be expected if one realizes that this problem and that of the circulation and cloud physics of that complex and little-understood phenomenon—the convective storm—are inseparable. Furthermore, as evidenced by the recent dates of most references given in this chapter, research into the problem has barely begun. So perhaps it is not surprising that we find ourselves in the situation of that proverbial group of blind men, each describing a different part of the same elephant.

It is clear that additional research is required for the ultimate solution of the problem and it is hoped that the research reported here will contribute to that solution.

CHAPTER 2

A STATEMENT OF THE PROBLEM

2.1 PURPOSE OF THE RESEARCH

The literature review given in Chapter 1 indicates a need for additional evidence relevant to the determination of the important process(es) of input of contaminants to convective storms. Incomplete understanding of the interrelationships of contaminant concentrations, rainfall rate, and mechanisms of contaminant input and capture is also evident. It is the purpose of this study to provide quantitative evidence concerning the input mechanism and to clarify the relationships between:

1. time profiles of contaminant concentrations,
2. time profiles of rainfall rate,
3. input mechanism, and
4. mechanism of particle capture

for two dissimilar contaminants.

2.2 SIGNIFICANCE OF THE PROBLEM

With regard to the scavenging function of rain as a natural agent for cleansing and restoring the atmosphere, this investigation is of basic practical importance. Knowledge of input and mechanism are essential if one is to estimate quantitatively the effect of rainfall events on the budget of atmospheric particulate matter. A very practical example of this which may be faced in the relatively near future is the

public health hazard associated with the use of nuclear explosives for canal or harbor excavation.

In addition to pollution applications, the identification and quantification of sources of tracer input offers potential aid to studies of mass budgets and circulations of convective storms.

2.3 THE APPROACH TO THE PROBLEM

The approach to the problem was experimental, rather than theoretical. The experiment was designed to collect very detailed data on rain scavenging at a single station and so timed and located as to obtain maximum benefit from complementary meteorological and rain scavenging data. Airborne plant pollens, which are emitted near the ground, were used as a natural tracer for air from the lowest layer of the atmosphere. In addition, the uniform large sizes and simple shapes of pollens offer a convenient basis against which to compare the scavenging characteristics of radioactive particles. The data were interpreted

1. by comparing observed time profiles of concentration against those computed from observed raindrop-size distributions and certain assumptions concerning input and attachment mechanisms of the respective contaminants, and

2. by application of mass-budget techniques to compare input of radioactivity and water in low-level air with their observed deposition (output) over an area of 582 square nautical miles.

2.4 DATA COLLECTION

The primary aim of the data-collection phase of this study was to obtain a more comprehensive and more detailed set of data pertinent to rain scavenging of the atmosphere at a single station than had been gathered previously. Of central importance is the improved time resolution of the sequential rain samples. During heavy rain, samples were taken at a rate of over 1 per min. The shortest sample period was 18.6 sec. Complete interpretation of such detailed data would require appropriate meteorological data of similar resolution; techniques for obtaining such data are not currently available. Maximum use was made, however, of available synoptic-scale and meso-scale data in an attempt to reconstruct the pertinent meteorological events in as much detail as possible.

The samples were collected in Oklahoma during May, 1964, as part of Project Springfield-1964, a comprehensive study of the transport and deposition of artificial radionuclides, sponsored by the U.S. Atomic Energy Commission and the Defense Atomic Support Agency. The field observational program is described in Appendix A. Each sample was analyzed for its content of artificial radioactivity and plant pollens. The rain water analysis procedures are described in Appendix B. Procedures used in the analysis of other data are given in Appendix C. Estimates of errors of measured and derived parameters are also given in the appropriate appendix.

CHAPTER 3

DATA ANALYSIS

The data reported in this chapter were collected from two severe squall line rain systems which occurred within a 24-hour period on May 9 and 10, 1964. The data of central interest, namely the temporal variations of the rain water contaminants, are presented first on each date. The supporting meteorological documentation is given next, starting with gross features and proceeding to the finest detail possible.

3.1 THE RAIN OF MAY 9, 1964

The basic character of the rain event, as it occurred at our station, is reflected in the time profile of rainfall rate R_g, computed from tipping-bucket rain gauge data, and shown in Figure 3.3. Note that two heavy showers occurred approximately 15 min apart. Total rainfall was 0.86 in. (21.8 mm).

3.1.1 Rain Water Analyses

Several individual radionuclides and parent-daughter groups were determined by gamma spectrometry. (See Appendix B.) Examples of their temporal variation and that of their sum and total beta radioactivity are shown in Figure 3.1. A high degree of parallel variation is evident. A check of all individual radionuclide concentration data from May 9 and 10, 1964 yielded the same result. Owing to a greater counting error

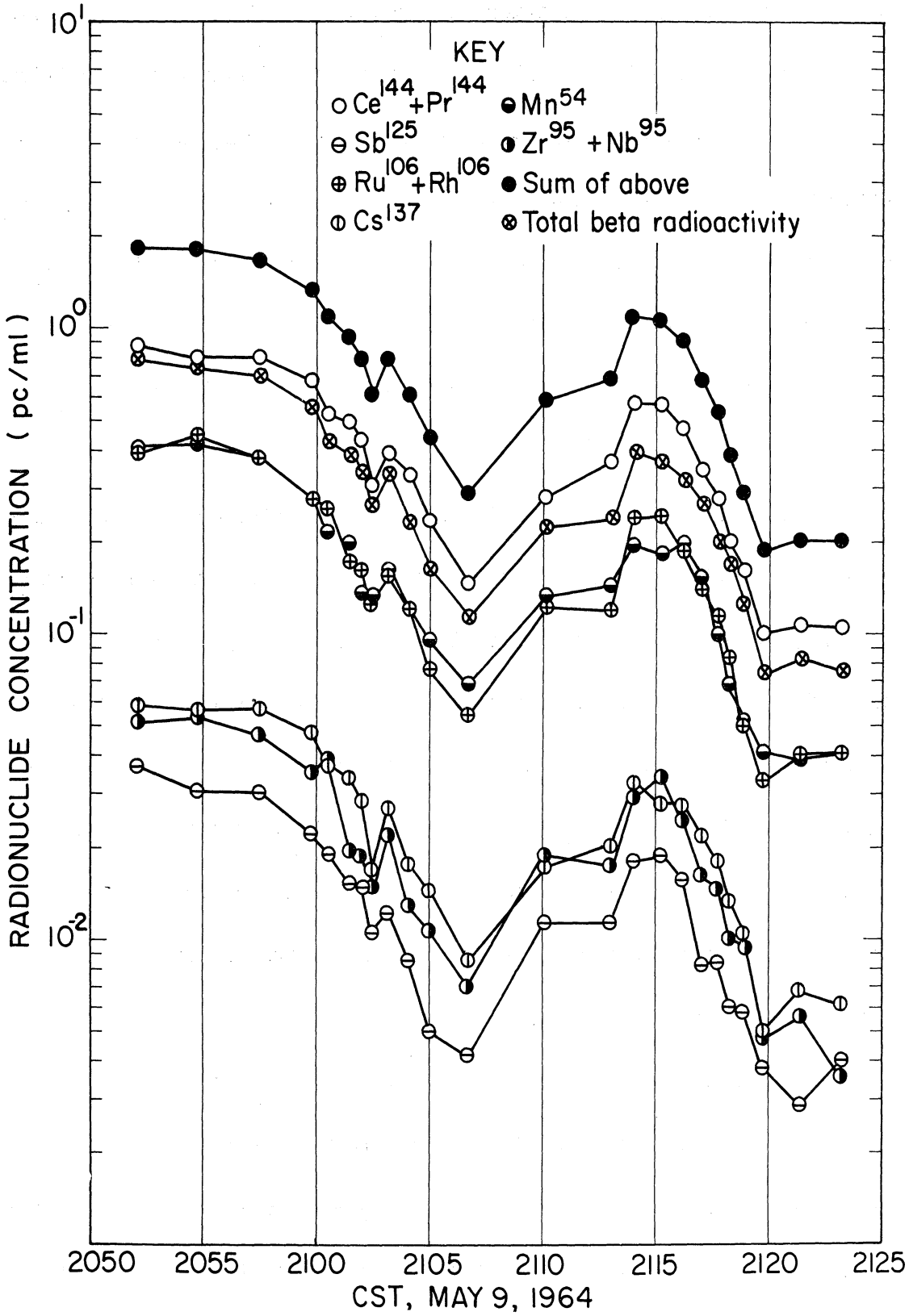

Figure 3.1. Portion of radionuclide concentration data from May 9, showing parallel variations between individual nuclides, total gamma radioactivity, and total beta radioactivity.

the degree of parallel variation is somewhat less in those radionuclides of lowest concentration. Still, the variations of any of the individual curves are closely approximated by those of their sum, and also by the curve for total beta radioactivity. Because comparative radionuclide data, such as concentrations on airborne dust and in precipitation, are usually reported as total beta activity, it is reasonable to plot only total beta concentration curves for comparison with other data (e.g., Figures 3.3 and 3.13).

Figure 3.2 is an example of the temporal variation of concentrations of several pollen types. A high degree of parallel variation is again evident, although the parallelism is perhaps not as great as in the case of the radionuclides. Most cases of non-parallelism between the pollen types occur at low concentrations, where concentrations are based on a very small number ($\leq$ 10) of counted grains. Concentrations of individual pollen types and their total are tabulated in Appendix D. Comparison with the other contaminants (e.g., Figures 3.3 and 3.13) are based upon total pollens.

Concentrations of radioactivity, pollen, and total residue are shown as a function of time and compared with the rainfall rate in Figure 3.3. Vertical bars on the pollen concentrations indicate three standard error limits. Two standard error limits of radioactivity concentrations are approximately ±10% (not indicated in the figure). Computation of these errors is discussed in Appendix B. The situation in

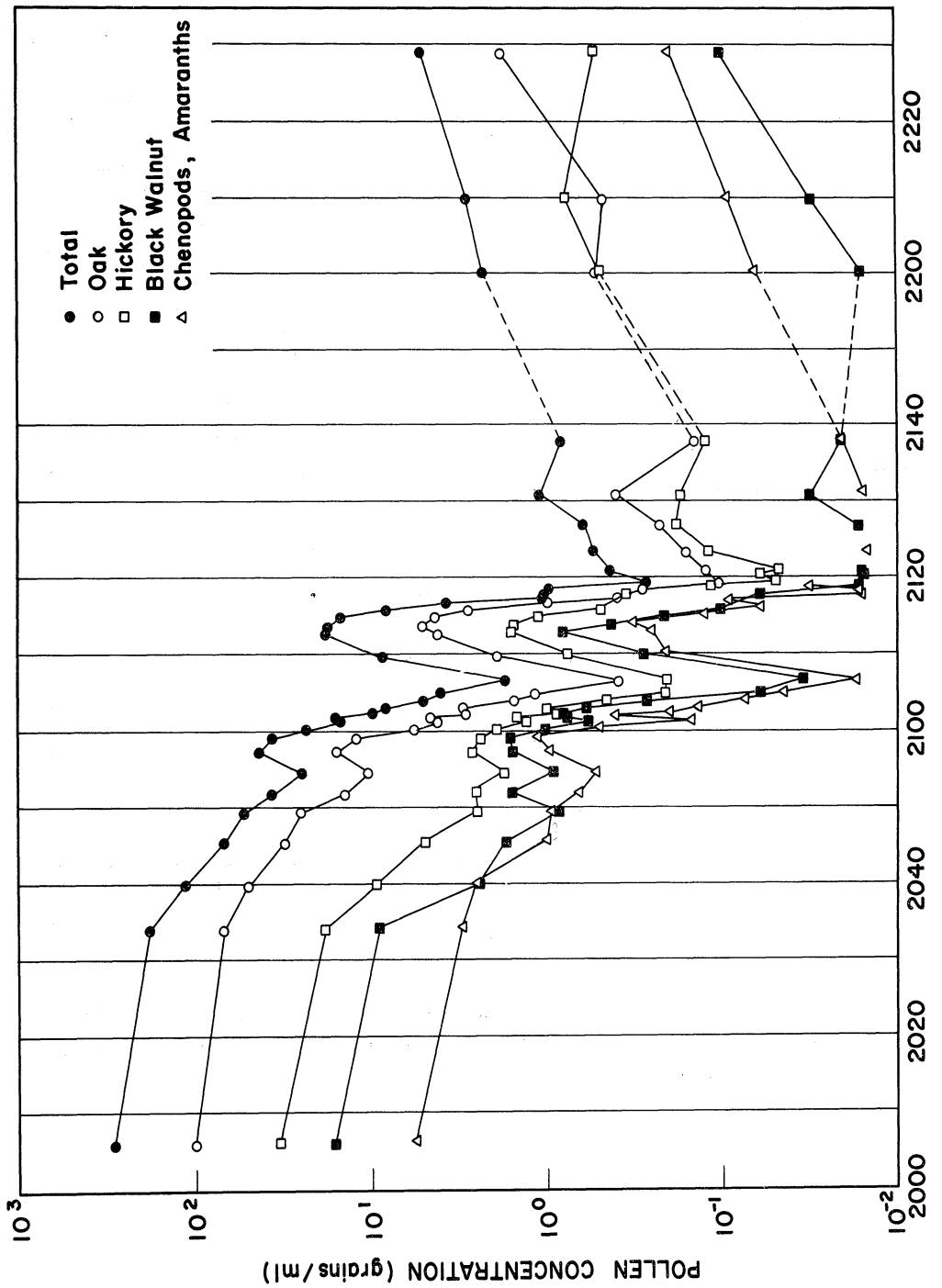

Figure 3.2. Portion of pollen concentration data from May 9, showing parallel variations between individual pollen types.

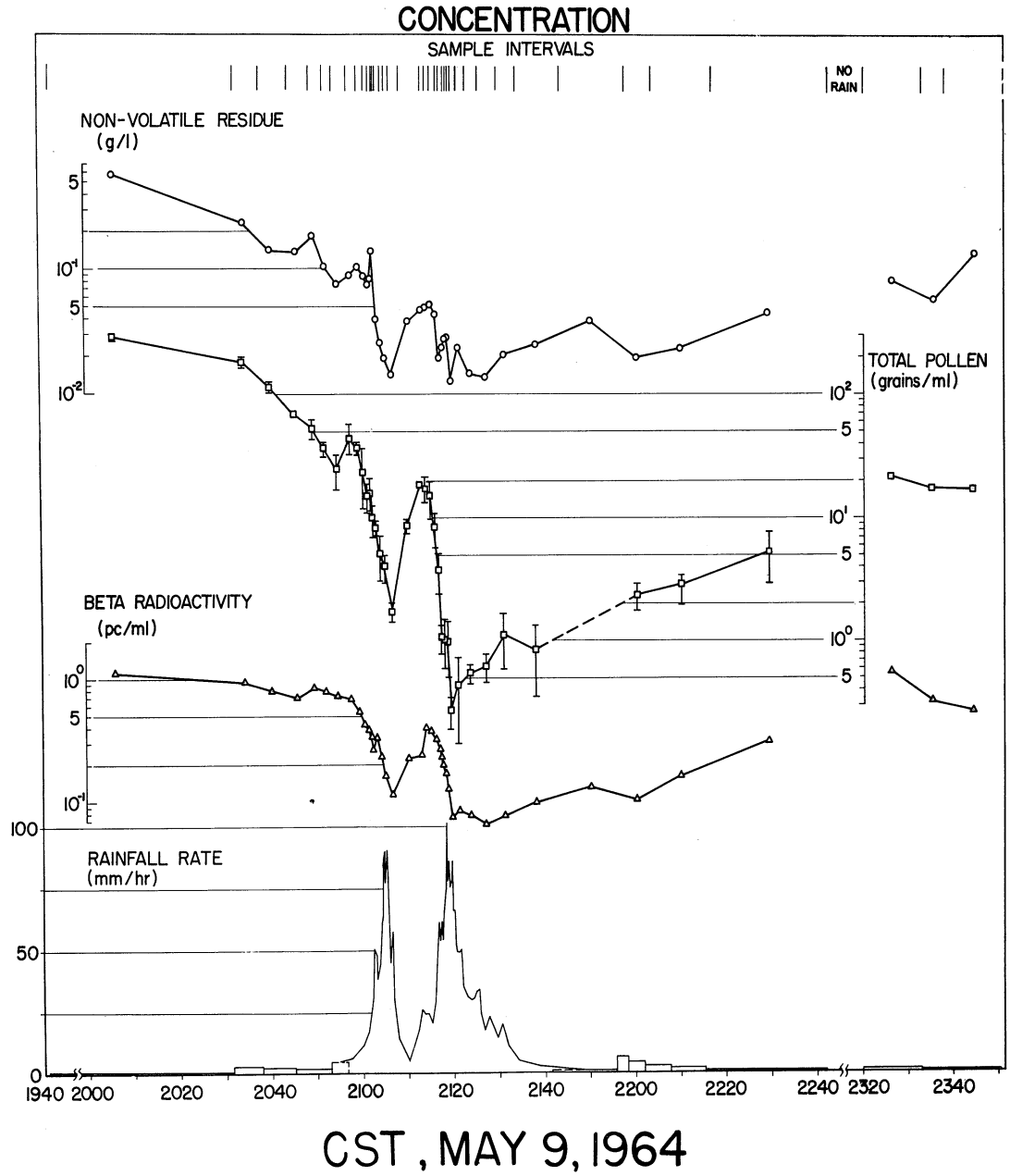

Figure 3.3. Temporal variations of concentrations of three classes of rain water contaminants, May 9, 1964. Three standard error limits are shown for pollen concentrations.

the case of the total residue concentration is less satisfactory than with radioactivity and pollen. As explained in Appendix B, the addition of unknown and varying amounts of zirconium salts to each sample introduced an indeterminate error into the residue concentrations. Maximum possible residue concentrations arising from this error are larger than any of the observed concentrations. Nevertheless, general trends appear to be significant.

It is of interest to compare the ranges of concentration values obtained for the three classes of contaminants. One may see from Figure 3.3 that the following approximate ratios of maximum to minimum values were obtained:

pollen:	100
residue:	50
radioactivity:	20

As will be shown in detail later, the same order prevails in the mean particle sizes of these three constituents.

Another feature of importance is the position of relative maxima and minima with respect to the rainfall rate curve. The three contaminant concentrations decreased slowly (but not at the same rate) during the period of light rain before the first shower. As the shower began, with a rapid increase in rainfall rate, the slopes of the concentrations increased. All three concentrations reached a relative minimum in the sample which was collected just after the first rainfall rate peak. The next three samples, collected as rainfall rate increased at the be-

ginning of the second shower, showed increasing concentrations. Peaks were reached about 4 min before the rainfall rate peak, which occurred during a period of rapid decreases of concentration for all three contaminants. Again a relative minimum was reached in the same sample for all three curves. This sample was collected after the primary rate maximum of 101 mm/hr, but during a period of relatively high rate. The rainfall rate R_s, computed from sample volume and collection time, was 73.6 mm/hr. Between this sample and the end of the rain, all concentrations increased gradually, again at slightly different rates. The dashed portion of the pollen curve indicates the absence of an intermediate sample, which was sacrificed to test the pollen analysis techniques and verify that the pollen grains were not charred during evaporation of the rain water.

In addition to the concentration of contaminants in rain, it is instructive to examine another parameter related to precipitation scavenging, namely the deposition rate. Deposition rate has units of mass per unit area per unit time and is equivalent to the product of concentration in rain and the rainfall rate. Deposition rates of radioactivity and pollens were computed from R_s and are shown in Figure 3.4; R_g is plotted for purposes of comparison. Three standard error limits are indicated by vertical bars in Figure 3.4 for the deposition rate of total pollen. Two standard error limits of approximately ±14% apply to the deposition rate of radioactivity.

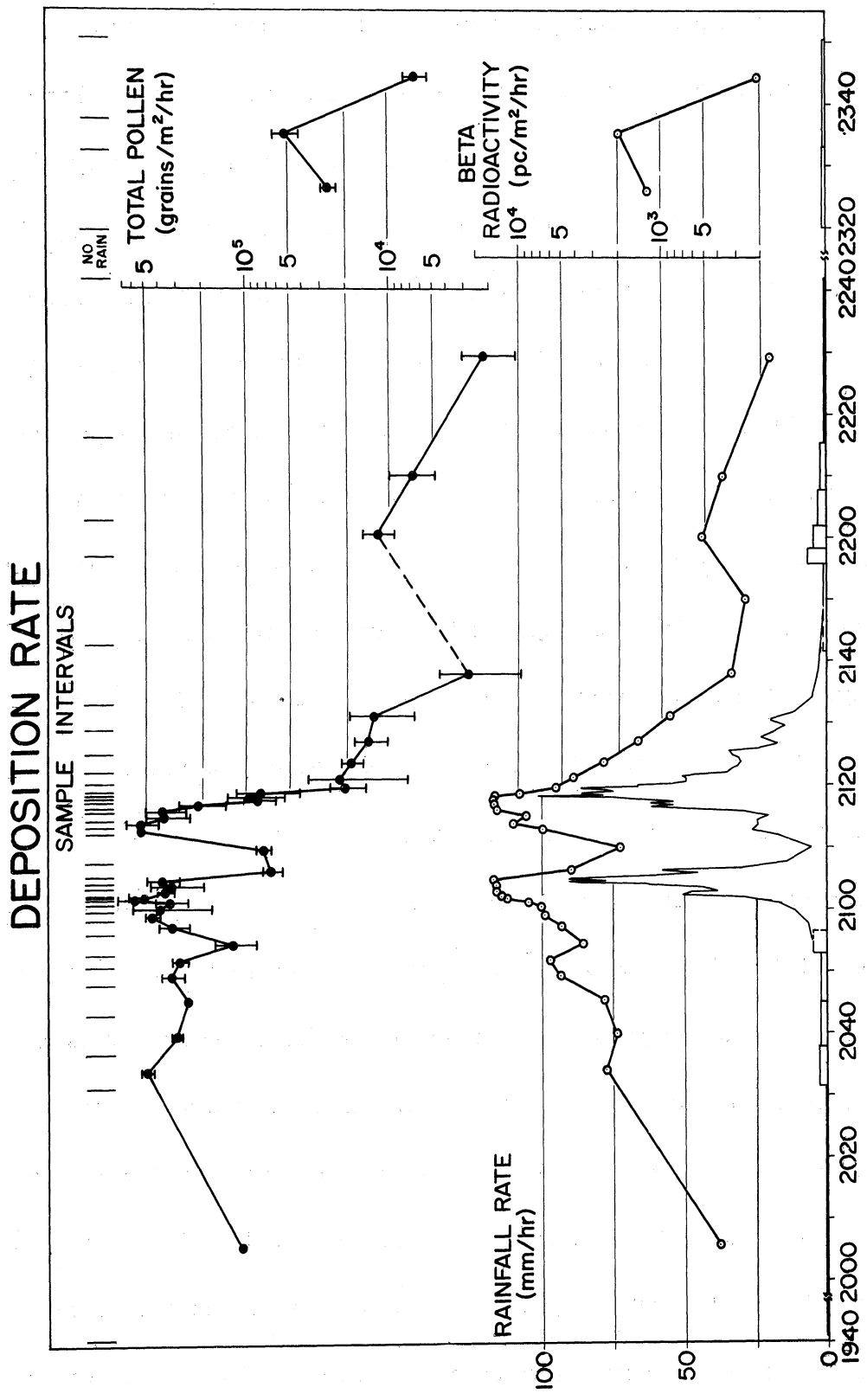

Figure 3.4. Temporal variations of deposition rates of total beta radioactivity and total pollens, May 9, 1964. Three standard error limits are shown for pollen deposition rates.

As expected, rainfall rate is the dominant factor in deposition rate. Both contaminants show peaks of deposition rate in association with the two prominent rainfall rate peaks. Close inspection of Figure 3.4 reveals that the radioactivity peaks lag the pollen peaks slightly; similarly, the rainfall rate peaks lag the radioactivity peaks slightly. The two contaminant curves are roughly parallel, except for the initial period of light rain, during which the pollen curve is at a relatively high value. This is attributable to the high concentrations of pollen in the first samples relative to the values at the beginning of the first shower, and is undoubtedly caused by impaction collection of pollens by the first rain to fall through the heavily contaminated air of the lowest layer of the atmosphere. Two features of the deposition rate curves are of special interest. The first is that approximately the same maximum value was reached in both major peaks for both contaminants. In the case of the pollens, the maximum value is about 6×10^5 grains/m^2/hr; for radioactivity about 1.5×10^4 pc/m^2/hr. The second notable feature is the "flat-topped" shape of both major radioactivity peaks. This means that the deposition rate remained constant, under conditions of rapidly increasing rainfall rate, for about 3 min in both cases, ending in each case at the R_g peak. This feature is not clearly evident in the pollen curve. Considered together, these two features may indicate that there is a maximum rate of deposition which can be attained by a rain system, given a particular level of contamination in the environmental air.

One possible mechanism comes to mind immediately: dilution of a limited contaminant supply by an excess of condensed water. This possibility is considered in greater detail in Chapter 4.

3.1.2 Concentrations of Airborne Pollen Grains

Concentrations of airborne pollens at the field site for May 9, 10, and 15, 1964, are tabulated in Table 3.1. The May 15 data are included to provide additional evidence regarding the general level of air concentrations during mid-May, 1964. Several uncertainties are associated with these data. In many samples, especially in the case of the longest sampling periods, the sampling surface was observed microscopically to be almost entirely covered with collected particles of all kinds. Because pollen grains impinging upon these particles would be likely to bounce off, it is likely that reported concentrations would be low, especially for the longest sampling periods. Examination of the data in Table 3.1 lends support to this hypothesis, because in general lower concentrations are associated with the longer sampling periods, but no firm conclusion should be drawn from such a limited sample. It is possible that diurnal variations of concentration in air could produce the same results. Computations of concentration were made on the assumption of a 100% collection efficiency of the bar for the pollen grains. It has already been pointed out that retention efficiency is likely to have been less than 100%; and the same is true for the theoretical collision efficiency (Brun and Mergler,

TABLE 3.1

CONCENTRATIONS OF AIRBORNE POLLENS—MAY, 1964

Date (1964)	Time, CST Start	Time, CST End	Duration (min)	Bar No.	Total Grains	Concentration (grains/m^3)	
5/9	1848	2006	78	1	43	33	
				2	40	31	
5/10	0948	1037	39	1	6	9	
				2	10	15	
	1053	1155	62	1	8	8	
				2	3	3	
	1254	1330	36	1	16	27	
				2	11	18	
	1800	1815	15	1	4	16	
				2	5	20	
5/15	0949	1052	63	1	18	17	
				2	lost	--	
	1056	1126	30	1	24	48	
				2	28	56	
	1129	1322	113	1	21	11	(rain)
				2	35	19	(rain)
	1325	1439	74	1	28	23	
				2	49	40	
	1442	1606	84	1	35	25	
				2	32	23	

1953). These combined errors could yield concentrations which are low by a factor of 2 to 5.

3.1.3 Synoptic Analyses

Investigation of almost any atmospheric phenomenon should be carried out in the framework of the large-scale features of the atmosphere prevailing at the time of interest. This framework will therefore be established, beginning with synoptic-scale features high in the atmosphere and adding detail as we proceed toward the surface and the locality of interest.

The 250 mb (jet stream level) isobaric analysis for 1800 CST* on May 9 is shown in Figure 3.5(a). The dominant feature of the flow on that day was a trough over the western U.S. The flow over Oklahoma was WSW. A jet stream was present across Kansas, Missouri, Illinois, and eastward to the Atlantic coast. Apparently, a broad zone of strong winds was present between Oklahoma City and Dodge City. This is suggested by winds at 250 mb and supported by vertical cross-sections normal to the flow. For example, see Figure 3.7. Flow at 500 mb at 1800 (Figure 3.5(b)) is very similar and shows some evidence for a westward tilt of the trough line with height. The surface feature of most pertinence to the Oklahoma area (Figure 3.6(a)) is a stationary front lying in an east-west orientation across southern Oklahoma at 0000 on May 10. The shaded area in cen-

*All times in this dissertation are Central Standard Time, unless specifically noted otherwise.

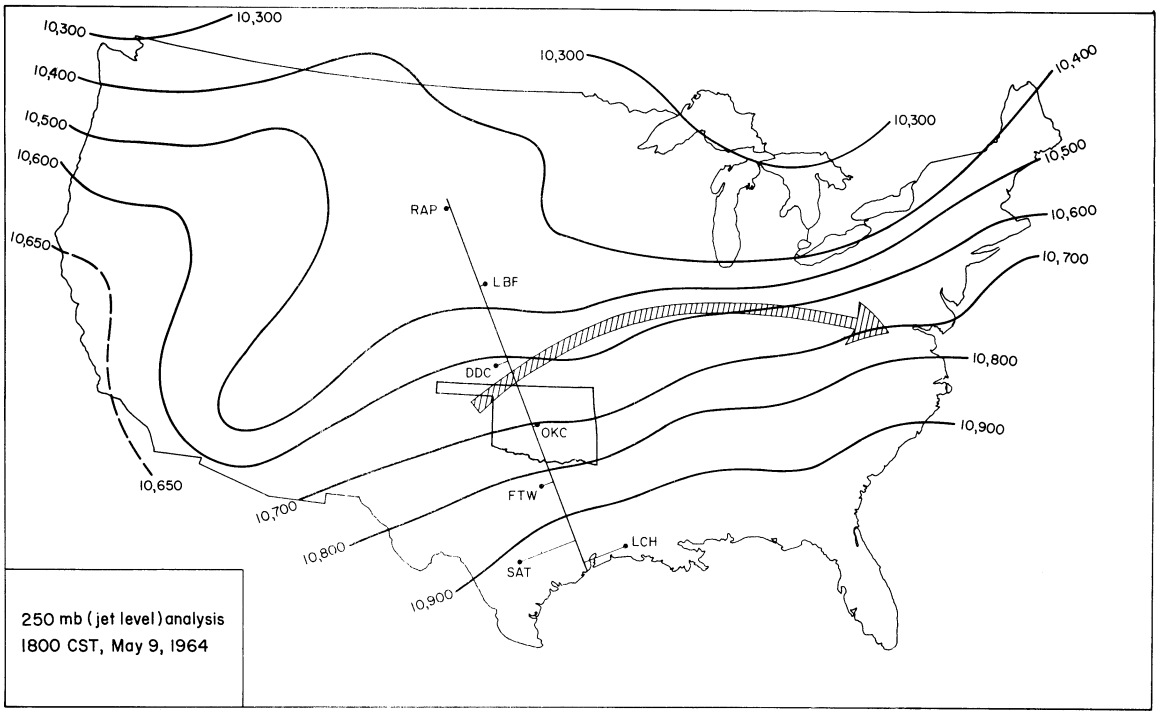

Figure 3.5(a). Constant-pressure analysis at jet stream level, 1800, May 9, 1964, showing location of cross-section shown in Figure 3.7.

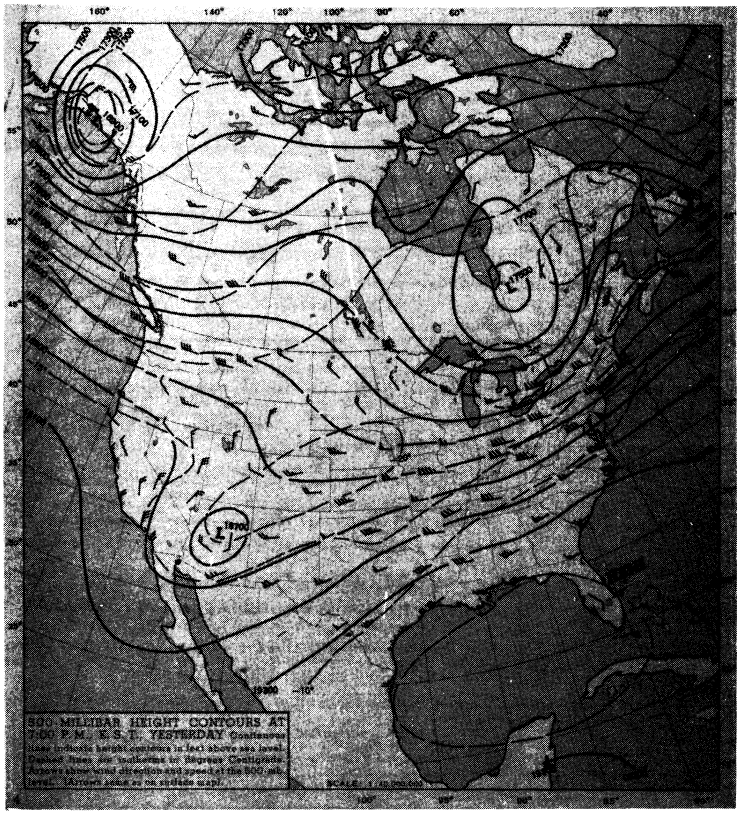

Figure 3.5(b). 500 mb analysis, 1800, May 9, 1964.

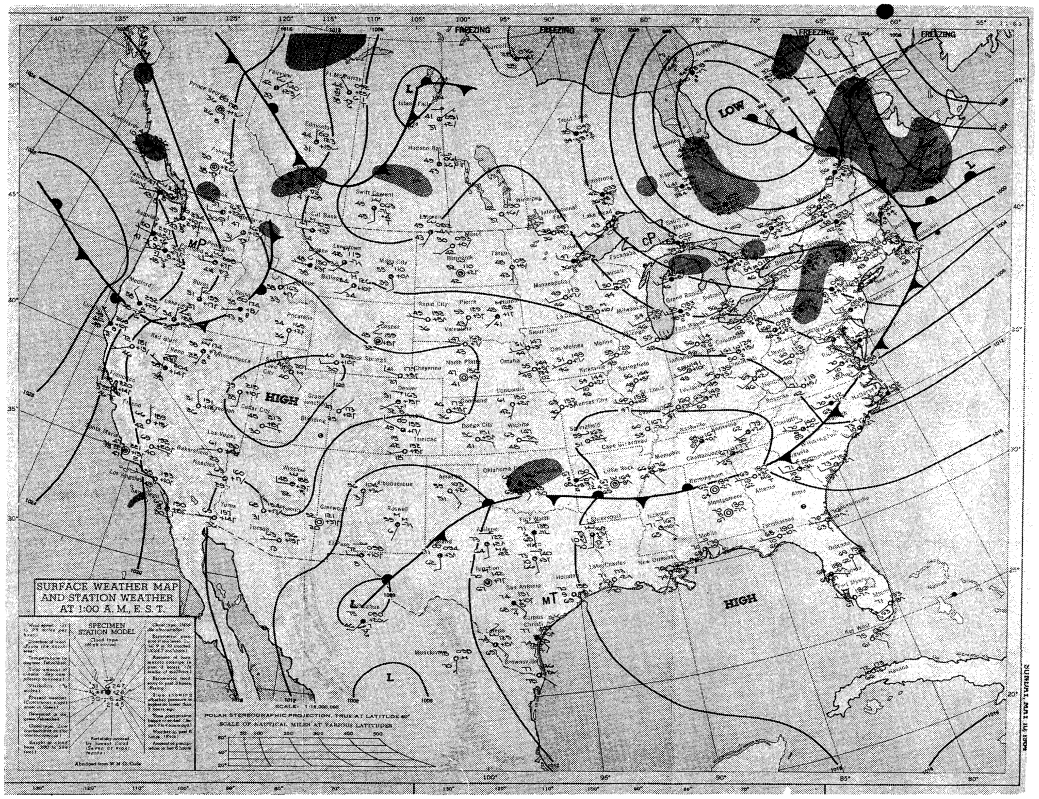

Figure 3.6(a). Sea-level pressure analysis, 0000, May 10, 1964.

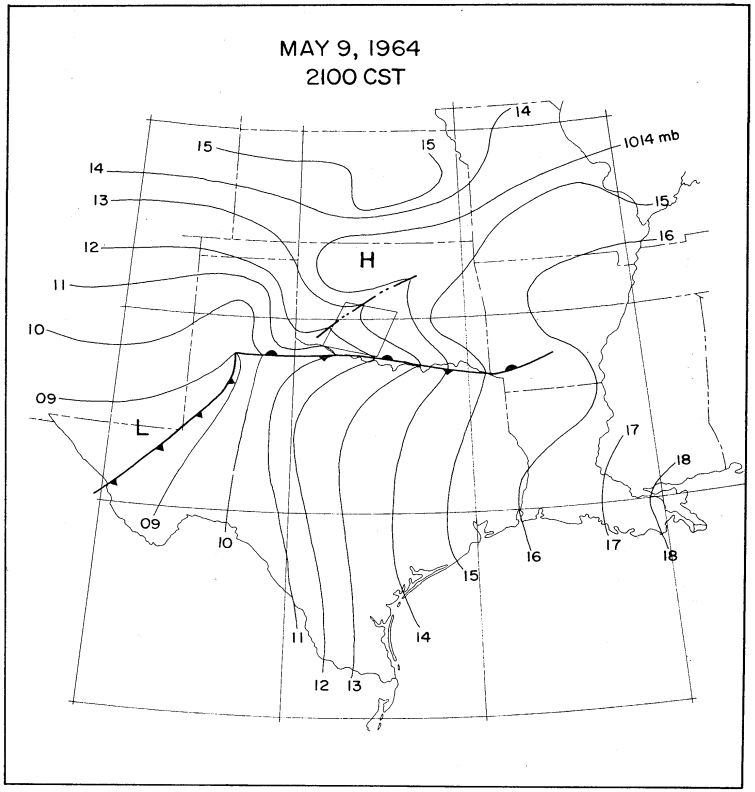

Figure 3.6(b). Detailed sea-level analysis over Oklahoma and adjacent states, 2100, May 9, 1964.

tral Oklahoma shows the location of the rain system which affected the area of our station on the evening of the 9th. Considerably more detail regarding the frontal system and the squall line is given by the surface analysis at 2100, which is shown in Figure 3.6(b). The front and the squall line are shown here in greater detail, and an additional feature now appears. The presence of a dew point discontinuity or "dry line" was clear from a comparison of dew points across the northeast-southwest line (indicated as a cold front) through western Texas. To the west of the line the dew points were less than 20F, whereas dew points of 50F and higher prevailed to the east. An intermediate dew point (28F) appeared at the interface of the dry and moist air. Observations suggest that the dry line may play a role in the development of squall lines in the south-central U.S. but the exact mechanism is not yet clear (Newton, 1963).

A synoptic analysis of special importance to this study is the cross-section analysis shown in Figure 3.7. By use of the cross-section normal to the flow, Danielsen (1964) has shown that it is possible to detect layers of air of recent stratospheric origin in the troposphere. The method of detection is based on the conservation of potential vorticity P_θ, approximated by

$$P_\theta = - g \frac{\partial \theta}{\partial p} (\zeta_\theta + f)$$

where g is the acceleration due to gravity, θ is potential temperature, p is pressure, ζ_θ is vorticity measured on a θ surface, and f is the

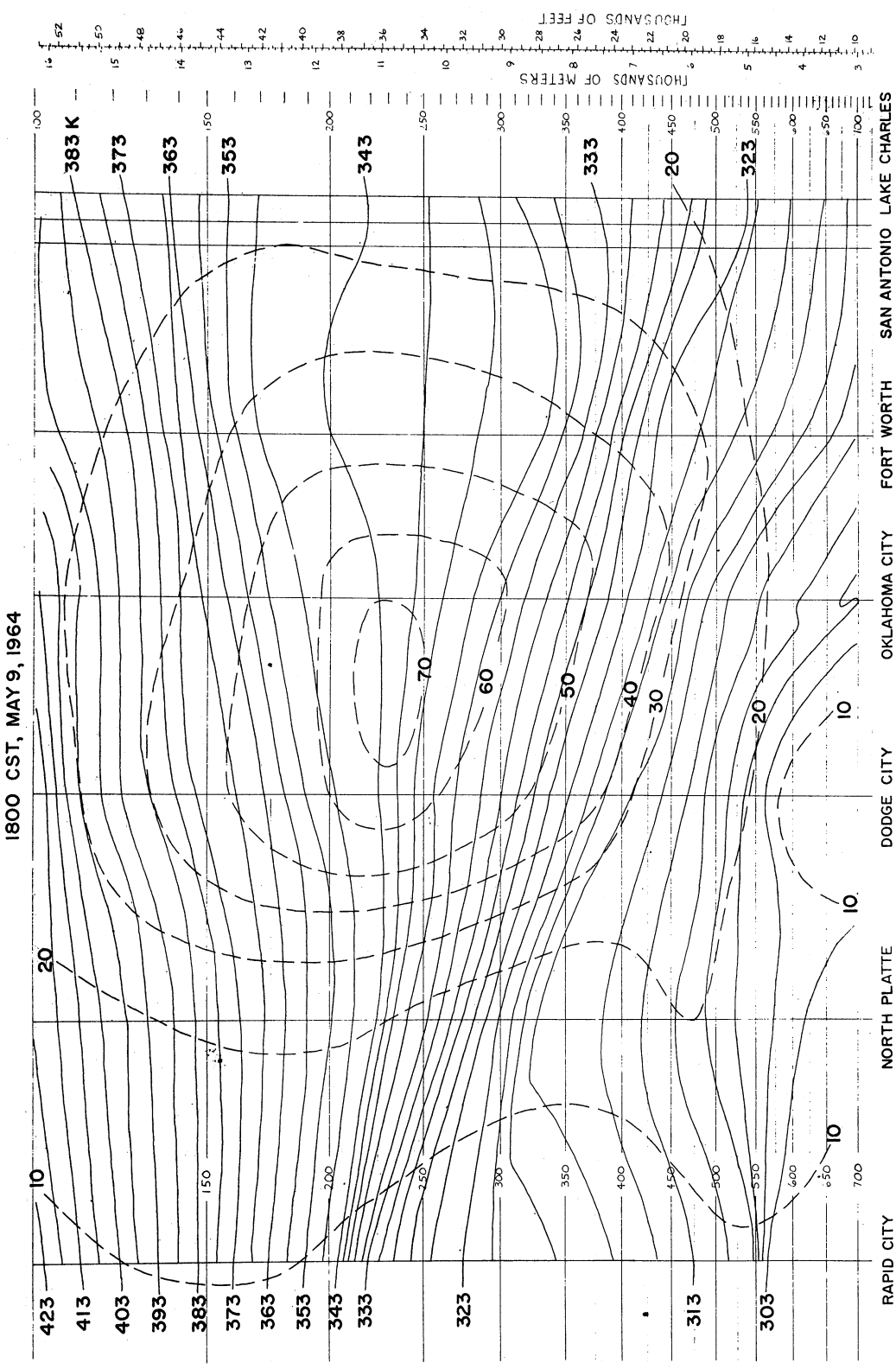

Figure 3.7. Vertical cross-section normal to flow at 500 mb, 1800, May 9, 1964. Solid lines are potential temperature in degrees K, dashed lines are isotachs in m/sec. San Antonio and Lake Charles data were averaged.

vertical component of the earth's vorticity. Danielsen has found high correlations between values of P_θ and concentrations of radioactivity in air. It can be seen that P_θ is a product of a vertical stability factor, $-\partial\theta/\partial p$, and $(\zeta_\theta + f)$, a measure of the stability relative to horizontal displacements. The term $-\partial\theta/\partial p$ will be large (positive), because θ increases upward and p increases downward, when the pressure difference between adjacent θ lines is small, i.e., when the lines are crowded together in the vertical. Following Danielsen, we may write

$$\zeta_\theta = \frac{V}{R_\theta} + \frac{\partial V}{\partial n_\theta} \simeq \frac{\partial V}{\partial n_\theta}$$

where V is wind speed, R_θ is the radius of curvature of the streamlines on the θ surface, and n_θ is distance along the θ line on the cross-section, positive to the right. The approximation of ζ_θ by the right-hand (shear) term may be made if R_θ is large. This is true in our case; as shown in Figure 3.5, there is very little curvature in the flow aloft over Oklahoma. Thus, high values of P_θ and hence high radioactivity concentrations in air may be expected in regions of vertical packing of θ lines and packing of isotachs along θ lines. A region of this kind was possibly present on May 9 between Dodge City and North Platte, as may be verified from Figure 3.7. However, such a region was specifically <u>not</u> present in the troposphere over or near Oklahoma City. The extent of vertical penetration by convection in the squall line on May 9 has been investigated by Hall (1965) using data from the National Severe Storms

Laboratory (NSSL) WSR-57 radar at Norman. It is reported that an echo top of 55,000 ft was associated with the most intense portion of the storm which passed through the southern portion of the ARS network. This is the storm identified below as storm A. Hall reports that the highest echo top over any of his stations reached 37,000 ft over station 6 between 2030 and 2035. The highest top over station 5 (WB11) reached 35,000 ft between 2105 and 2115. Of course the pertinence of echo tops over a collector is questionable because precipitation trajectories are rarely if ever vertically downward. Still, these heights indicate the general level of the tops over the ARS network. Reference to the tropopause height, reported by Hall as 41,300 ft at 1800 on May 9, shows that probably only the most intense portion of the storm entered the stratosphere. This is not to imply that high concentrations of radioactivity would be encountered above the tropopause. Values of the potential vorticity (P_θ) in the anticyclonic stratosphere (such as over Oklahoma City) are intermediate between the high values characteristic of the cyclonic stratosphere and the low values of the troposphere. However, the relationship between P_θ and the radioactivity concentration is not firmly established for the anticyclonic stratosphere (Danielsen, 1965). In any case, no tropopause penetrations were observed in the vicinity of any of the stations, and it is unlikely that high concentrations of radioactivity were encountered by the storms in the troposphere.

Attention is now directed toward a more detailed documentation of the squall line rain system, using several kinds of meso-scale data.

3.1.4 Meso-Scale Data

The time series of radar echo intensity distributions given in Figure 3.8 shows immediately the sequence of events as the squall line approached and passed our station (near mesonetwork station 11). The first presentation of the series, at 2023, confirms the general NE-SW orientation of the squall line shown in Figure 3.6. Only the southwestern end of the line is shown. Three main storms (labeled A, B, and C in Figure 3.8) are apparent. Storm A was the largest and most intense. At 2023 it was entering the ARS rain gauge network (dashed outline); light rain was falling at station 11, northeast of storm A (cf. rainfall rate in Figure 3.3). Seven minutes later, at 2030, the three main storms had moved eastward, and development of more intense echoes had taken place near station 11. A slight increase in rainfall rate was observed at this time (Figure 3.3). By 2045 additional eastward movement and further development to the northeast of storm A had taken place.

Station 11 was situated between two NE-SW bands of heavy precipitation. At 2054 the band to the northwest had disappeared, but the other was oriented as before but had moved slightly northward. Further northward movement occurred by 2100. A 30-db contour was then located very close to station 11 on its southeast. Between 2100 and the following

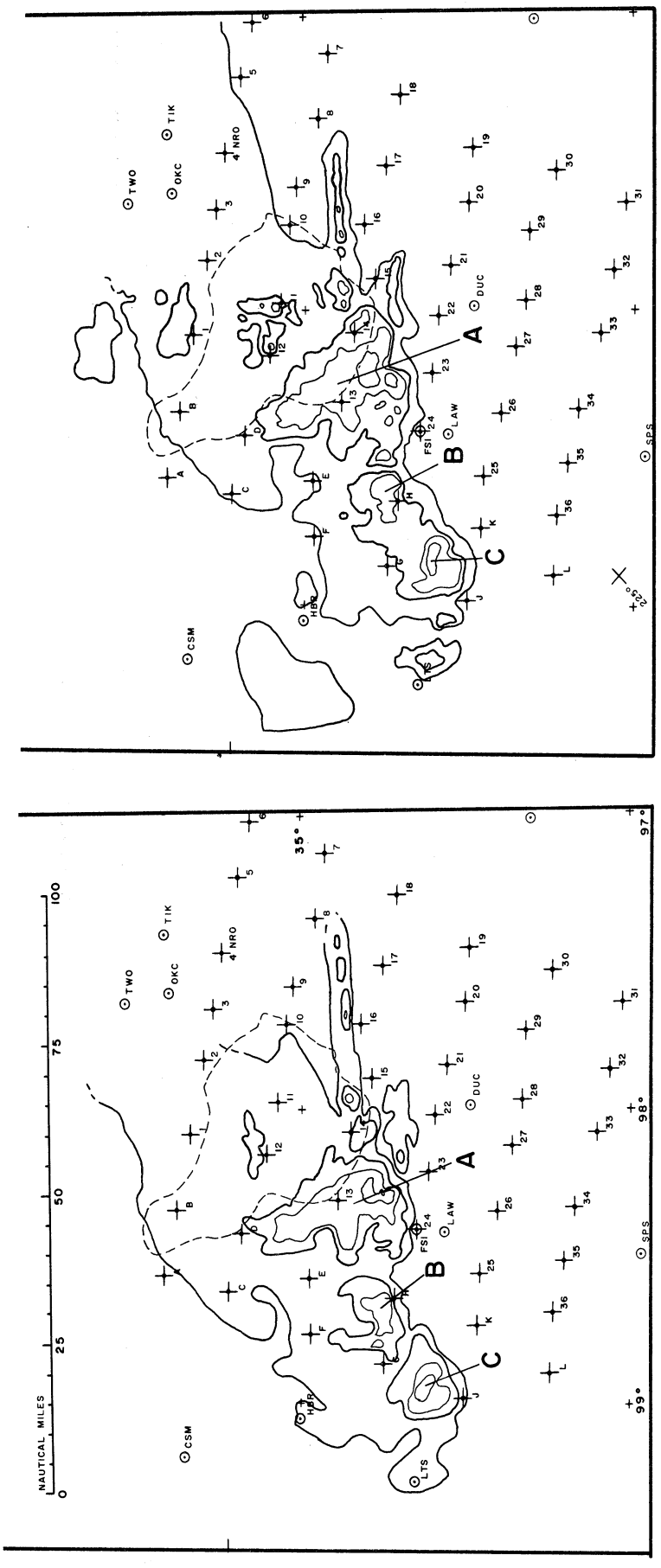

Figure 3.8. Time sequence of radar echo intensity distributions over the mesonetwork, May 9, 1964, using data from WSR-57 radar at NRO. Successive contours represent the minimum detectable signal and gain reductions of 18, 30, 42, and 54 db. Corresponding values of Z_e are given in Table C.2. The dashed line is the outline of the ARS network. Time is given in the upper left corner.

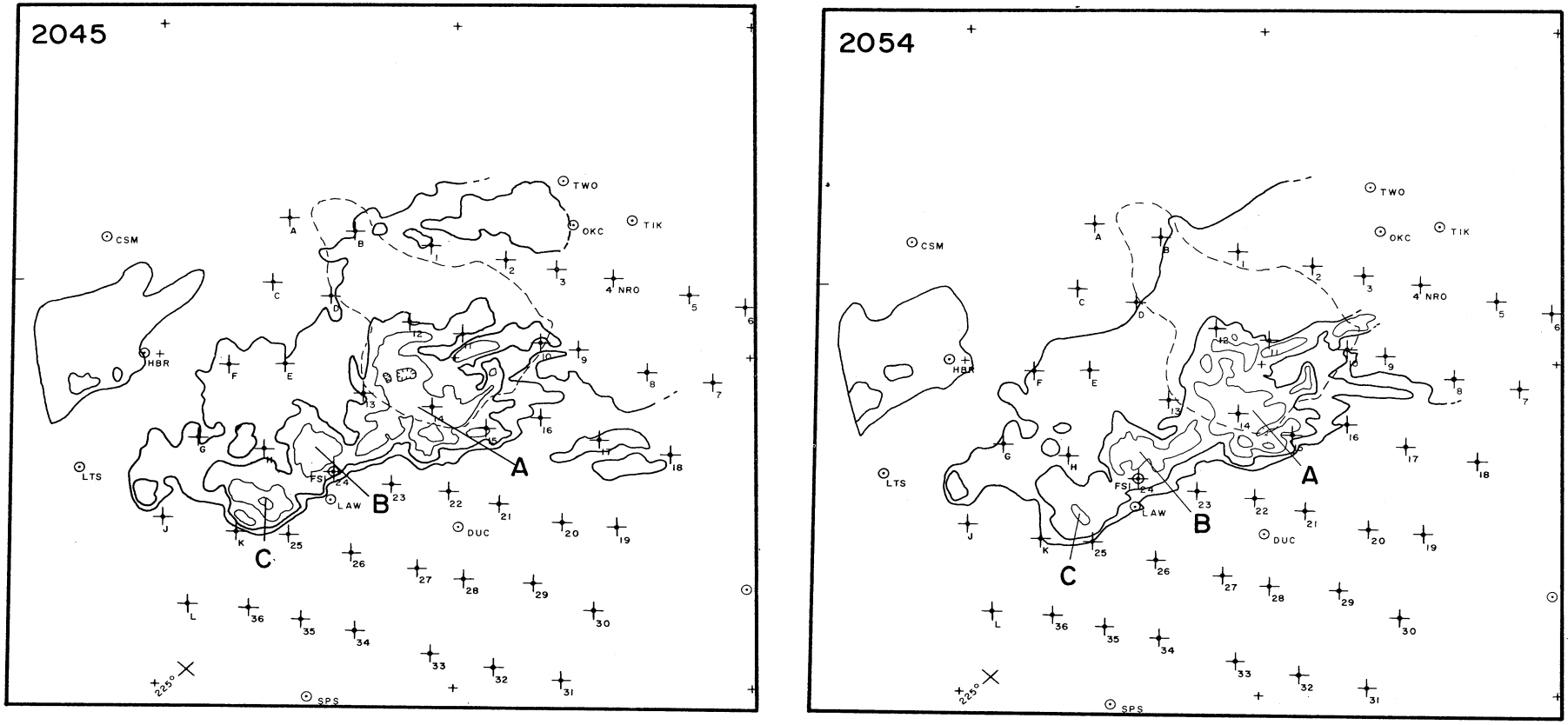

Figure 3.8 (Continued)

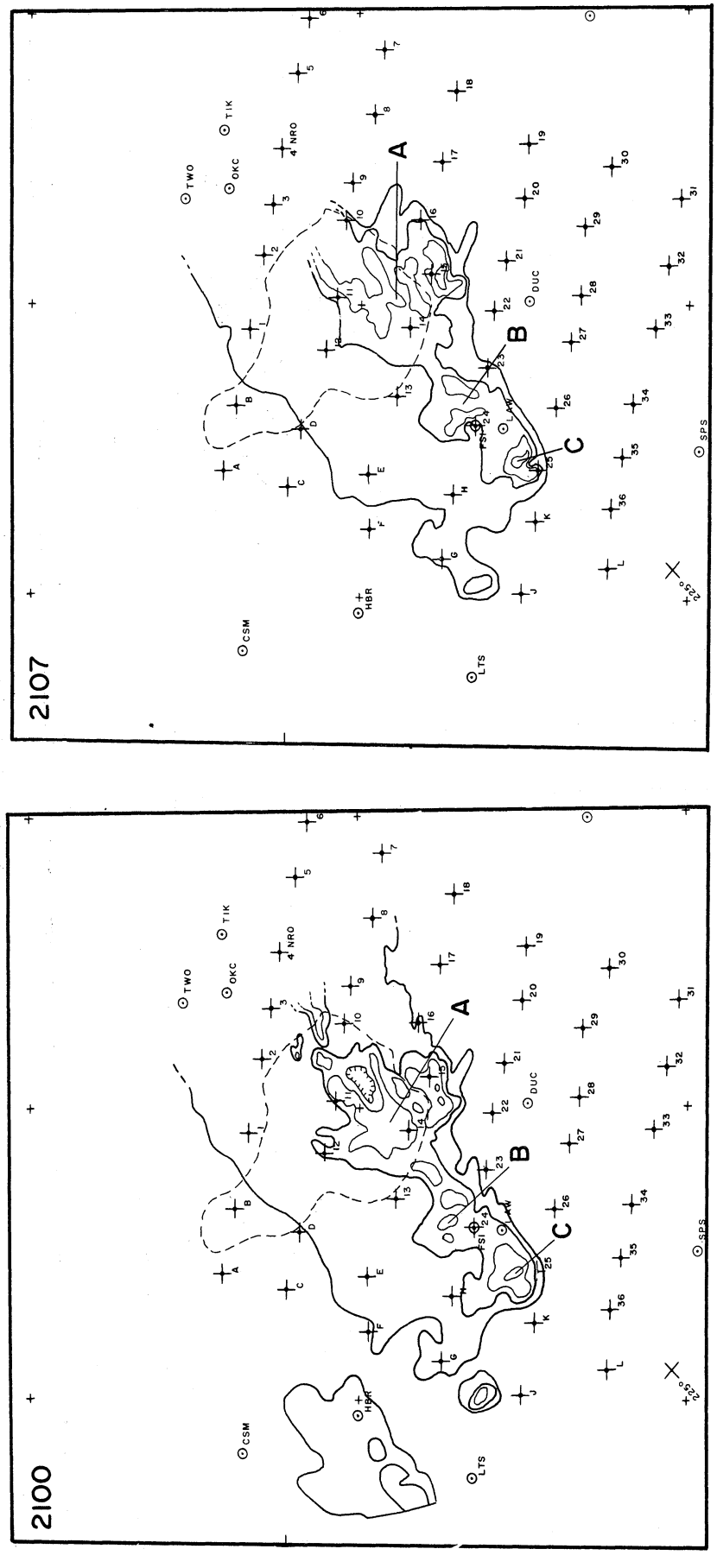

Figure 3.8 (Continued)

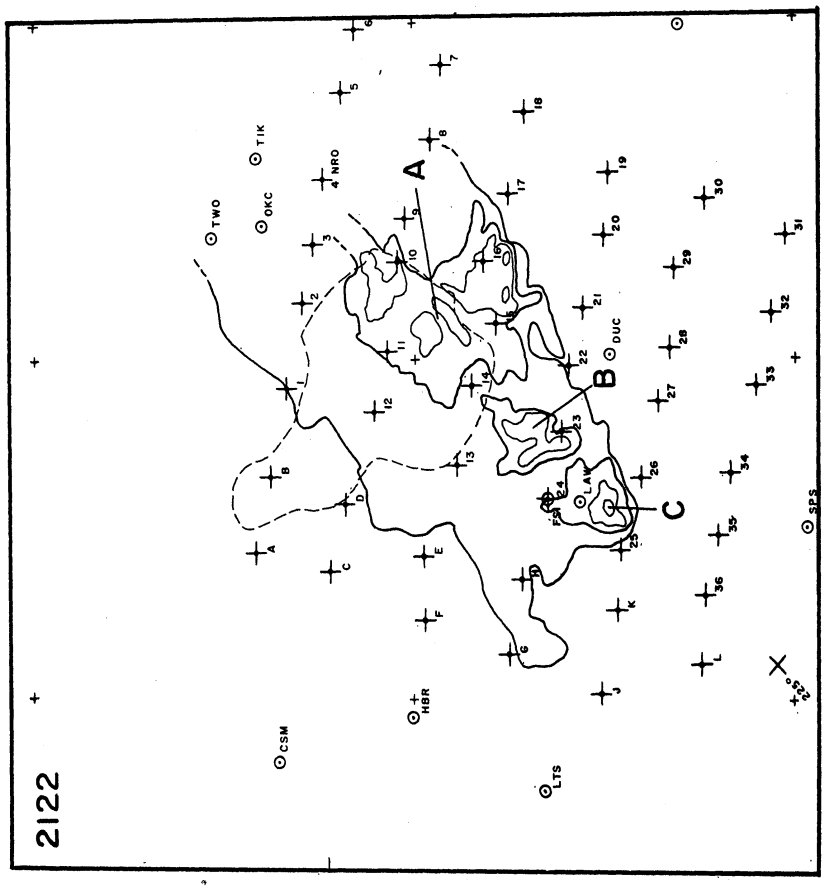

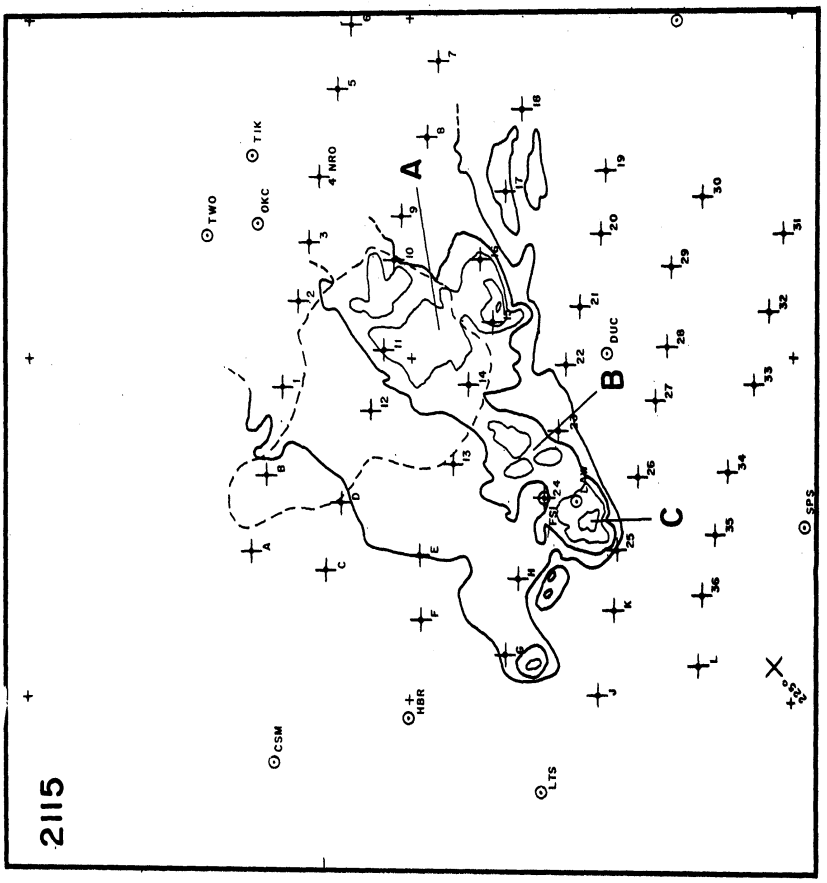

Figure 3.8 (Concluded)

map at 2107, the first rain burst occurred. Although it is not clear from the 0° elevation radar data, it is feasible that this heavy shower was the result of a northward extension of the heavy rain to the SE. This is consistent with information provided by the radar from a series of scans with the antenna tilted upward, as discussed later. The next map, at 2115, coincides with a time of rapidly increasing rainfall rate at the beginning of the second shower. It is clear by comparison with the map at 2107 that the rain area which affected station 11 was associated with a general expansion of the rain area to the south and east. The next presentation, at 2122, comes during the final stages of the second shower. It is rather surprising that evidence of heavy rain at station 11 is lacking. The absence of strong echo is probably an indication that the shower at that time filled only a small fraction of the radar beam.

During the period of time represented in Figure 3.8, storm A, which affected our station, was decreasing in peak intensity; in addition, the degree of organization was decreasing. This is inferred from the changes observed in the intensity distribution. That is, at 2023 the intensity contours are quite concentric, with the highest gradient in the southeast quadrant of the storm. By 2122, after a period of 1 hr, the gradient has weakened and several intensity maxima are present, somewhat randomly distributed throughout the storm.

The radar antenna tilt sequence makes 360° scans in 1° increments of elevation angle from 0° through 6° and in 2° increments up to 14°. These data provide information on the vertical distribution of precipitation and the height of echo tops. Important additional information concerning the history of the two rain bursts on May 9 was obtained through examination of these data. Both of the heavy showers received at our station were evidently associated with a region of relatively intense local convection to our east. This region of convection was imbedded in the broader rain area, but its "motion" was different from the mean motion of the squall line or any of its component storms. In contrast to the general eastward motion of the squall line and its elements, the convective region identified above was observed to move, or propagate, northward, or even slightly northwestward. The region was somewhat rectangular in shape, oriented NE-SW, about 8 n mi wide and 15 n mi or more long. The showers which affected our station were peripheral to the most intense area and were located to its west or southwest. Small towers (about 1 n mi diameter) were observed aloft in the radar data in the vicinity of station 11 several minutes prior to both heavy showers. At 2104, the same time as the first rainfall rate peak, a very small echo was present at 26,000 ft over station 11. Echoes were also observed at the same height less than 1 n mi west of and about 4 n mi northeast of station 11 at 2112, as the second heavy shower began. Therefore it appears that the two rain bursts received at our station

were from very small cells which were associated with a larger, northward-propagating convective region to the east of our location.

In summary, station 11 was affected by storm A, the peak intensity center of which passed south of station 11. The storm was probably in the early stages of dissipation during the traverse.

The pressure mesoanalysis for the mesonetwork at 2045 is shown in Figure 3.9. Comparison with the radar data at the same time (Figure 3.8) shows a squall front (I), thunderstorm high, and wake depression, familiar features of severe storm situations, in association with storm A. A second squall front (II), located in the NE quadrant of the network, was apparently associated with an earlier storm in an area north of the mesonetwork. The presence of the wake depression at 2045 indicates that storm A was in the dissipation stage before the heavy rain began at our station.

The next data to be presented are fields of rainfall rate over the Agricultural Research Service (ARS) network, and are the most detailed data on the motion of this rain system yet examined. Rainfall rates over the ARS network are shown in Figure 3.10 at 10 min intervals from 2030 to 2130. At 2030 an area of heavy rain, designated in Figure 3.8 as storm A, was entering the SW corner of the network. This feature, as well as the intensity centers NW and SE of our location, are identifiable on the radar map at the same time. The detail of the development NE of storm A in the radar map of 2045 is brought out in the

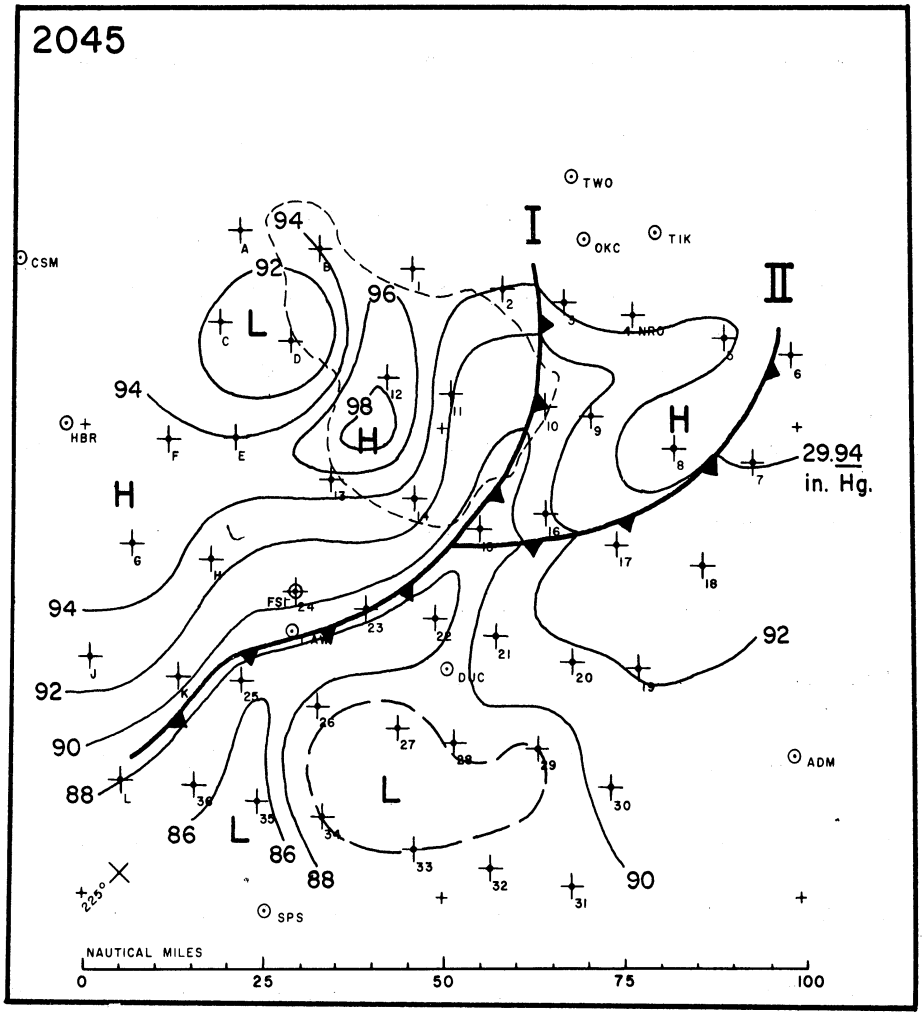

Figure 3.9. Pressure mesoanalysis for 2045, May 9, 1964. Isobars of altimeter setting were drawn, as described in the text.

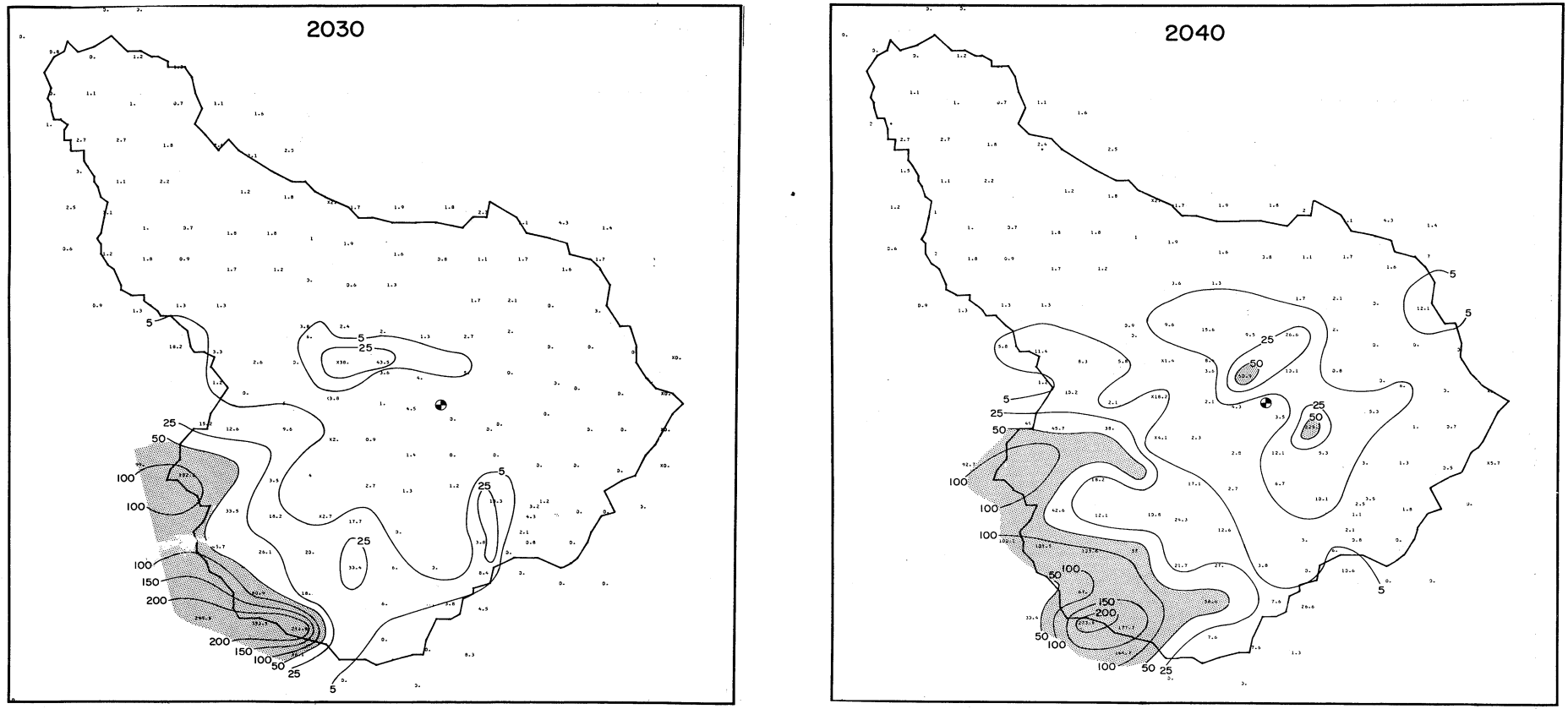

Figure 3.10. Rainfall rate sequence over ARS network, May 9, 1964. Units are mm/hr. See text for description.

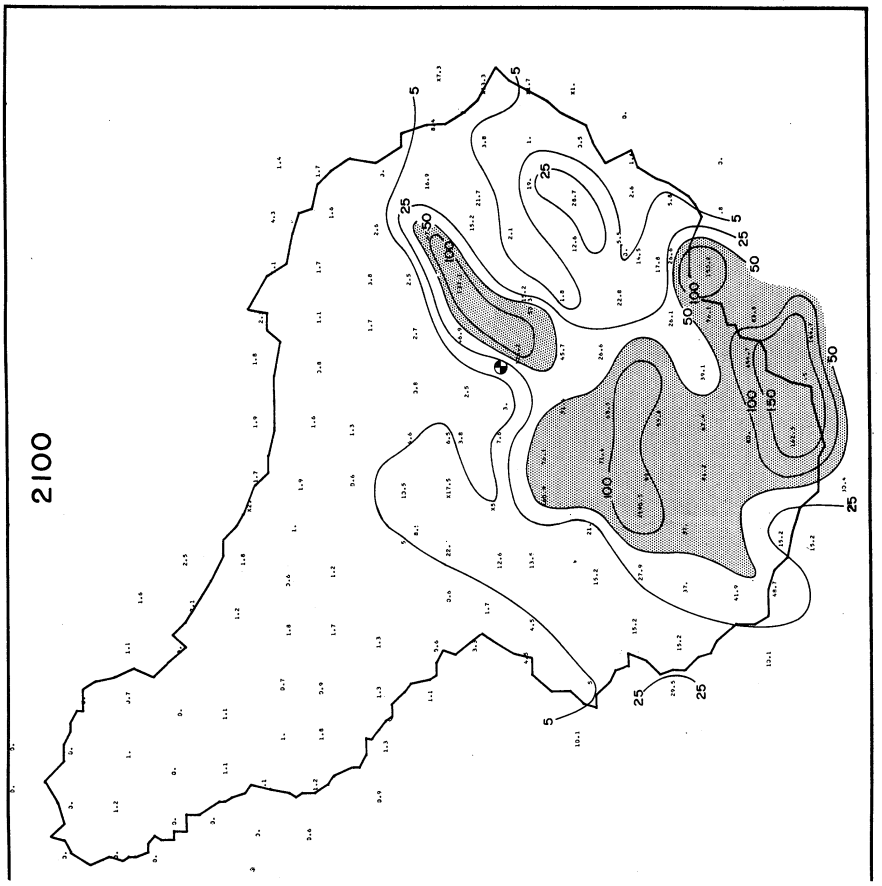

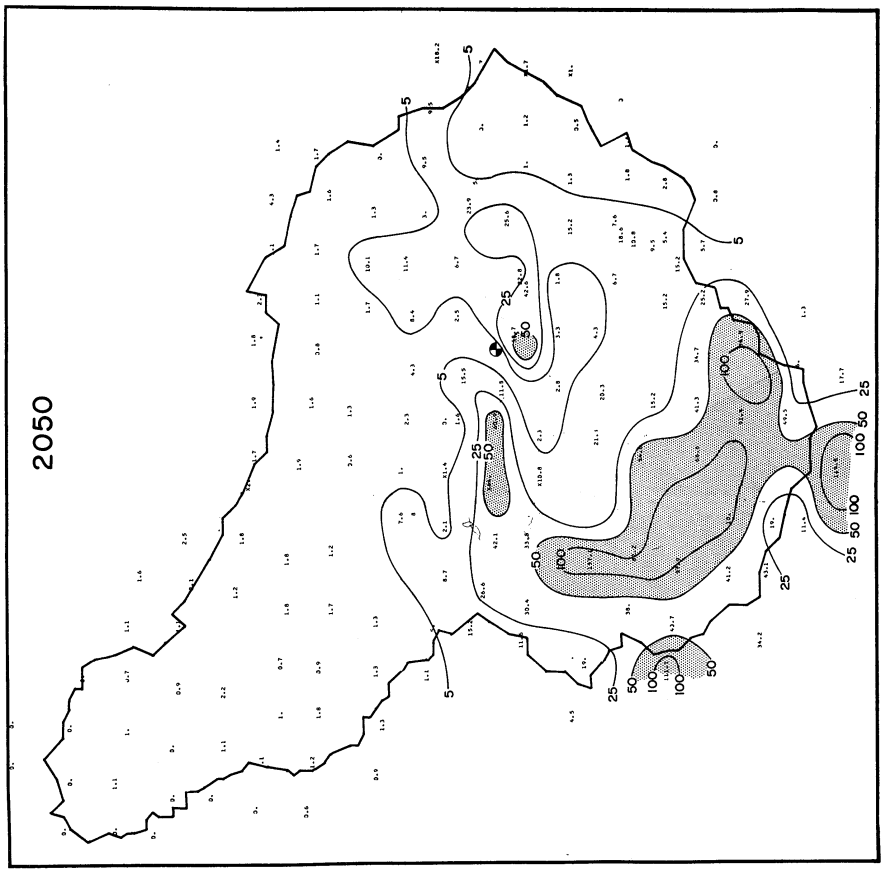

Figure 3.10 (Continued)

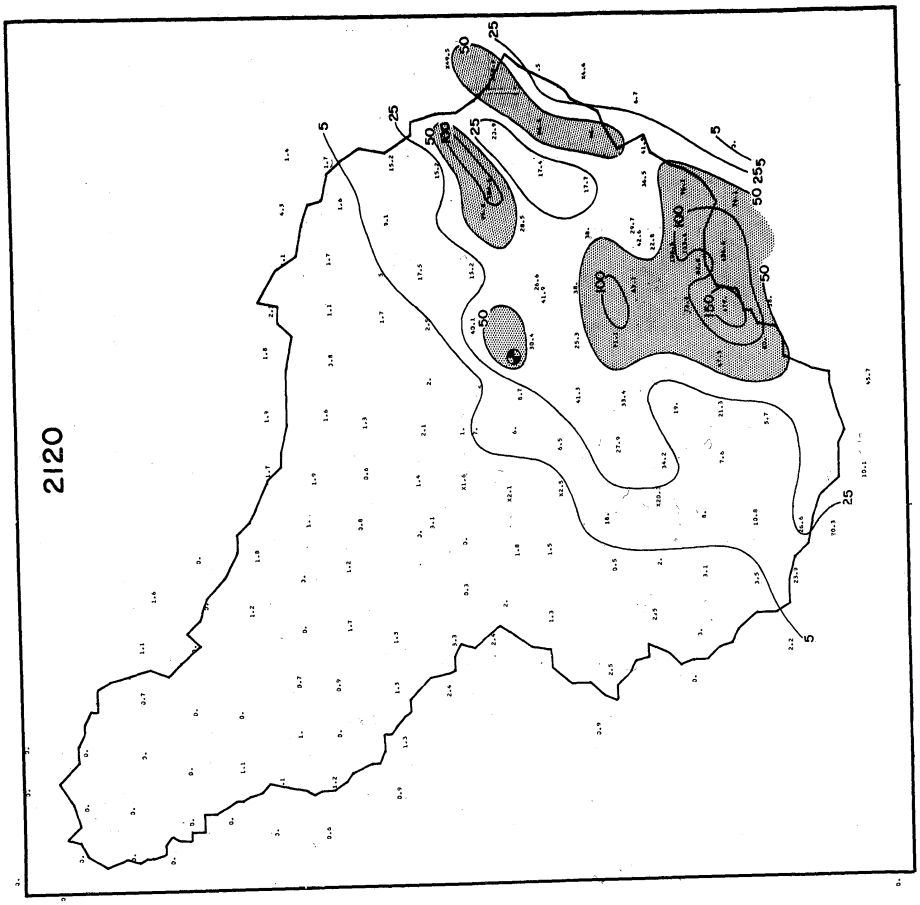

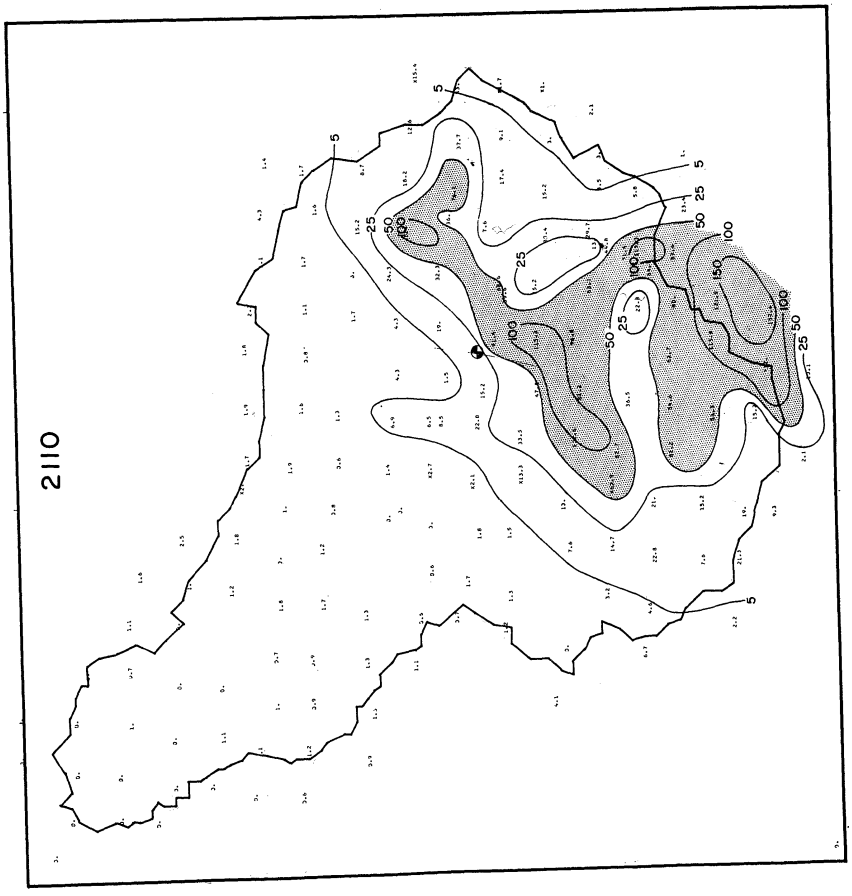

Figure 3.10 (Continued)

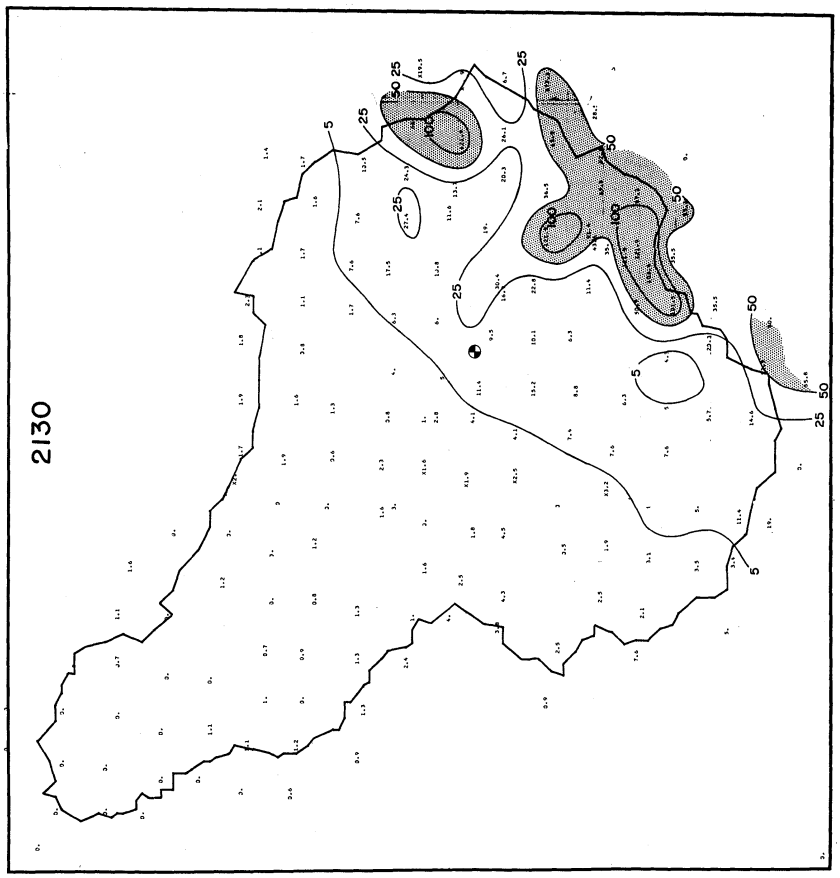

Figure 3.10 (Concluded)

rainfall rate map at 2040. The intensity centers NW and SE of our location are clearly shown. The main storm has moved farther into the SW corner of the network at this time. The next two rainfall rate maps, at 2050 and 2100, show in detail the situation just preceding the first heavy shower at our station. The rainfall rate map at 2050 shows intensity maxima very close to our station to the south and west. By 2100, however, the situation had changed radically. The shower to our south had increased in intensity and extended northeastward, while the shower to our west disappeared. During this 10-min period, the southern part of the network experienced a general eastward movement of the main storm and the development of several individual intensity centers. The rainfall rate map at 2110 shows in general the same NE-SW zone of heavy rainfall SE of our station, and no evidence at all of our first shower, which occurred between this and the previous map. It seems apparent that the shower at our station resulted from a brief westward or northward extension of the band of showers to our southeast. The shower structure in the southeast part of the network was exceedingly complex at 2110. The following map (2120) coincides with the peak rate of our second shower and shows that the rain which fell at our station was from a brief local shower, again to the rear of the band of heavy rain to our east. The transitory nature of this heavy shower is illustrated by the fact that none of the ARS gauges (3 mi grid interval), in the vicinity recorded a rainfall rate

over 40 mm/hr, although the rate at our station was > 60 mm/hr. Evidence of this shower is lacking on the radar map at 2122, also. The final rainfall rate map, at 2130, shows the further eastward movement of the heavy rain and the light rainfall which was occurring at our station and westward of it at that time.

The use of the rainfall rate charts provides details of motion and rain system structure not available from the radar data alone. The degeneration of the organized storm into many relatively isolated and transient showers was especially clear, and the detail concerning the origin of the first shower at our station would have been incorrectly inferred from the radar data.

The total squall line rainfall over the ARS network is shown in Figure 3.11. As might have been expected, the heaviest rainfall occurred in the southern and southeastern parts of the rain gauge network. Our station was in an area of steep gradient; neighboring ARS gauges to the west and south had totals of less than half and more than twice our total, respectively.

Variations of station pressure, temperature, and relative humidity at station 11 during the course of the rain are shown in Figure 3.12. A prominent pressure rise occurred during the period of heavy rain between 2100 and 2130. Breaks in the temperature curve seem to be associated with the two rainfall rate peaks. The humidity curve shows a maximum at 2100, followed by an irregular decrease until about 2115, about the same time as the second temperature break, and apparently associated

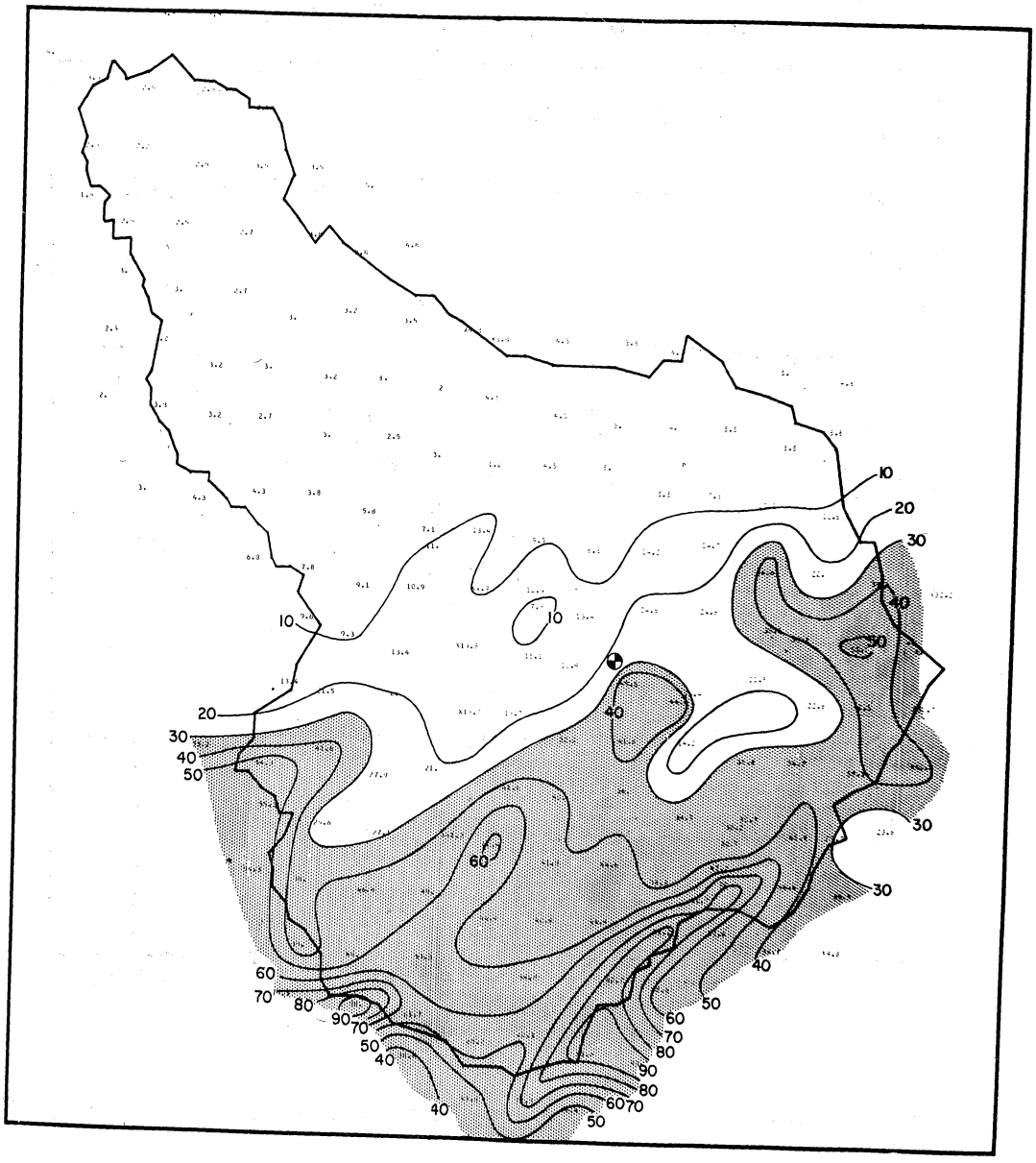

Figure 3.11. Total squall line rainfall over ARS network, May 9, 1964. Units are mm.

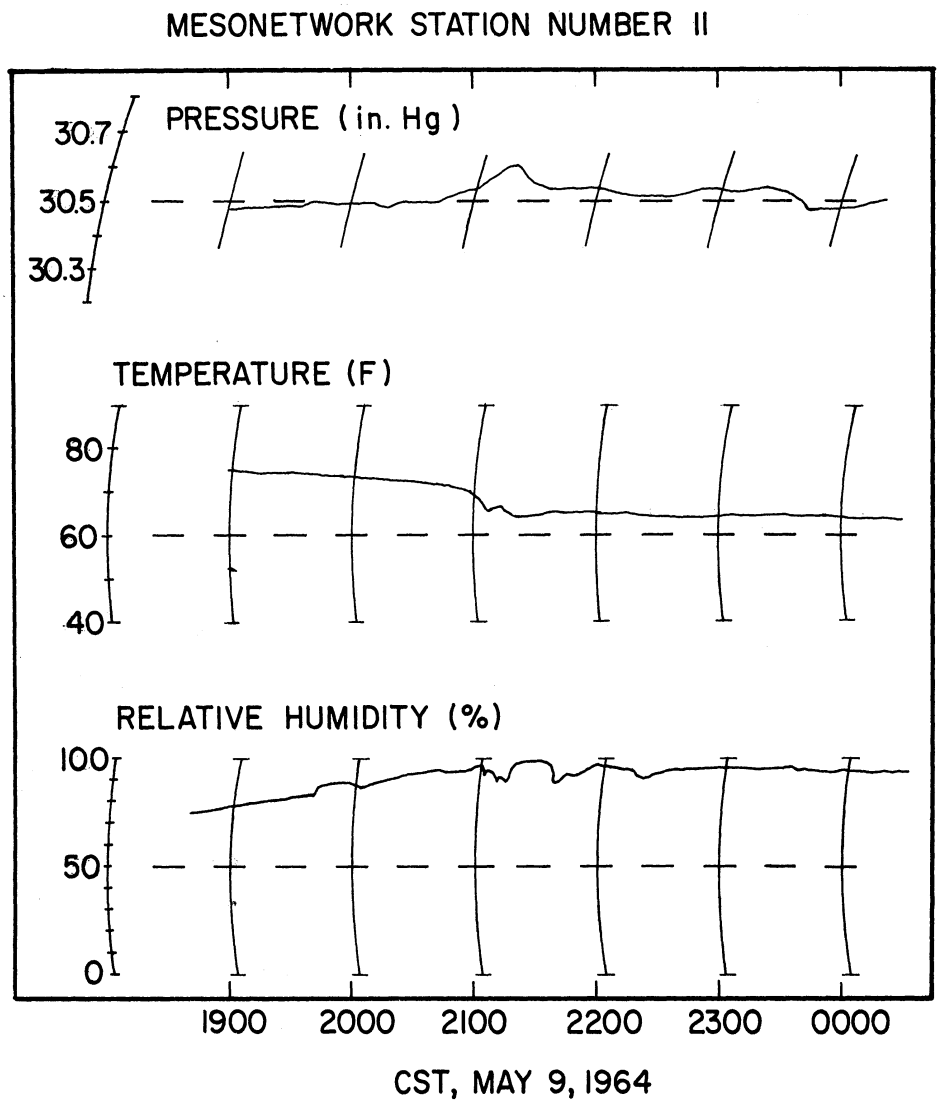

Figure 3.12. Variations of pressure, temperature, and relative humidity at mesonetwork station 11 on May 9, 1964.

with the second shower. A rapid increase in humidity occurred beginning at 2115. Nearly 100% humidity was reached within 5 min; this value was maintained for the duration of the heavy rain, and was followed by a temporary dip between 2130 and 2140.

3.1.5 Summary

This storm is characterized chiefly by the occurrence of two bursts of rain at our station. The results show positively that temporal variation of the concentration and deposition rate of contaminants in rain which falls at a point are determined within individual convective cells, which may be too small to be observed by radar or even by a network of rain-gauges on a 3 mi by 3 mi grid.

The outstanding feature of the results is that concentrations of particles of three distinct size spectra vary in phase, and are associated with major variations in rainfall rate. The relationship between temporal variations of concentration and rainfall rate were the same in both rain bursts if one is careful to exclude other effects. In this case the effects of the initial light rain are to be excluded in consideration of the first burst and those of the first burst are to be excluded in consideration of the second. Thus, a relative maximum of concentration was found slightly before each rainfall rate peak. After this maximum, the concentrations decreased very rapidly and were doing so at the time of the rainfall rate peak. Soon after the rate peak a relative minimum concentration was reached. This pattern occurred during both rain bursts.

Deposition rate, which is a product of concentration and rainfall rate, was controlled mainly by the latter, so that deposition rate was greatest during intense rainfall. The constant deposition rate of radioactivity during a period of increasing rainfall rate for a few minutes prior to both rainfall rate peaks is a particularly interesting feature of these curves.

The precipitation system was a squall line located north of a stationary front—dry line system in Texas. The center of the storm which produced the rain samples at station 11 moved from approximately 270° and passed south of the sampling station. Most of the rain which fell at station 11 came in the two heavy bursts, which were associated with small convective cells of short duration. These developed ahead (NE) of the main storm during a period in which the main storm was dissipating and becoming less organized.

3.2 THE RAIN OF MAY 10, 1964

On this day rain fell intermittently in south-central Oklahoma during daylight hours. The event examined in detail here was a late afternoon squall line, which produced a single intense rainfall rate peak at our station, as shown in Figure 3.13. This storm, although superficially similar to the one of the previous day, was markedly different in many respects. These differences are made clear below.

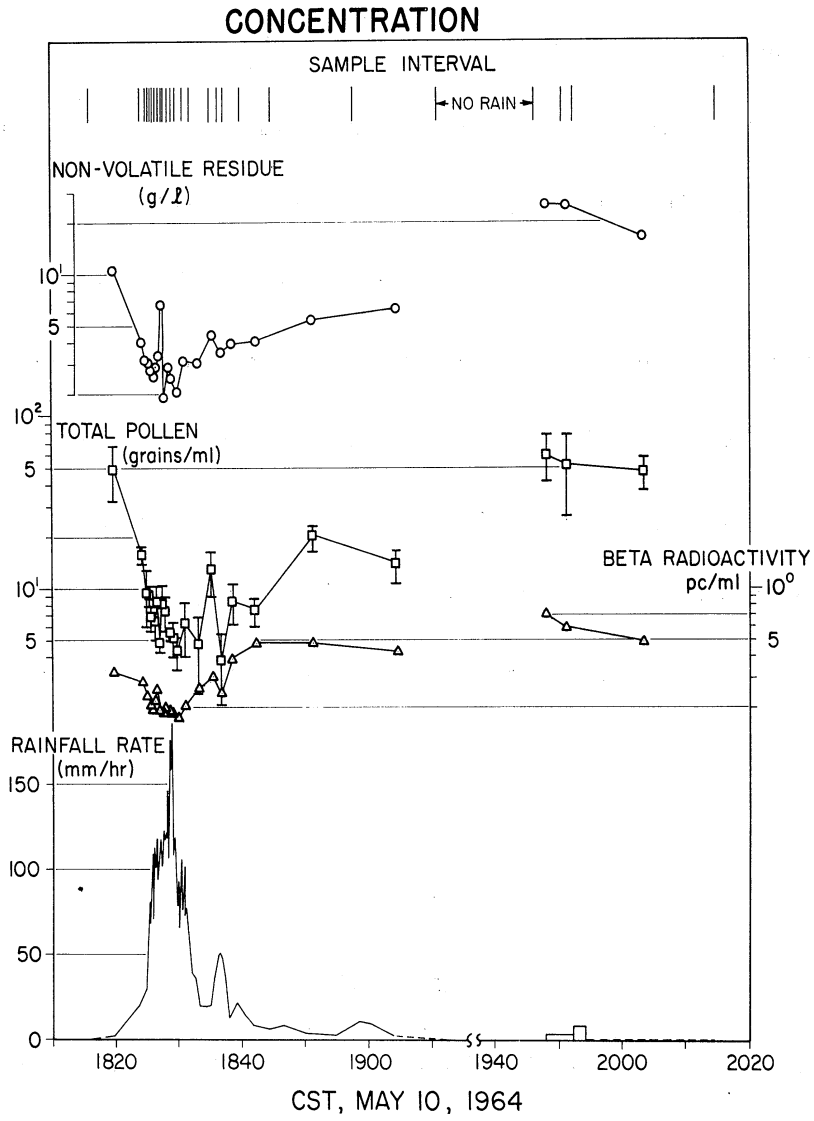

Figure 3.13. Temporal variations of concentrations of three classes of rain water contaminants, May 10, 1964. Three standard error limits are shown for pollen concentrations.

3.2.1 Rain Water Analyses

Contaminant concentrations and rainfall rate are shown as a function of time in Figure 3.13. The three contaminant concentrations decreased together at the beginning of the heavy shower, but in each case the difference between values at the start of the shower and those during the heaviest rain was much less than observed in the rain of May 9. The overall ranges of concentrations of the respective contaminants (exclusive of the shower between 1948 and 2015) was less on the 10th than on the 9th (see p. 33) but ratios of maxima to minima were in the same order

pollen:	12
residue:	6
radioactivity:	3

The negative slopes of the three curves during the period of the shower when rainfall rate was increasing are in the order pollen > residue > radioactivity, as was also observed on the 9th. A secondary shower, which occurred at about 1838, produced a minimum of all three concentrations in the sample collected during the rate peak, compared with adjacent samples. This decrease was very marked in the case of the pollens. Finally, a comparison of Figures 3.13 and 3.3 show that the highest concentration of each contaminant was greater on the 9th than on the 10th. In the case of radioactivity, the maximum on the 9th was almost twice that on the 10th; for the other two contaminants the factor was approximately 6.

Deposition rates of pollens and radioactivity are presented in Figure 3.14. The major peaks of both curves are in phase with the rainfall rate peak. The deposition rate of radioactivity remained constant from the time R_g exceeded about 100 mm/hr until its peak, at which time both began to decrease. The same behavior was noted on the 9th, except that deposition rate became constant in that case when the value of R_g was about 50 mm/hr.

Concentrations of airborne pollens on May 10 are given in Table 3.1 (p. 38).

3.2.2 Synoptic Analyses

To document the state of the atmosphere at the time of the rain event, let us again look first at the flow at the level of the jet stream, in this case the 200 mb level, which is shown in Figure 3.15(a). Comparison with Figure 3.5(a) shows that the trough in the western U.S. filled somewhat in the previous 24 hr and moved slightly eastward. Northeast of Oklahoma a minor perturbation was present in the vicinity of the jet stream, which was in general located in about the same position as on the 9th.

The 500 mb surface at 1800 is shown in Figure 3.15(b). Eastward motion and filling of the trough are evident at this level also. As seen from the surface map at 0000 on May 11 (Figure 3.16(a)), which is 4 hr after the storm ended at our station, a weak cyclone formed on the stationary front and moved eastward. This movement is clear by

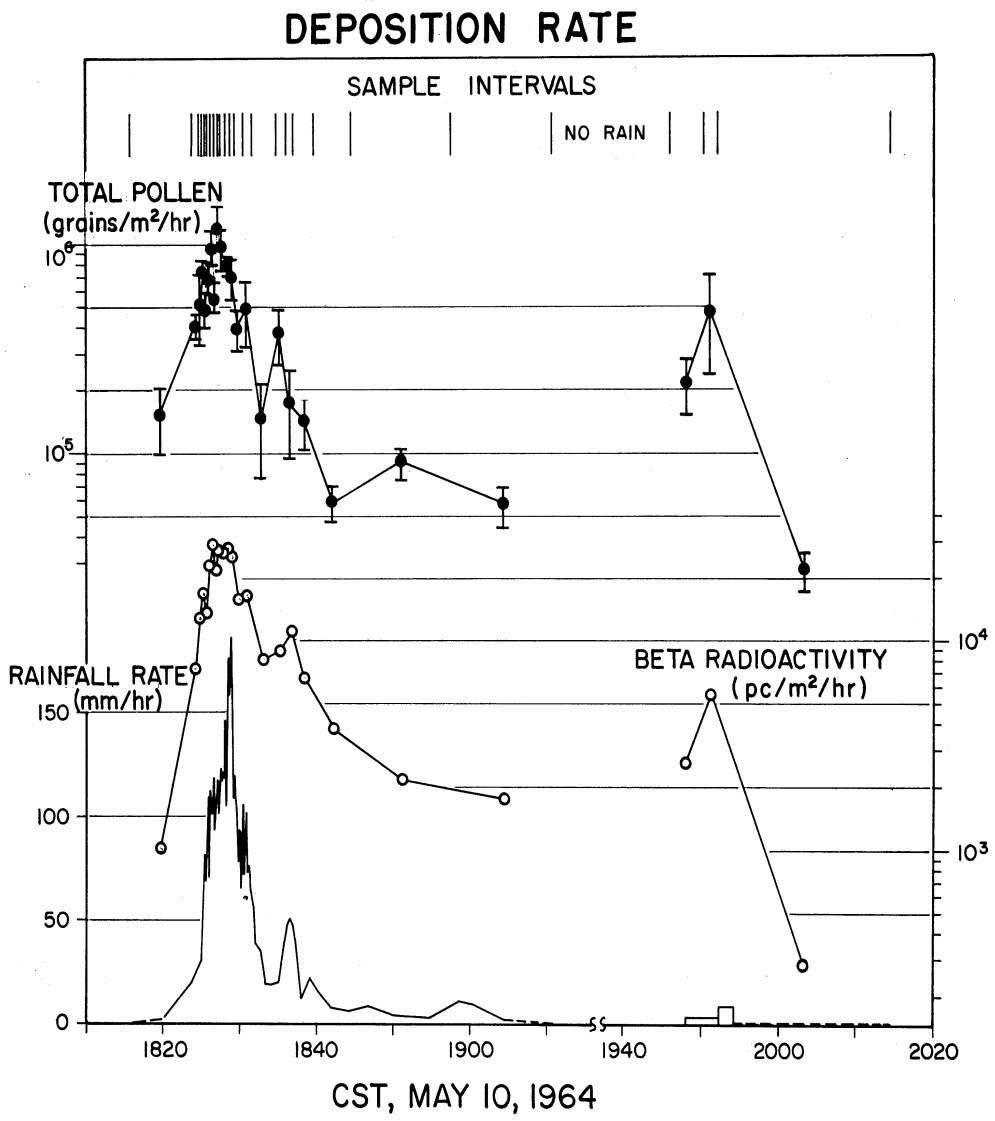

Figure 3.14. Temporal variations of deposition rates of total beta radioactivity and total pollens, May 10, 1964. Three standard error limits are shown for pollen deposition rates.

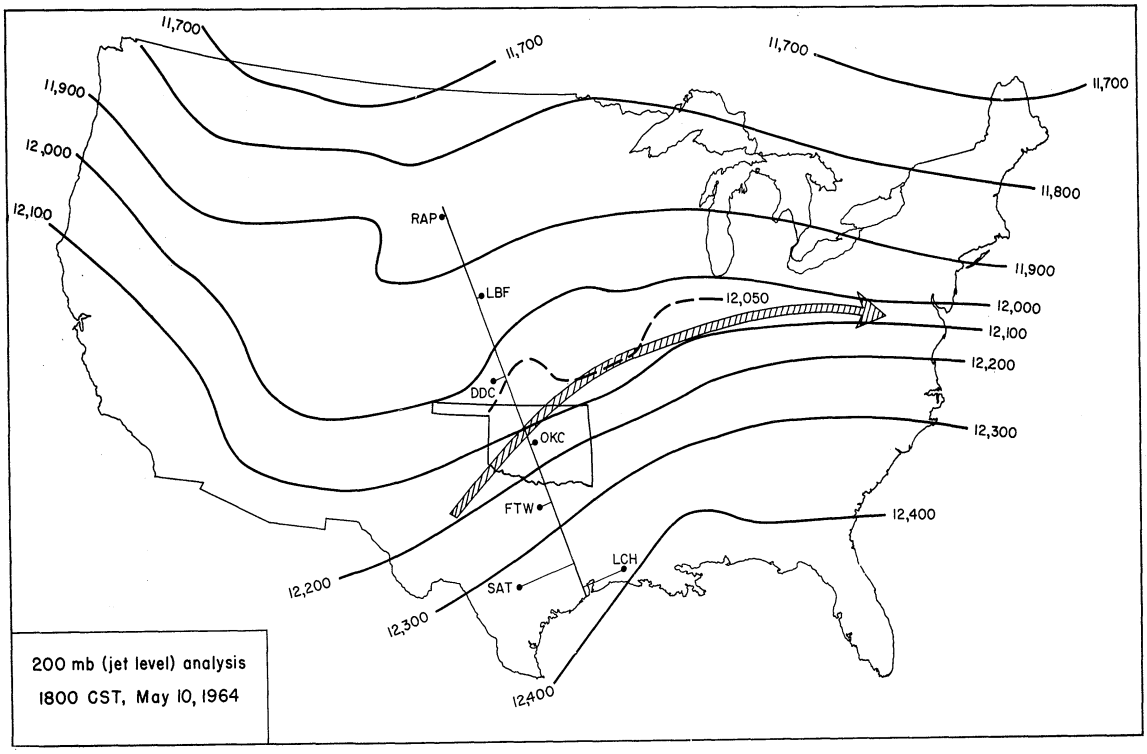

Figure 3.15(a). Constant pressure analysis at jet stream level, 1800, May 10, 1964, showing location of cross-section shown in Figure 3.17.

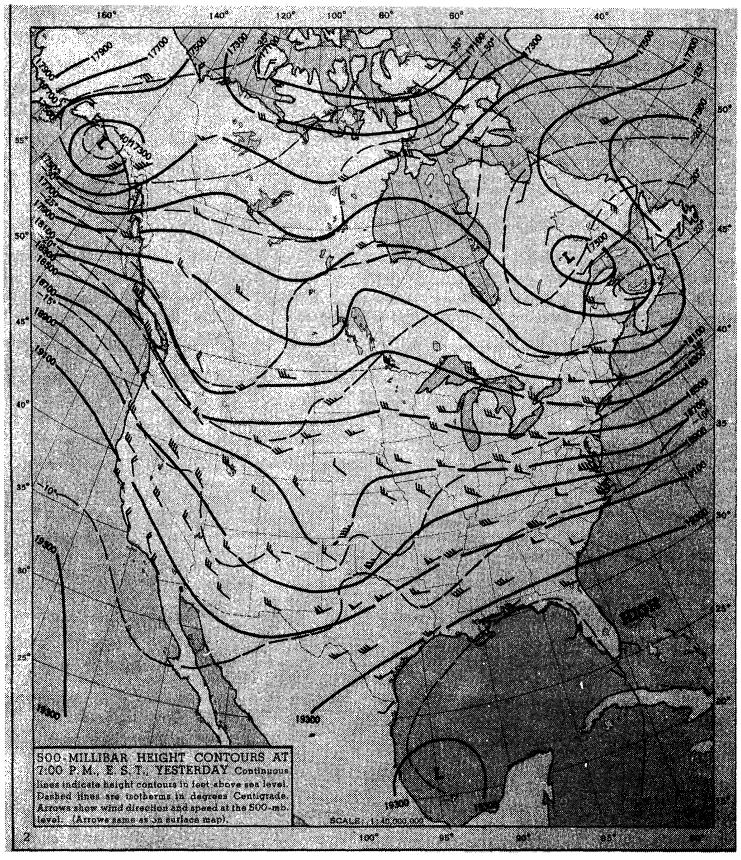

Figure 3.15(b). 500 mb analysis, 1800, May 10, 1964.

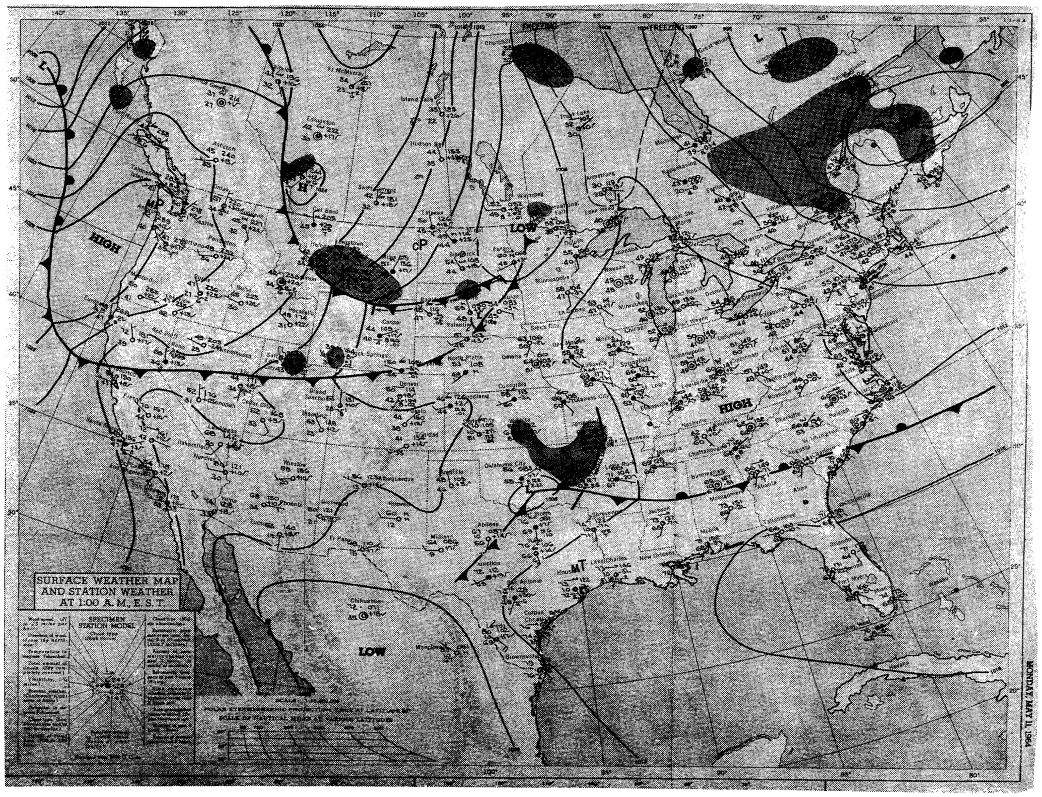

Figure 3.16(a). Sea-level pressure analysis, 0000, May 11, 1964.

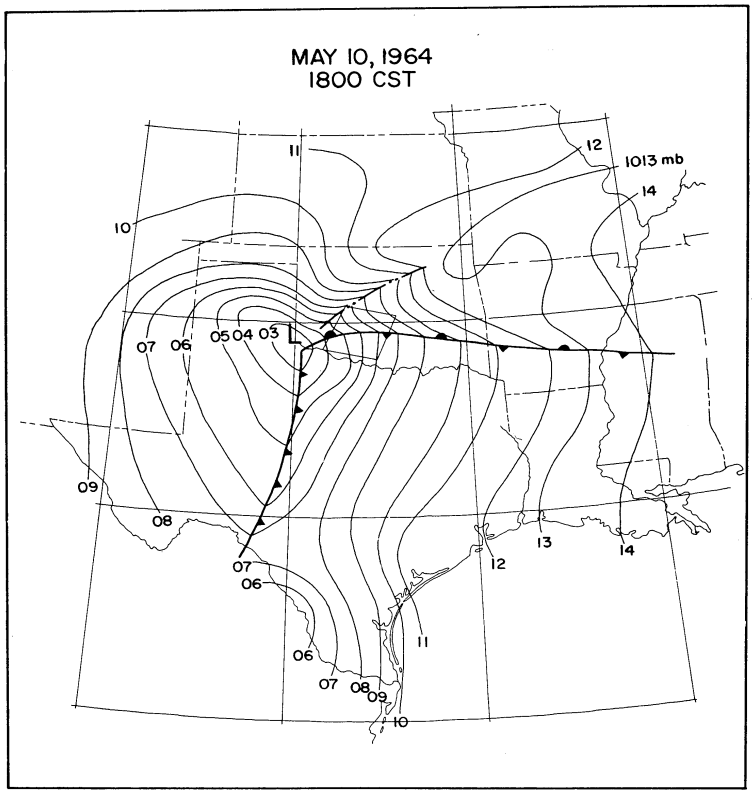

Figure 3.16(b). Detailed sea-level analysis over Oklahoma and adjacent states, 1800, May 10, 1964.

comparison with Figure (3.16(b)), a local synoptic analysis of the south-central U.S. at 1800 on the 10th; at this time the low pressure center was just entering the SW corner of Oklahoma. The center was the junction point for the dry front which extended southward from the low, the stationary front, which extended eastward, and the squall line, which extended northeastward.

Examination of the atmospheric cross-section for 1800, shown in Figure 3.17, reveals no indication of stratospheric intrusion which would be evidence for the presence of concentrated layers of high radioactivity in the troposphere. However, it is clear that the location of the jet stream had shifted slightly southward from its position of the previous day and the maximum wind speed decreased from 70 m/sec on the 9th to 50 m/sec on the 10th. A great instability in the vicinity of the squall line is clearly evident from the folded θ lines in the Oklahoma City sounding. The relationship between storm tops and features of the cross-section are found in the work of Hall (1965). He reports that the highest radar echo over his stations reached 43,000 ft, which is close to the tropopause height, which he reports to be 43,300 ft. This echo top maximum occurred over station 1 from 1730-1736, and was associated with the storm identified below as storm A, which passed about 20 n mi north of our station. The storm which affected our station reached 41,000 ft over station 4 between 1746 and 1814; its maximum height over station 5, adjacent to our station, was 35,000 ft from 1825-1847.

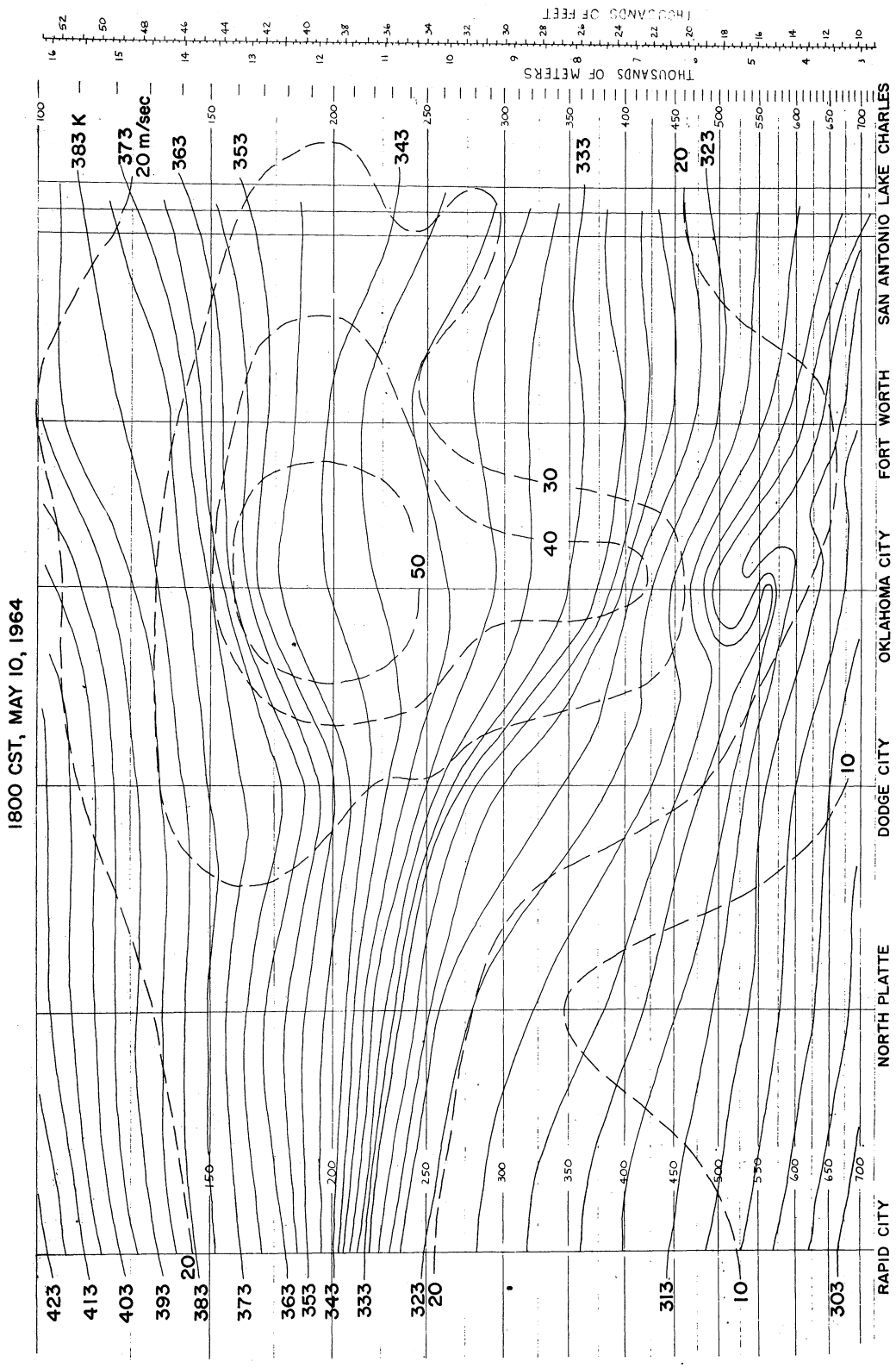

Figure 3.17. Vertical cross-section normal to flow, 1800, May 10, 1964. See legend, Figure 3.7.

3.2.3 Meso-Scale Data

The time sequence of radar echo intensity distribution is shown in Figure 3.18. At 1745, a half hour before rain began at our station, the southern end of the squall line was composed of three main storms, designated A, B, and C from north to south. By 1800 the four individual high-intensity echo centers of storm B had formed a single closed contour and moved eastward to a point just inside the western boundary of the ARS network. By 1815 further eastward movement had brought the intense core of storm B to a point 7 n mi west of our location. The radar map at 1827 shows the maximum intensity echo directly over our station. This coincides with the rainfall rate maximum observed at the same time. (See Figure 3.13) The position of the intense center at 1833 is east of our station and appears to have changed course slightly from a straight eastward path to one slightly north of east. At this time another shower, manifest on the radar map as a closed 30 db contour, was present about 4 n mi west of our station. This is evidently the source of the rainfall rate maximum observed at 1838 (Figure 3.13). At 1847 the radar map shows station 11 in an area of weak echo (< 18 db); however the northward extension of storm C, which passed mainly south of our station, was located to our west and southwest and is the likely source of the slight rainfall rate increase at about 1855. This is clearly shown in the map at 1900, where the position of station 11 is just westward of an 18 db contour. The final radar map at 1948 shows station 11 under the influence of storm D, which formed behind the main

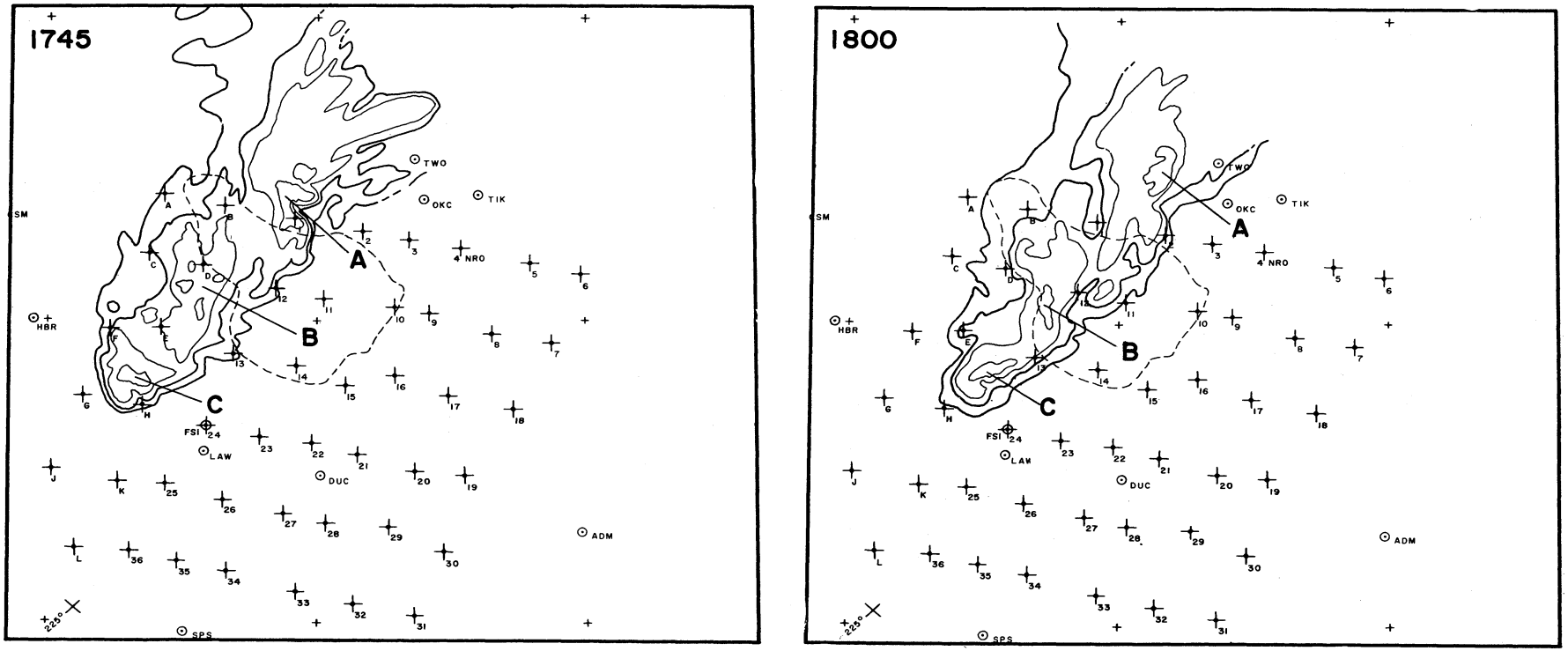

Figure 3.18. Time sequence of radar echo intensity distributions over the mesonetwork, May 10, 1964. See legend, Figure 3.8.

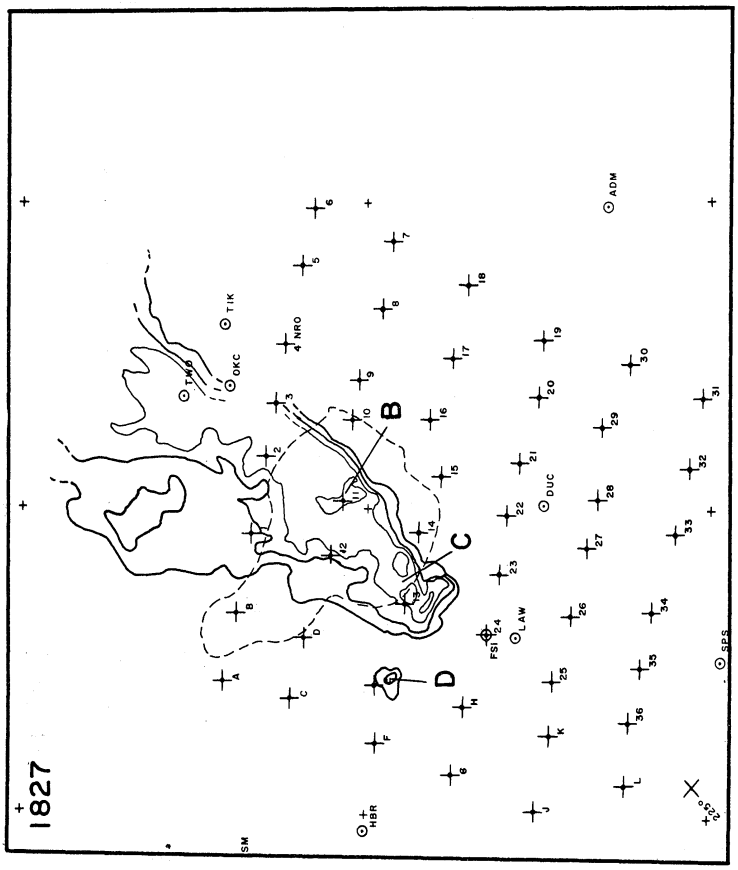

Figure 3.18 (Continued)

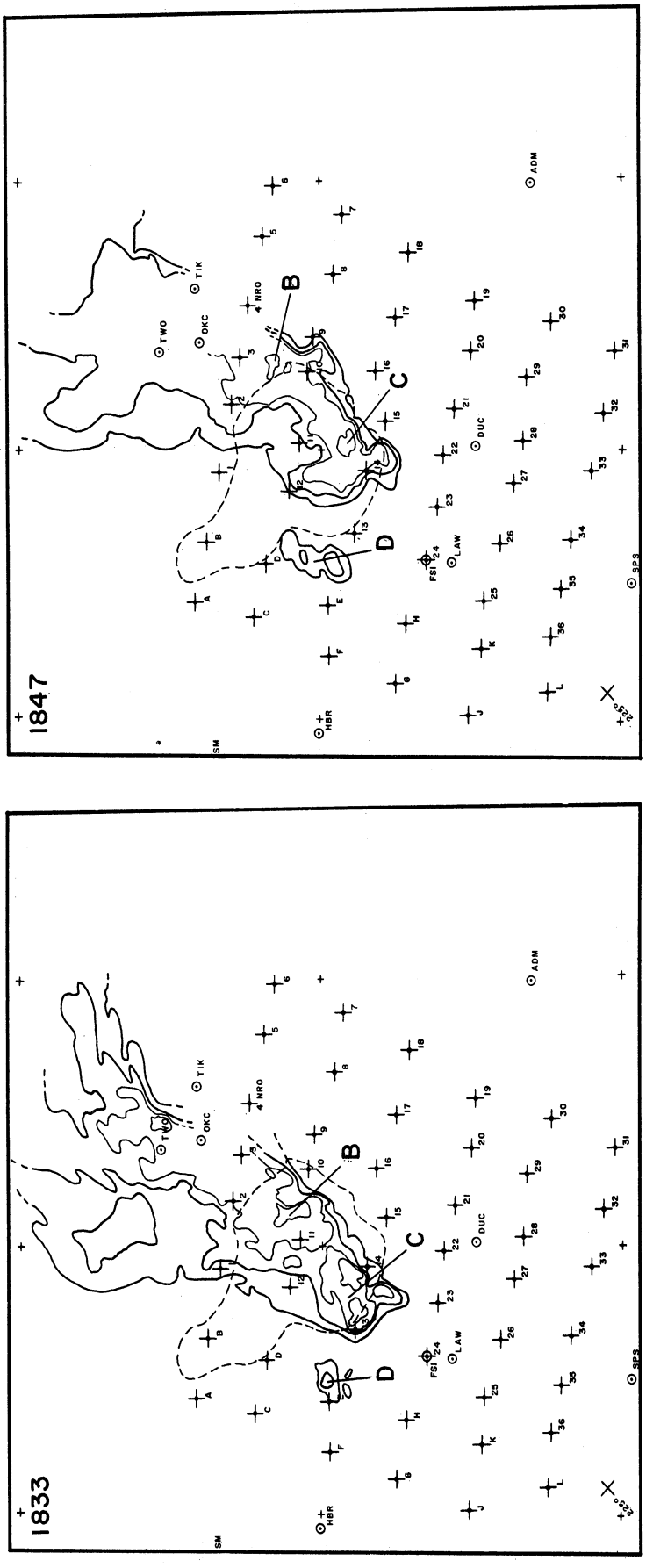

Figure 3.18 (Continued)

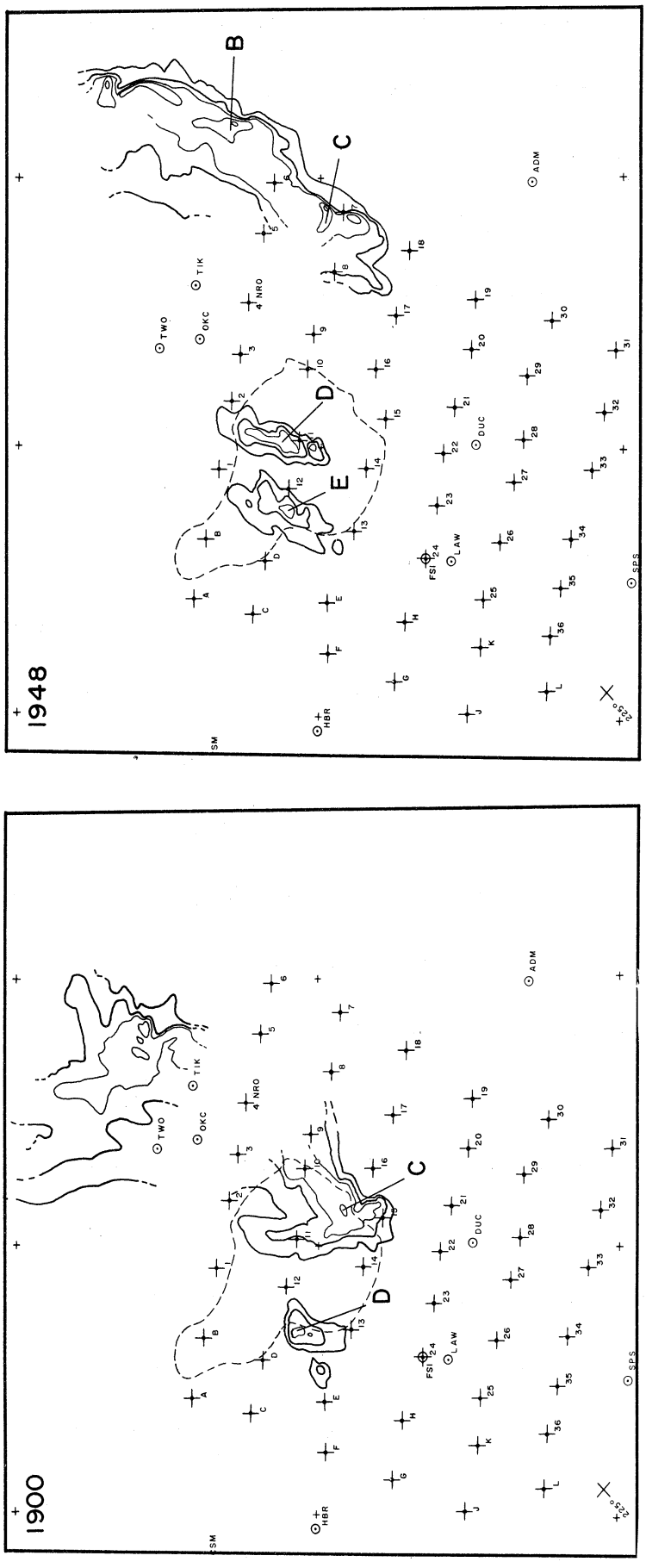

Figure 3.18 (Concluded)

squall line. Only light rain was experienced at station 11; however, it appears that some heavier showers associated with storm D passed both to our north and south.

The pressure mesoanalysis (Figure 3.19) for 1815, just after the rain began at station 11, shows the squall front already past and the high pressure center located to the WNW. Station 11 was in a region of large pressure gradient at that time. The location of the pressure system near the boundary of the mesonetwork makes it difficult to tell if a wake depression was present.

The sequence of rainfall rate maps, prepared from the ARS network data, is shown in Figure 3.20. The time of the first map is 1800, just as the intense core of storm B moved into the network. The "hook" configuration of the heavy rainfall is apparent here, even at the edge of the network, but this configuration was not apparent in the radar data. The second map shows that the center of the storm had completely entered the network at 1810. The intense core of the storm appears circular in shape, with two crescents of intense rain, oriented opposite each other on a NW-SE axis. It is clear, from examination of variation of rainfall rate at the individual rain gauges, that this area of maximum rainfall was undergoing cyclonic rotation as well as translation during this time. The following maps show this feature also, but in a less striking manner. The band of rain to the NW had diminished slightly in intensity but was still clearly present at 1820, as the dashed 90-mm/hr contour shows. Comparison of the maps at 1820 and 1830

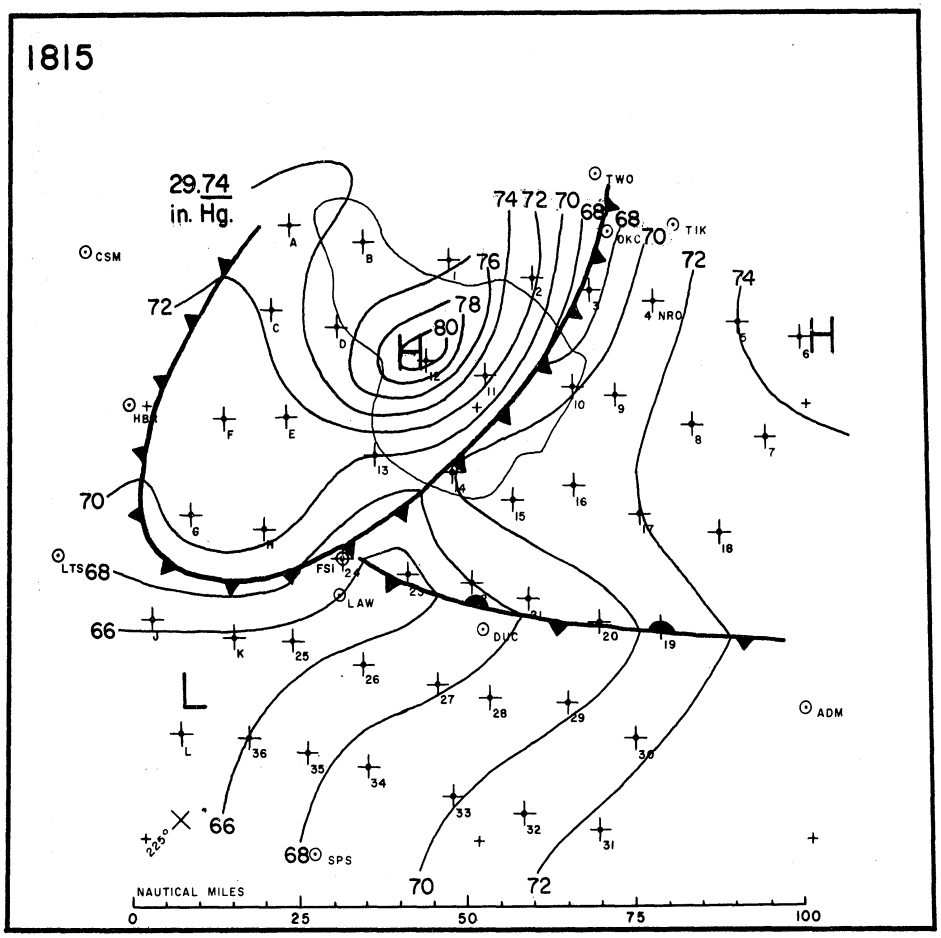

Figure 3.19. Pressure mesoanalysis for 1815, May 10, 1964. See legend, Figure 3.9.

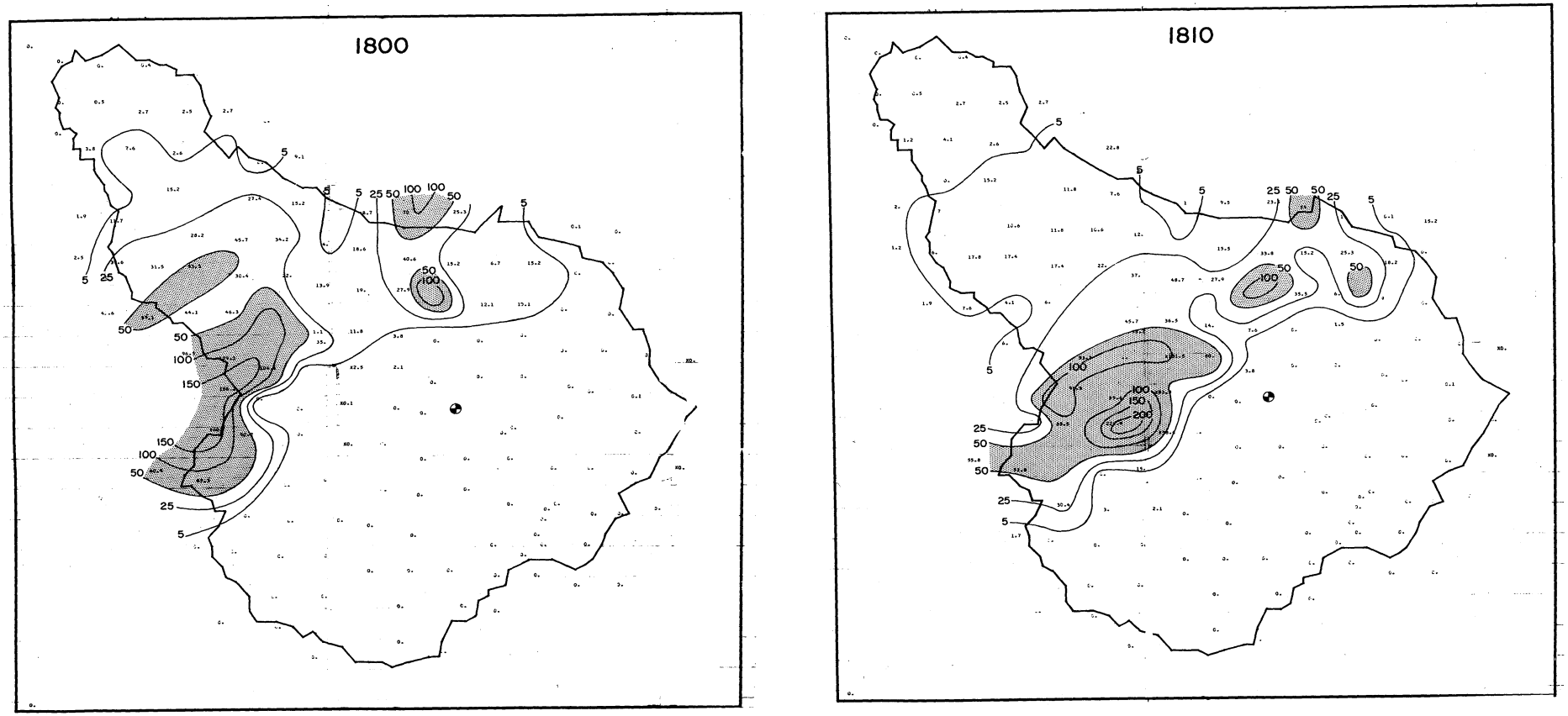

Figure 3.20. Rainfall rate sequence over ARS network, May 10, 1964. Units are mm/hr. See text for description.

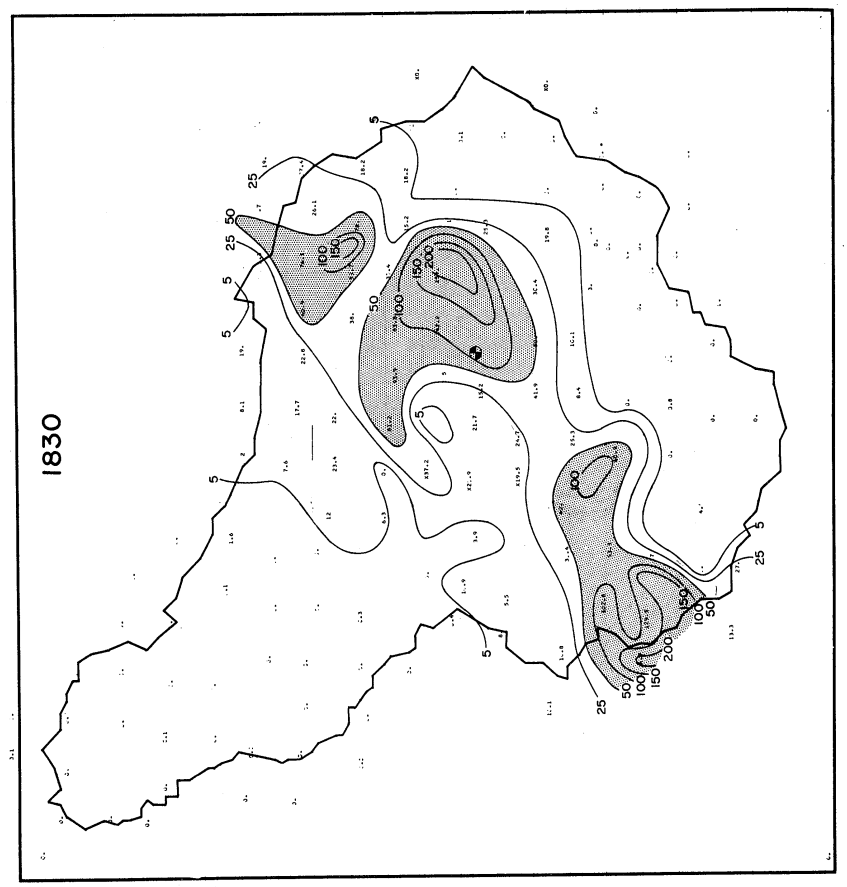

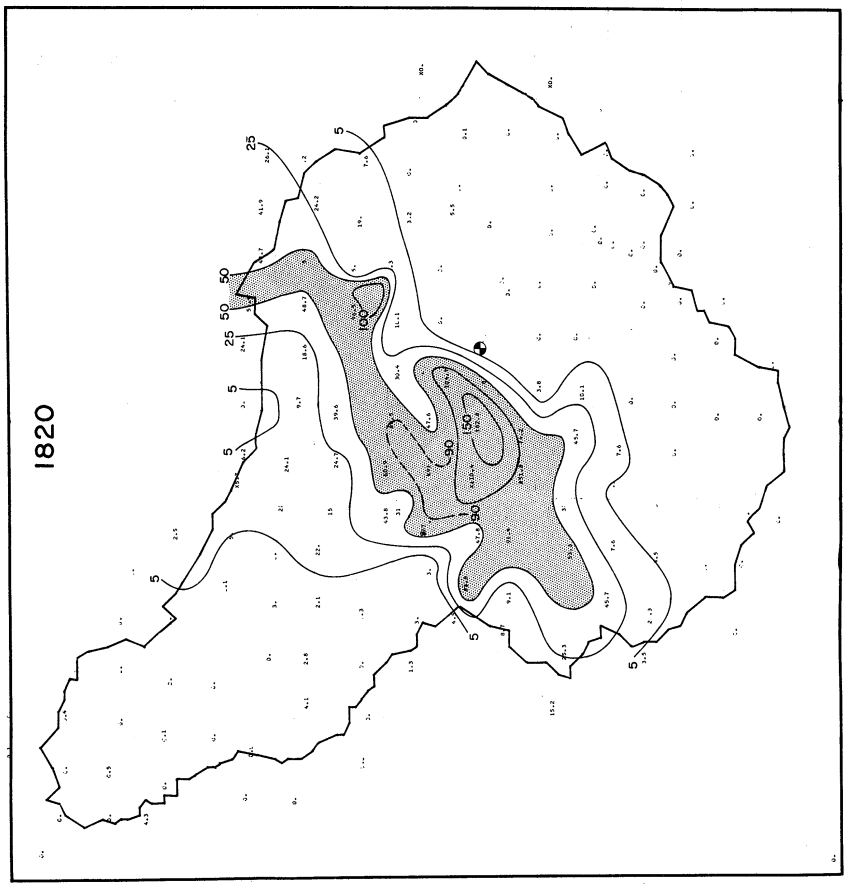

Figure 3.20 (Continued)

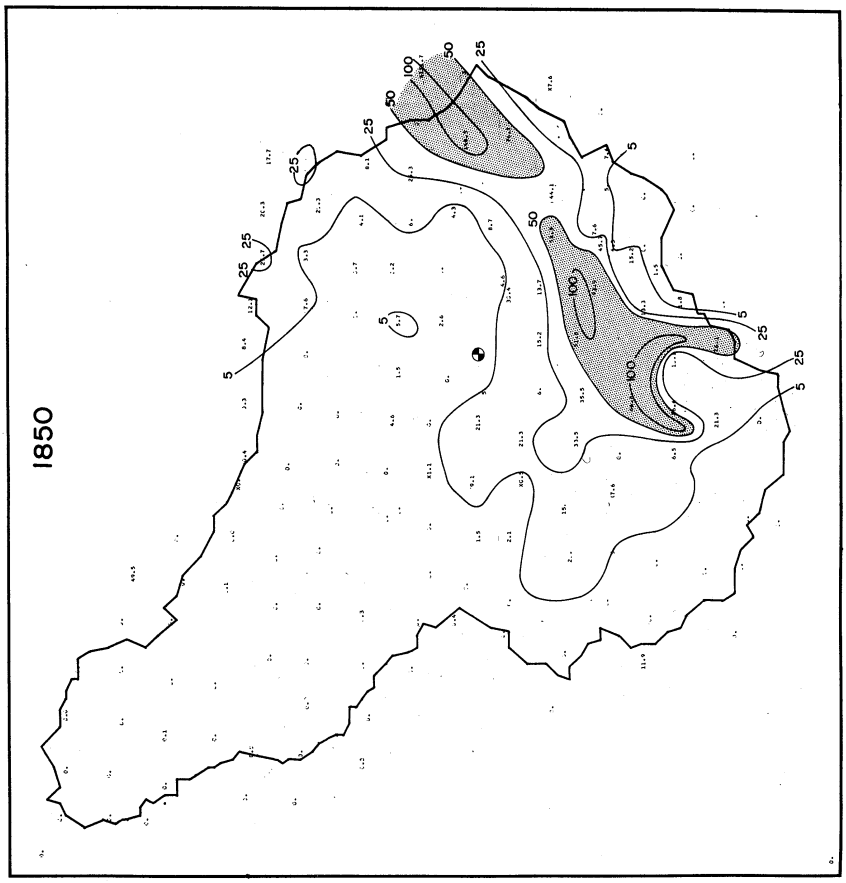

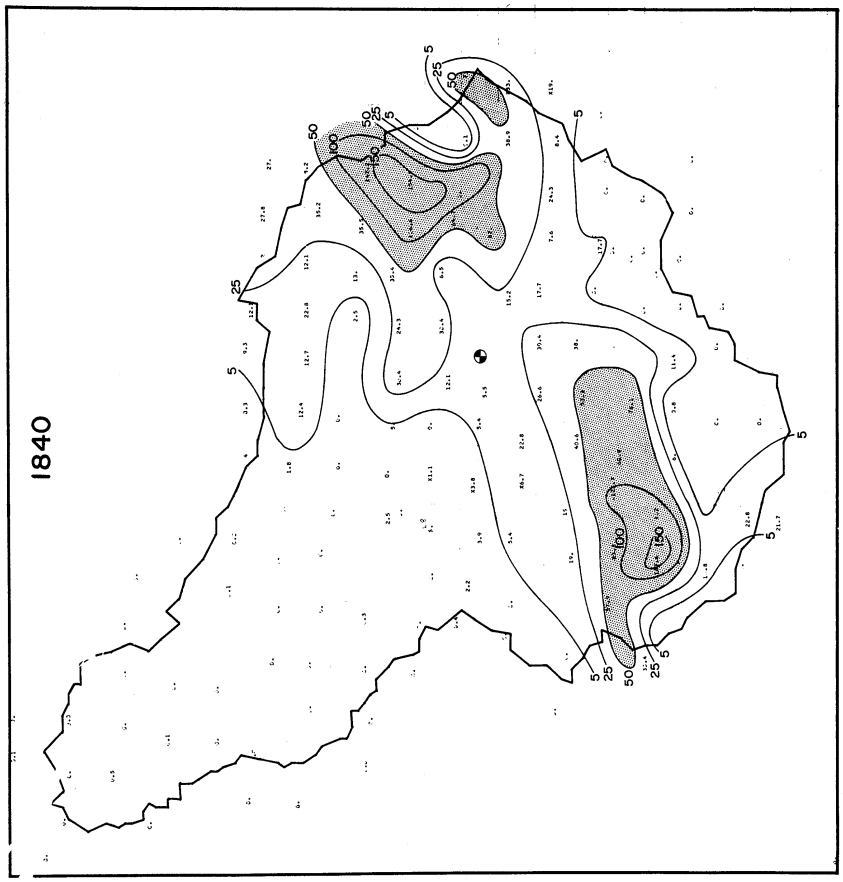

Figure 3.20 (Concluded)

shows that the most intense storm core passed over our station during this interval. This observation is in complete agreement with the rainfall rate observations at our station (Figure 3.13) and the radar data (Figure 3.18). Also evident from a comparison of these two maps is a sudden acceleration of the most intense core. It moved at least 10 miles during the 10-min interval, a speed of at least 60 mph. During the intervals 1800-1810 and 1810-1820 the speed was 50.4 and 44.8 mph, respectively. Cyclonic motion of the center of storm B is clear. This map also shows that storm C was beginning to enter the network at this time. Because the storm is at the edge of the network, the indicated extreme hook of this storm is less certain than that of storm B; however, it is one of the possible ways to analyse the limited data in the area. The 1840 map shows storm B about to leave the network. One interesting feature of storm B at this point is that the hook configuration had been reestablished, the new hook forming on the SE quadrant of the intensity center. One interpretation of the evolution of storm B is that the hook echo which was present when the storm entered the ARS network "closed itself off" by cyclonic turning around the updraft and generated a new hook from a new updraft, ahead of the intense rainfall. Eastward motion of storm C during the previous 10-min interval is clear, but determination of the intensity configuration is hindered by lack of data at the edge of the network. The final map (1850) shows storm B nearly out of the network and further movement of storm C. The

northward extension of storm C, which produced the small intensity maximum at 1900, is evident west of the station.

The squall line and the brief following shower produced the distribution of total rainfall shown in Figure 3.21. The distribution is remarkably uniform—between 20 and 35 mm—over most of the ARS network.

Pressure, temperature, and relative humidity variations at station 11 on May 10 are reproduced in Figure 3.22. The temperature and humidity graphs reflect the passage of the squall front at about 1800, both recording sudden decreases. A pressure jump occurred some minutes later at about the time rain began. The temperature curve shows a second discontinuity at about the time of the heavy rain burst, and a rapid increase of relative humidity began at the same time.

3.2.4 Summary

There are several important distinctions between the storm sampled on the 10th and that of the 9th. The one on the 10th produced only one major rain burst at station 11, and this burst came from the main storm center, which passed directly over the station. Furthermore, this center was clearly identifiable both on radar maps and on rainfall rate maps for a considerable time as it approached the station. In other words, a persistent circulation was involved here, in contrast to the situation on the 9th, when transient cells were involved.

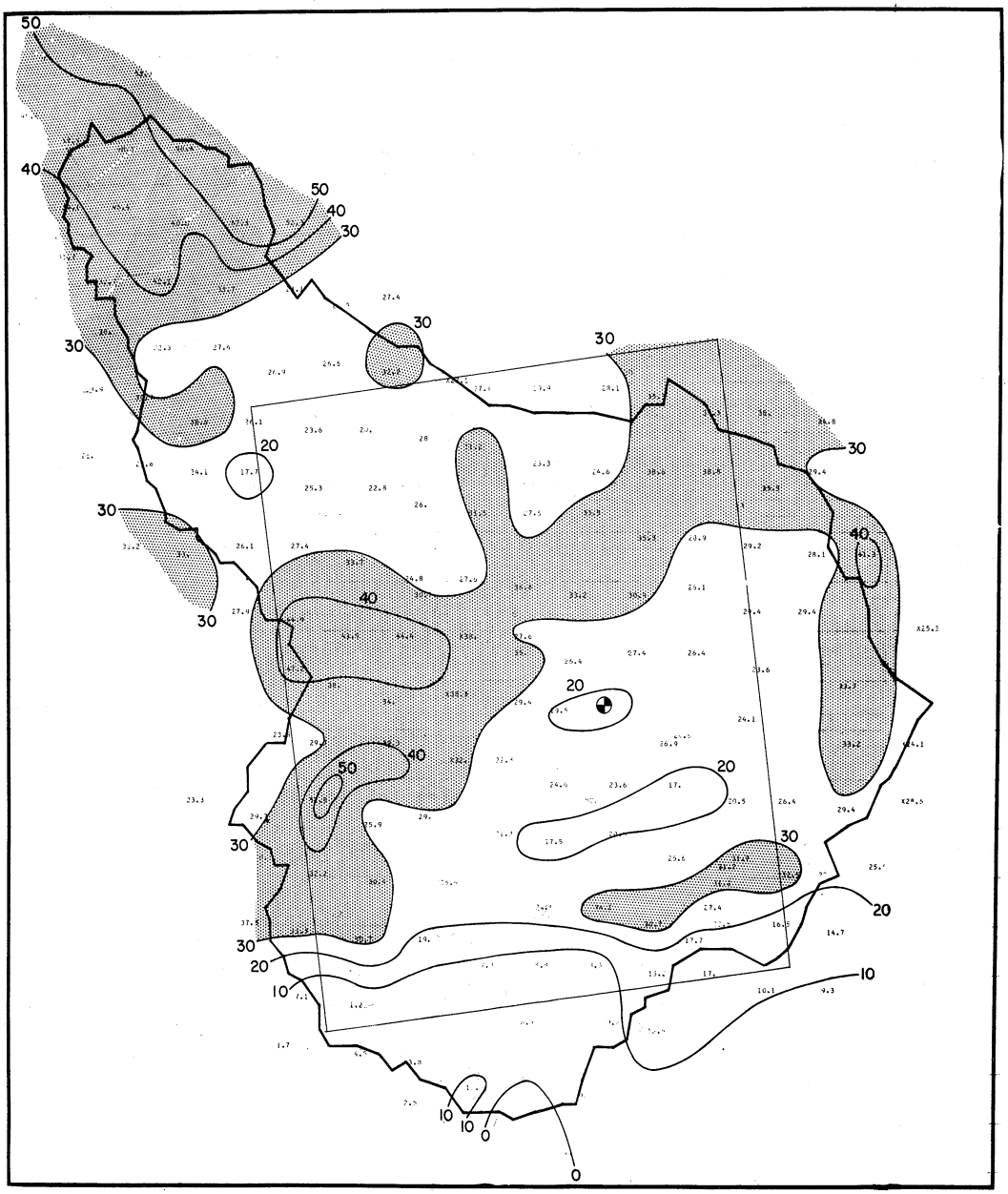

Figure 3.21. Total squall line rainfall over ARS network, May 10, 1964. Units are mm. The rectangle outlines the "test zone" in which depositions of water and radioactivity were measured.

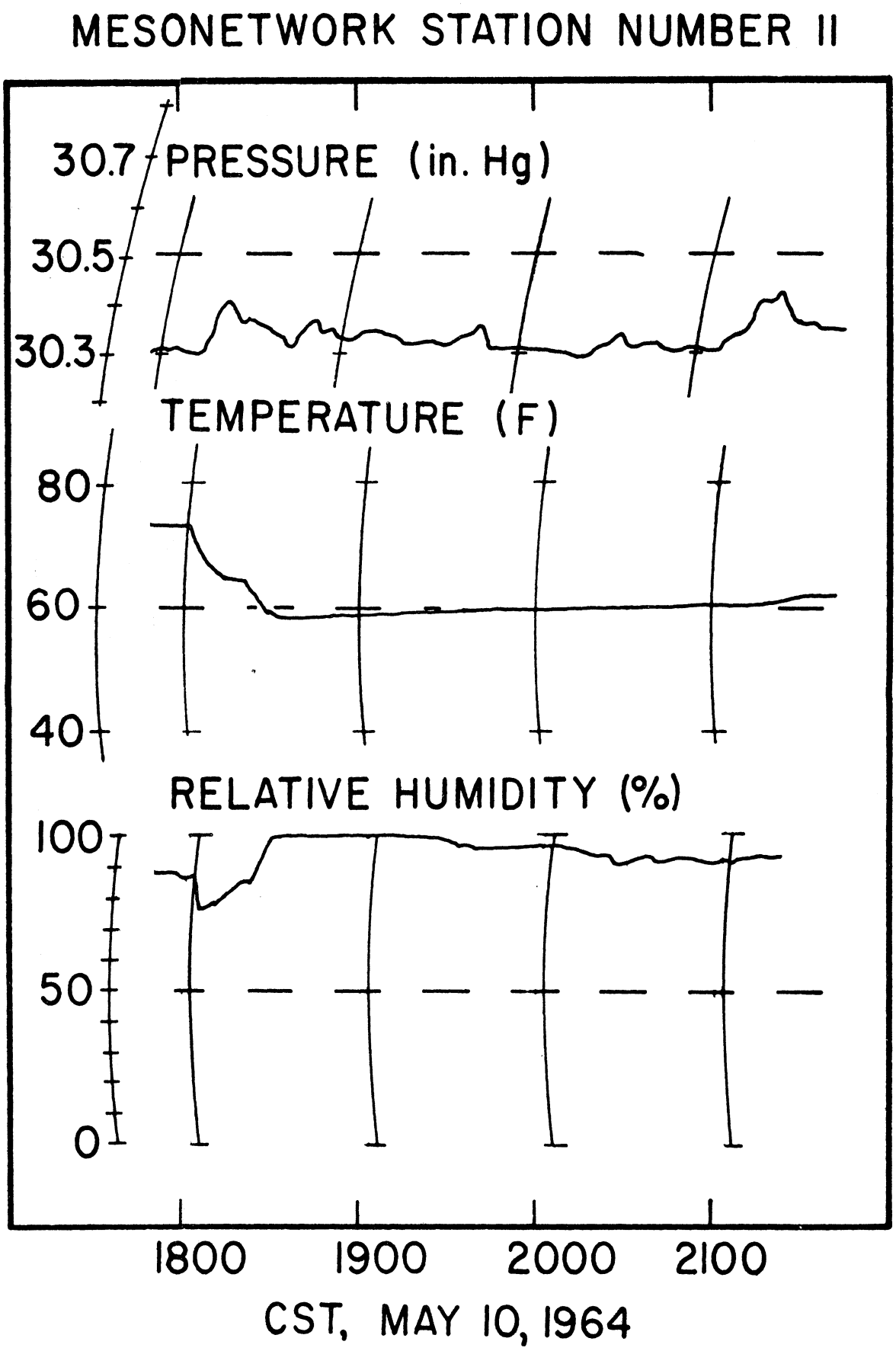

Figure 3.22. Variations of pressure, temperature, and relative humidity at mesonetwork station 11 on May 10, 1964.

For all these differences in the character of the two storms, the relationship between temporal variations of concentrations, deposition rates, and rainfall rate are not greatly different from those observed on the 9th. Again the three concentrations varied together and had the same relationship to the rainfall rate peak as on the 9th, as did the deposition rate. A significant difference between the two days is found, however, in the amplitude of the variations, those of the 9th being about 8 times greater.

The synoptic-scale features were very similar on the 10th to those on the 9th except that the pressure systems both aloft and at the surface were beginning to develop and move eastward on the 10th.

3.3 DISCUSSION OF THE DATA

The size distribution of airborne particles is an important factor with respect to the physical mechanism by which particles become attached to precipitation particles. The following paragraphs constitute a brief review of the size characteristics of the several classes of particles of interest in this study.

Three classes of particles are dealt with: non-volatile residue, fission product radioactivity, and plant pollen, the latter two categories being sub-classes of the first.

The non-volatile residue is made up of particles of all sizes which are capable of remaining airborne for periods of the order of one hour. Particles with diameters of $10^{-2}\mu$ and smaller have very short

lifetimes owing to their rapid rate of agglomeration with other particles. In the present context it must be considered that the upper size limit of the gross residue is at least 100μ diameter. Particles this large can easily be maintained aloft under unstable conditions.

Airborne plant pollens range in size from about 10μ to 100μ diameter. Those types identified in this study have a somewhat smaller range. Measured and literature values of sizes of the several types are given in Table B.2. (Also see photographs in Figure B.1.)

Shleien, Galvin, and Friend, (1965), using three filters in series concluded that particles having diameters less than 1.75μ contained at least 88% of the total fission-product gamma activity. The samples were collected in the spring of 1964. These authors conclude further that "long-lived fission-product activity in air at ground level is for the most part associated with airborne materials having the same diameter as particles prevalent in the surrounding air." Lockhart, et al. (1965), using a series of four filters, came to essentially the same conclusions based on sampling during 1963 and 1964. They found fission products in tropospheric air to be associated with particles having an average diameter between 0.3 and 1.1μ (assuming spherical particles of 1.8 g/cm^3 density). Shalmon (1964) determined the radioactivity associated with different sizes of ground-level airborne dust collected from April to September, 1963, and concluded that 90% of gross beta radioactivity was attached to particles larger than about 0.7μ diameter. Taken together, these three papers indicate that about 80%

of low-level airborne radioactivity was associated with particles between 0.5 and 1.75μ diameter. The sampling periods indicate that the results would apply to periods other than those during which atmospheric tests were carried out.

The size ranges of non-volatile residue, plant pollens, and gross beta (artificial) radioactivity are summarized in Figure 3.23, in which the size ranges in which the respective attachment mechanisms are effective are also included. By comparison of the two groups of size ranges, one may determine which attachment mechanisms are effective for the particles identified in this study.

Of the attachment mechanisms considered, only impaction and condensation appear to figure prominently in the attachment of the three classes of particles of present interest. Let us consider each contaminant separately.

The gross residue represents the largest size range and is therefore subject to several attachement mechanisms in different parts of the size spectrum. As Figure 3.23 shows, the smallest particles may be captured by the Brownian diffusion mechanism. However, the greatest mass is above the range of effectiveness of Brownian diffusive capture and should be scavenged by condensation and impaction. Impaction will be effective for all particles larger than 3μ diameter. Nucleating ability of particles is a function of their solubility, wettability, and size. All soluble particles larger than about 0.1μ will serve as condensation nuclei, and insoluble particles will do the same if their

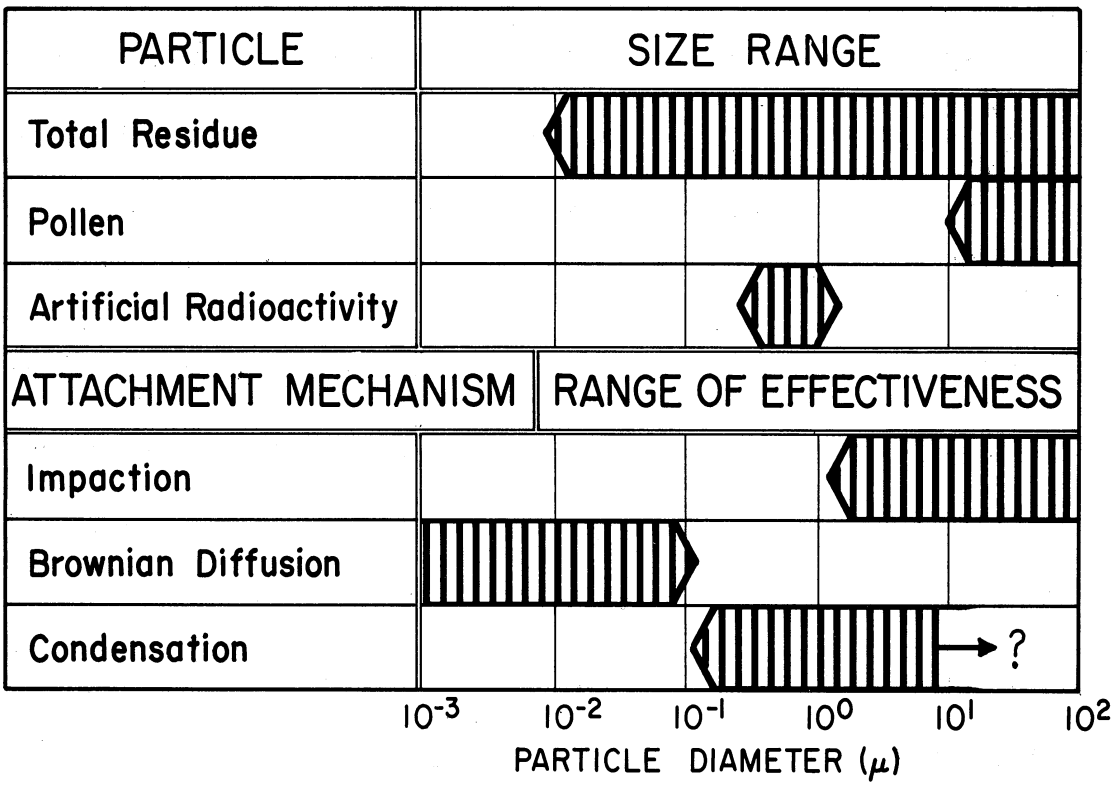

Figure 3.23. Schematic diagram showing attachment mechanisms of importance for the three classes of contaminants studied.

contact angle θ for water is very small (McDonald, 1963). Without a detailed knowledge of the size spectrum and chemical nature of the gross residue, it is impossible to assess the relative contributions of these three scavenging mechanisms.

The size range of the plant pollens is such that raindrops collect these particles very efficiently by impaction. However it is important to determine whether this is an exclusive mechanism. In particular, it is possible that the pollen grains could act as condensation nuclei. As discussed in Chapter 1, insoluble particles, such as pollen are thought to be, must be highly wettable (θ near 0°) in order to serve as condensation nuclei, at least in the absence of surface roughness effects (McDonald, 1963). That this may be the case, at least for some types of pollen, may be inferred from the qualitative results of McDonald (1964). He observed microscopically that several types of pollen, when brought into contact with a water surface, behaved in much the same manner as the fully wettable ($\theta = 0°$) grains of silicate which were also tested. That is, the particles moved rapidly across the air-water interface and continued into the water for a distance of about 100μ. This suggests that some pollens may serve as condensation nuclei, purely as a result of the wettability of their surface. In addition, surface features such as pores, furrows, and reticulations may serve as preferred nucleation sites.

The size of the particles carrying most of the artificial radioactivity would seem to limit the possible attachment mechanisms to con-

densation, judging from the position of the theoretical lower limit of the impaction mechanism, as indicated in Figure 3.23. However, several investigators (Reiter, 1961; Goldsmith, et al., 1963; Itagaki and Koenuma, 1962) noting an increase in the concentration of fallout radioactivity in rain as it approached the earth's surface, attributed at least part of the effect to the impaction process. Owing to the proximity of some of these experiments to periods of active bomb testing, radioactive particles larger than 3μ diameter would be expected in significant quantities in the atmosphere. Such particles could have been collected by impaction. However, it appears that not enough attention was paid by these investigators to the effect of evaporation of the raindrops which also serves to increase concentrations of non-volatile matter in rain. For the period of the rain collections reported here, the size spectrum for particles bearing artificial radioactivity given in Figure 3.23 should hold, and there is no reason to expect that attachment could occur in any manner other than by condensation.

It may then be said in summary that the particles bearing artificial radioactivity are expected to be collected almost exclusively through their use as condensation nuclei. The pollens should be collected mainly by impaction, but may possibly serve as condensation nuclei also. The gross residue will be collected by both impaction and condensation, and probably also by Brownian diffusive capture.

Specification of the attachment mechanism(s) of the respective particles has important consequences regarding the explanation of observed time variations of their concentrations. The particles bearing artificial radioactivity offer a convenient starting point because theoretically they must be collected as condensation nuclei. These particles fall into that region of the aerosol size spectrum between 0.1 and 1.0μ, in which particles are too large for efficient removal from the atmosphere by Brownian diffusive capture and too small for capture by impaction. Even though capture by condensation is effective on these particles, it seems likely that they may have a longer residence time in the atmosphere than some larger and smaller particles because of their relative resistance to scavenging. Perhaps this is the reason that they contain most of the artificial radioactivity. Because they are present in the atmosphere for a longer time, they have a chance of collecting by agglomeration the radioactive particles, which leave the stratosphere about 1 order of magnitude smaller in size. The same mechanism tends to make these particles "mixed nuclei," i.e., agglomerates of both soluble and insoluble particles and effectively upgrades the sizes of the basically soluble constituents. Such particles act essentially as large soluble particles with respect to nucleation and are thus readily nucleated.

On the assumption that the radioactive particles are collected by condensation, it follows that there should be little spatial variability of radioactivity concentration within a convective cloud. Thus is would

appear that concentration variations observed at the ground must come about as a result of variations in the mass of water lost from the raindrops by evaporation. If one assumes that the lowest concentration observed at the ground is representative of the concentration in the cloud, i.e., that that sample underwent no evaporation, the relative evaporation loss required to produce other observed concentrations may be computed. For example if one assumes the minimum concentration of radioactivity observed during the rain of May 9 to represent the concentration in the cloud water, evaporation of over 90% of the water present at the cloud base is required to produce the concentration observed in the first sample. Computations of evaporation, based on measured ambient temperature and humidity profiles and raindrop-size distributions at the ground, are necessary to test such a hypothesis. Such computations are presented in Chapter 4.

The fact that observed amplitudes of the concentrations of pollens and total residue are greater than that of the radioactivity indicates that concentrations of these particles cannot be controlled exclusively by evaporation. (If they were, the amplitudes would be equal.) This is not unexpected because the pollens are all large enough to be collected by impaction, and many of the residue particles are also.

The observation of in-phase variations of radioactivity, pollen, and residue concentrations and similar variations of their deposition rates, as well as that of water, suggest qualitatively that all are removed from the same air, namely low-altitude air. Qualitative support

for such a mechanism is gained also by consideration of the requirements for attachment of particles to the rain elements. Attachment of particles to cloud and rain elements is favored by the intimate association of the particles with large amounts of water or water vapor. Input via the well-known convective updraft provides such an association as well as a transport of the particles to the raining core of a storm in a simple and direct way. Conversely, input by mixing with the environment at high altitudes provides association with only the small amounts of water and ice available in the peripheral parts of the clouds. Neither can high-altitude input provide access to the raining core since divergence away from the center of the storm is characteristic of the tops of convective storms. Quantitative tests of the low-altitude input hypothesis are presented in Chapter 4.

CHAPTER 4

QUANTITATIVE APPLICATIONS OF THE DATA

4.1 INTRODUCTION

A likely contributor to past differences of opinion concerning rain scavenging processes is the fact that the available data permitted the formulation of only qualitative relationships. Quantitative evidence was not available, owing to the lack of comprehensive mesometeorological and radiochemical data. The sets of data presented in Chapter 3 are of sufficient quality to permit, at the very least, a beginning toward the quantification of some of the relevant processes. It is to be emphasized, however, that reliable conclusions result only from reliable data; analytical techniques must be considered and applied with extreme care to insure accurate and consistent data.

Based upon the data presented earlier, this chapter is addressed to two important questions:

1. Can input of airborne radioactivity from low altitudes account for observed deposition of radioactivity by a convective storm?
2. Consistent with the answer to (1), can observed variations of contaminant concentrations be explained quantitatively?

4.2 COMPARISON OF SCAVENGING DATA AT CLOSELY-SPACED STATIONS

On several days during May, 1964, rain collections were made simultaneously at the University of Oklahoma automatic station 5, located at WB11 (Figure A.1) and at The University of Michigan station. A distance of approximately 0.25 mi (0.4 km) separates the two sites. The existence of sets of radioactivity concentrations in sequential rain samples collected at neighboring sites suggests a comparison of the data. Such a comparison is valuable for checking the accuracy of the respective analysis procedures. In addition, it may serve to bring out possible small-scale variations in storm structure and/or deposition or concentration. This section is devoted to comparisons of data collected on May 9 and 10.

Beta radioactivity concentrations and rainfall rates at the two stations are compared in Figure 4.1. Comparison of the rainfall rate variations shows that two rain bursts occurred at each station, and that in neither instance did the peaks occur together. The precise times of the maximum rates at the automatic sampler site are not known because of the relatively poor resolution of the weighing-type rain gauge from which the WB11 rates were computed. Nevertheless, it seems apparent that the respective peaks were separated in time by several minutes. The variations of concentration at the two stations are roughly in phase during the initial decrease and following increase, but the subsequent decrease at the automatic station lags that of our station, just as the corresponding rainfall rate peak does. At each

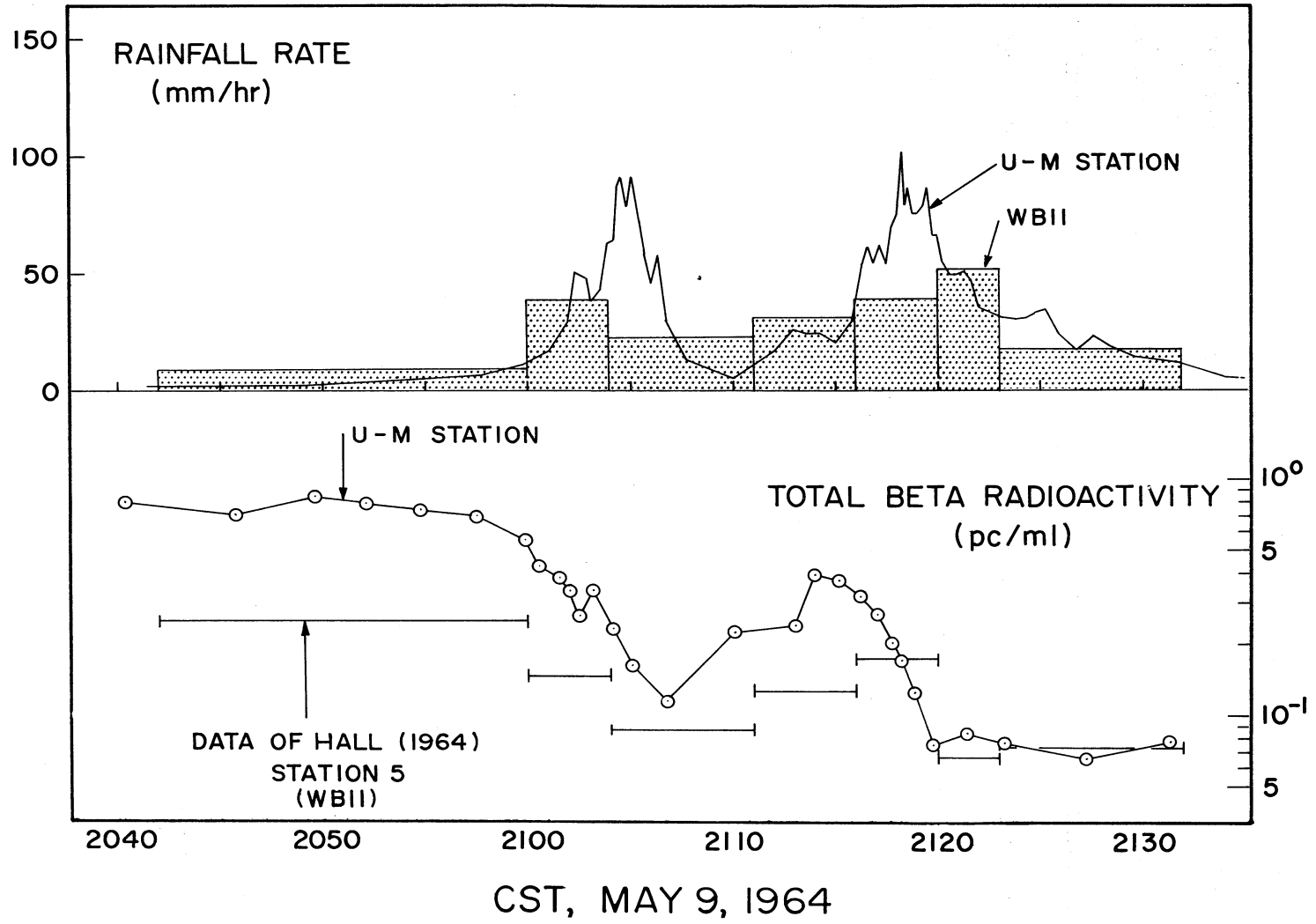

Figure 4.1. Comparative radioactivity concentrations and rainfall rates at nearby stations.

station, the frequently observed pattern of concentration change occurred during both bursts; namely, the maximum was slightly ahead of the rate peak and was followed by a rapid decrease of concentration, which ended in a minimum slightly after the rate peak. Two aspects of the comparison give cause for concern. The amplitude of the variations at the automatic station are considerably less than at our station. Qualitatively, this is to be expected, because of the longer periods required to collect each sample. Further discussion of this point is given later. The second, and more serious, aspect is that there appears to be a significant difference in the absolute value of the concentrations. For example, during the period between 2042 and 2100, concentrations at The University of Michigan station were higher by a factor of over 2.5. The best comparison, however, is between depositions per unit area at the two stations. These are given in Table 4.1. On May 9, deposition of radioactivity, as computed from concentration measurements, and corrected for rainfall differences, was 3.18 times greater at our station.

The comparative concentration data for May 10 are given in Figure 4.2. This time there is a clear time displacement of the rainfall rate peaks at the respective stations. Perhaps two minutes of this difference could be attributed to timing errors, but this would still not eliminate it. Reference to the configuration and direction of movement of the heavy rain area in Figure 3.20 shows that a time difference

TABLE 4.1

COMPARISON OF DEPOSITIONS AT COLLECTION SITES WHICH ARE 0.25 MILE APART

Date (1964)	Manned Station	Automatic Sampler No. 5	Ratio
	Beta Radioactivity Deposition During Squall Line (pc/m^2)		
5/9	5536	1622	--
5/10	5311	1779	--
	Total Rainfall During Squall Line (mm)		
5/9	21.8	20.3	--
5/10	18.3	18.3	--
	Radioactivity Deposition for Equal Rainfall Amounts (pc/m^2)		
5/9	5536	1742	3.18
5/10	5311	1779	2.98

of several minutes between the two sites is not unlikely. The automatic station, being located north and slightly west of ours, would be expected to have received heavy rain first.

Comparison of the concentration variations shows that they are not at all alike at the respective stations. At each, the absence of a substantial drop in concentration at the beginning of the heavy rain is notable. A nominal decrease was observed at our station, but none at all occurred at the automatic station. In this case the amplitudes of the respective concentration variations are about equal, but comparison of deposition (Table 4.1) again shows a significant difference, this time with equal rainfall.

Comparison of these data should be made with due regard to certain differences which should be expected owing to different sample collec-

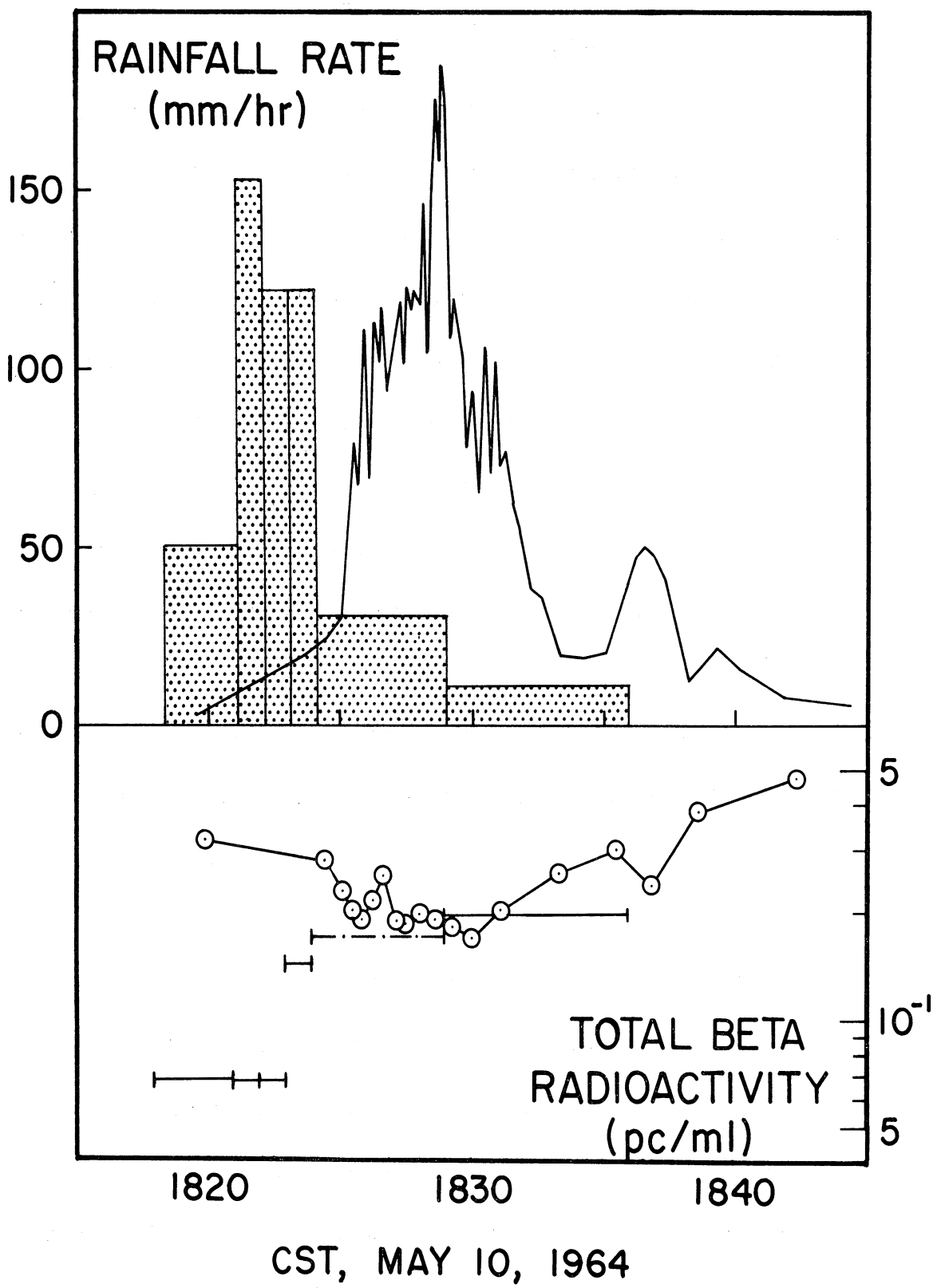

Figure 4.2. Comparative radioactivity concentrations and rainfall rates at nearby stations. Identification of curves is the same as in Figure 4.1.

tions periods, or "averaging times" (Pasquill, 1962). Collection periods at the manned station were of the order of 1 min, whereas those of the automatic station varied between about 1 min and 10 min or more. During periods when collection periods at the respective stations were dissimilar, one should expect that amplitudes would be reduced in the case of the larger averaging times. That this amplitude reduction can be substantial is demonstrated in the following example. Consider a sinusoidal variation with a period of 15 min. This is roughly the period observed on May 9. Whereas a 1-min averaging time retains 98% of the amplitude of the original variation, a 5-min averaging time retains only 80%. The amplitude of the automatic sampler data is less than 50% that of our data; thus it is likely that factors other than different averaging times must be involved. Furthermore, differences in averaging time cannot account for the discrepancy in deposition.

It is very unlikely that concentration and deposition differences of the magnitudes observed would occur within a quarter of a mile. A more likely explanation is that the sample handling procedures used by Hall (1965) were not adequate to obtain an accurate assessment of the radioactivity in the rain samples. The procedure used (Hall and Klehr, 1963) was to remove an aliquot of 300 ml from each sample, after shaking to suspend insoluble matter. After removal of insoluble particles by filtration, the water was evaporated and the soluble residue

deposited in a planchet and counted for radioactivity. The insoluble residue was counted separately.

This method is likely to leave significant amounts of radioactivity in the sample bottle. Our analysts report that up to 80% of the activity from a rain sample may be left attached to the walls of the sample bottle unless careful measures are taken; these may consist of adding carrier to prevent sorption on walls and/or scrubbing with acids to remove attached material.

There is a tendency for the discrepancy in radioactivity concentrations to be greatest at times of high concentrations of both radioactivity and residue at the manned station. (Compare Figures 4.1 and 4.2 with 3.3 and 3.13, respectively.) High concentrations of total residue at the beginning of showers indicate large amounts of insoluble matter which can adhere strongly to bottle walls. This is evidence that the observed deficiencies in radioactivity arose because the aliquots were not representative of their respective samples. Additional evidence is found in comparing the measurements of beta radioactivity in rain at the U.S. Public Health Service Radiation Surveillance Network Station in Oklahoma City. Between 1700, May 10, and 1400, May 11, 37.5 mm of rain deposited 14,500 pc/m^2. The equivalent deposition for 18.3 mm (received both at WB11 and at our station), using direct proportionality, is 7070 pc/m^2. Although comparison of data at sites separated by about 65 km is somewhat risky, the differences in magnitude are such as to

suggest that the concentrations from the automatic sampler network are too low.

4.3 MASS BUDGET ANALYSIS OF THE STORM OF MAY 10, 1964

An obvious test of the hypothesis that most of the deposited activity enters a convective storm from low levels consists in evaluating the low-level input and the total deposition and comparing the two results. Evaluation of mass input was made using the kinematic model of Newton and Fankhauser (1964). The volume of air intercepted by the storm was computed layer by layer from the storm motion and the vertical distribution of wind velocity. Water input was computed by integrating the product of air input and water vapor mixing ratio, q, over the moist layer. The moist layer is characterized by high values of q and extends from the surface to about 600 or 700 mb, at which point q begins to decrease rapidly with height. Radioactivity input in the same layer was computed as the product of the total air input and the radioactivity mixing ratio, assumed to be constant with height. Depositions of water and radioactivity were computed from sampling networks within a rectangular "test zone" at the surface.

To collect the data necessary to evaluate input and deposition, it is necessary not only to have a comprehensive program for collection of meteorological and scavenging data, but also to have all component systems operational when the storm occurs. Furthermore, it is desirable that the storm center pass through the center of the rain-

gauge and rain-sampling networks. Data collected on May 10, 1964, show that the storm which occurred on that day is particularly well-suited to a mass budget analysis. The center of one of the severe storms which comprised the squall line on that day passed directly over the ARS network. The availability of several soundings at Fort Sill (FSI) in the warm moist air ahead of the storm and data on the concentration of radioactivity in air from the U.S. Public Health Service (1964) permits computation of the input of radioactivity at low levels. Data on deposited radioactivity was available from the University of Oklahoma sampling network (Hall, 1965). The ARS rain-gauge network provided data on water deposition. Evaluations of water input and deposition provide a standard against which the radioactivity budget may be compared.

4.3.1 Budget Model

Input and deposition of water and radioactivity were evaluated with respect to a surface test zone. This zone is defined so that its north and south boundaries are parallel to the mean storm track over the network, as determined from radar data. The test zone has dimensions of 21.8 x 26.9 n mi (582 square n mi) and is shown in Figure 3.21.

Deposition of water in the test zone was evaluated by planimeter measurement of areas on the map of total squall line rainfall shown in Figure 3.21. Radioactivity deposition was evaluated similarly from an isopleth analysis of deposition over the University of Oklahoma sampling network. The locations of the automatic samplers are shown in Figure 4.5.

Input rates of radioactivity and of moisture to the storm were computed from soundings ahead of the squall line using a procedure adapted from Newton and Fankhauser (1964), as follows. In unit time, the mass of any atmospheric constituent intercepted by the storm between pressure levels p_o and p_1 is

$$M \simeq \frac{D}{g} \int_{p_o}^{p_1} V\, q\, dp$$

where V is the speed of the air relative to the moving storm, D is the diameter of the (circular) storm, q is the mixing ratio of the constituent in air, p is pressure, and g is acceleration due to gravity. In practice, M was computed and summed over discrete layers from the surface to the top of the moist layer using the relation

$$M \simeq \frac{D}{g} \sum_{i=1}^{n} \bar{V}_i\, \bar{q}_i\, \Delta p_i$$

where i is the layer index and n is the number of layers in the moist layer. The presence of a bar over a parameter means that its mean value in the layer is used. To obtain the total input in the moist layer, M was multiplied by the time required for the storm to pass over the test zone. Total inputs of water and beta radioactivity in the moist layer were computed and compared against the respective depositions.

4.3.2 Results

Input evaluations were made for D equal to the dimension of the test zone normal to storm velocity, i.e., D = 26.9 n mi. Except for

the lowest layer, which extended from the surface to 950 mb, a constant pressure interval of $\Delta p_i = 50$ mb was used. The $\bar{V}_i$ were computed by subtracting the mean storm velocity from the mean velocity in each layer, i.e., from one-half of the vector sum of the winds at top and bottom of the layer. The mixing ratio of beta radioactivity in air was computed from data on the activity per unit volume of air, as determined from 24-hr filter samples. Estimated mean pressure and temperature for the 24-hr period were used to convert activity per unit volume to the activity mixing ratio. Because only 24-hr average measurements were available, it was assumed that the mixing ratio was uniformly distributed in time and space. The data on concentrations of radioactivity in air relevant to the choice of a representative value are given in Table 4.2. Because of a motor failure at the Oklahoma City

TABLE 4.2

CONCENTRATIONS OF TOTAL BETA RADIOACTIVITY IN AIR

Location	Time of End of Sample, CST, May, 1964		Length of Sample (hr)	Concentration (pc/m^3)
	Day	Hour (CST)		
Ponca City	10	1200	24	1.50
Little Rock	10	0900	24	1.52
Ponca City	11	1000	22	1.63

sampling site, the closest site was Ponca City, Oklahoma. Little Rock, being upwind (surface wind) of central Oklahoma, would have sampled the relevant air on the previous day. The table indicates that the nearest value on the day of sampling (Ponca City sample ended 1000 on May 11) is 1.63 pc/m^3. However, to be conservative with respect to the hypothesis of a low-level input, the lowest value, 1.50 pc/m^3, was selected. Using a mean density of 1.14 kg/m^3, computed from a mean station pressure of 969 mb and a temperature of 20.5 C, approximately the average conditions at Ponca City during the sample collection, a mixing ratio of 1.32 pc/kg is obtained.

Input rates of radioactivity and water in the layer from the surface to 650 mb were evaluated from the FSI soundings at 1200, 1500, and 1700, and a space extrapolation to the beginning of the storm at FSI (1800) was made. The results are shown in Figure 4.3. As indicated, input rates of 4.3×10^9 pc/sec and 3.9×10^{10} g/sec were chosen for radioactivity and water, respectively. The input rate chosen for radioactivity represents an extrapolation of the values computed for 1500 and 1700, both of which were less than that computed for 1200. It was felt that the 1200 value could be ignored in the extrapolation because of its remoteness from the time of the storm. At worst, by ignoring the 1200 value we tend to be conservative with respect to the hypothesis. The choice of 650 mb as the upper boundary of the moist layer was based primarily upon Figure 4.4 which shows the vertical distribution of input

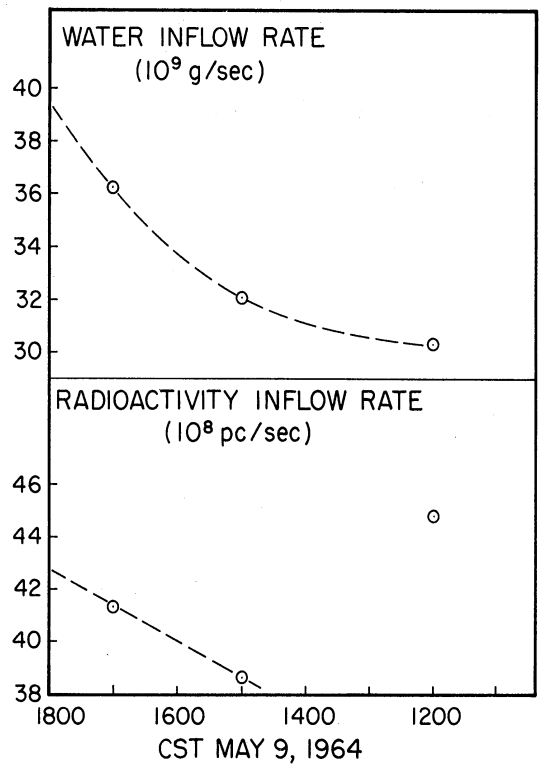

Figure 4.3. Time extrapolation of input rates of water and radioactivity computed from FSI soundings.

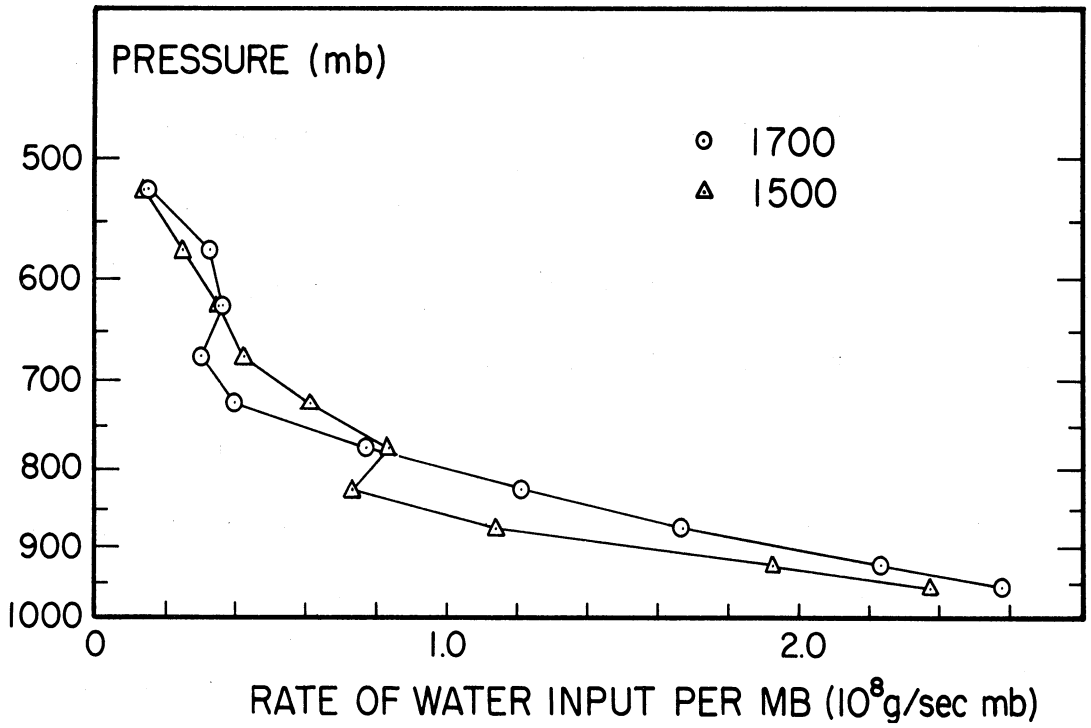

Figure 4.4. Vertical distribution of water input rate on May 9, 1964, at FSI.

rate of water per mb. It may be seen that nearly all of the water input must have occurred below 650 mb at both 1500 and 1700. At the mean storm speed of 19.7 m/sec, it took the storm 2.07×10^3 sec to cross the test zone. During this time a total of 8.9×10^{12} pc of radioactivity and 8.1×10^{13} g of water were intercepted by the storm.

Total deposition of radioactivity in the test zone was evaluated from isopleth analyses of the deposition pattern in the zone, based on deposition at 10 sites. Because such analyses are highly subjective, especially in view of the relatively few data points, several analyses were evaluated. The four analyses are shown in Figure 4.5, along with the evaluated deposition, d, of each. The deposition value $d = 3.38 \times 10^{12}$ pc obtained from analysis IV is considered to be the maximum which is consistent with the observations. Although in general deposition is correlated with rainfall, attempts to improve the analysis of deposition by reference to rainfall patterns were not successful owing to the absence of a systematic relationship between rainfall and deposition at the 10 data sites. The agreement in computed deposition from the four analyses of Figure 4.5 is striking and lends confidence that the deposition cannot have been greatly different from the values determined from these analyses. One additional factor must be considered, however. The comparison of our data with the automatic sampler data, which was discussed above, indicates that deposition estimated from the automatic sampler data may be too low. The question of how much too low can only be answered roughly, from comparison of the available data on

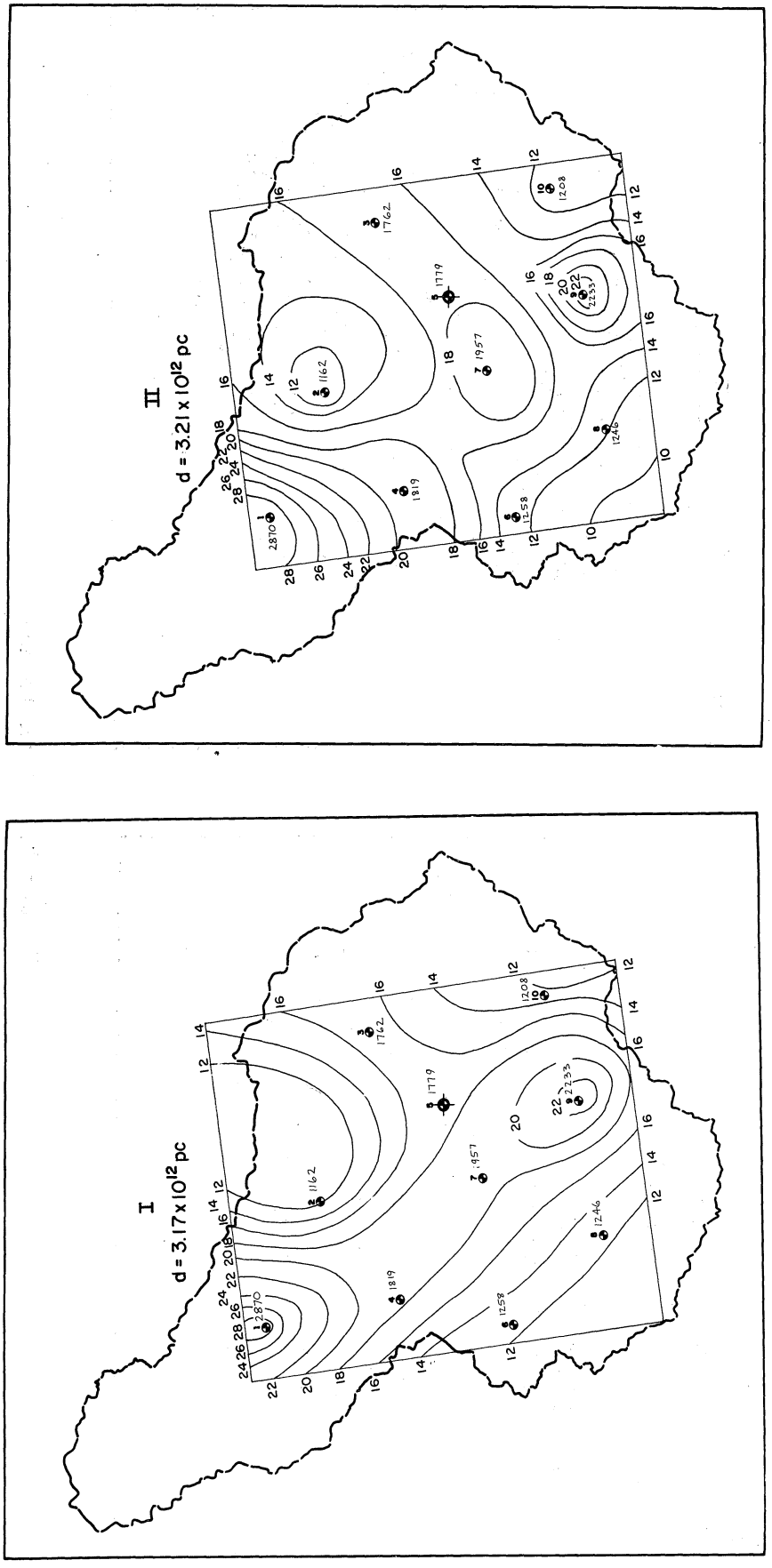

Figure 4.5. Comparison of d for different analyses of the deposition pattern in the test zone from the squall line on May 10, 1964.

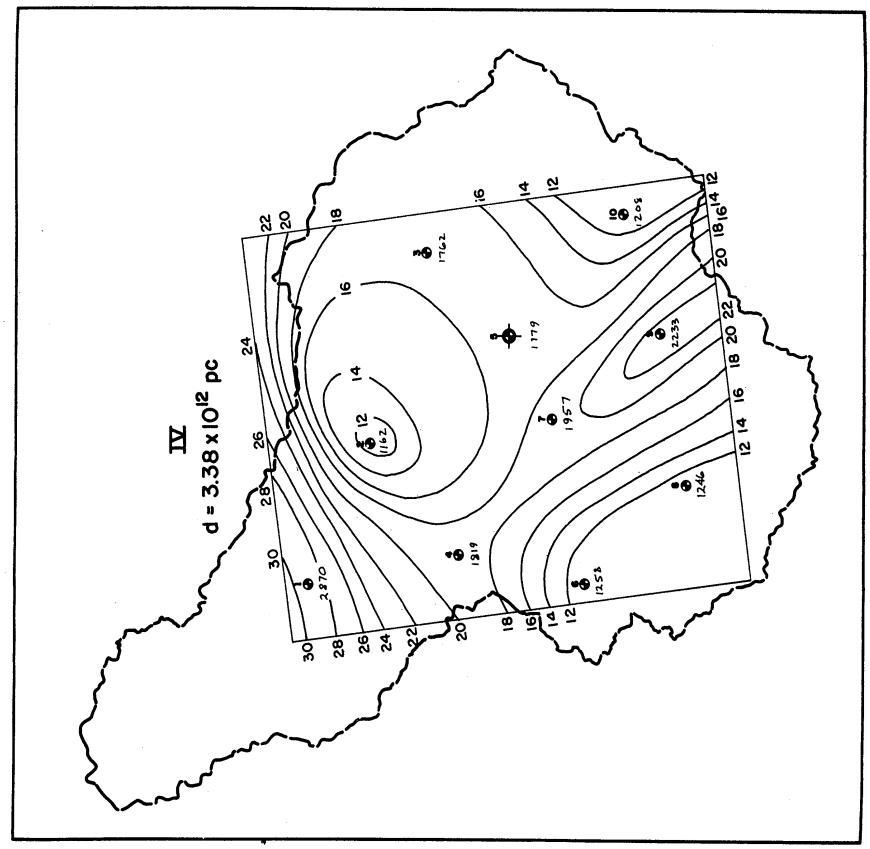

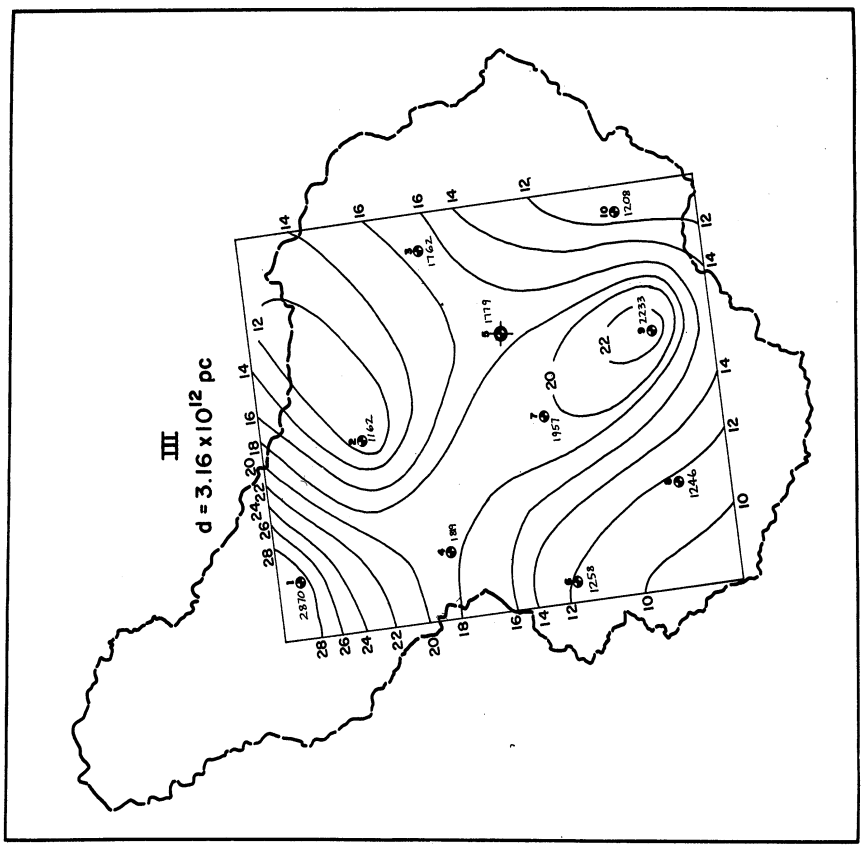

Figure 4.5 (Concluded)

total deposition at the respective adjacent stations. The total depositions (during the squall lines only) on May 9 and 10 are compared in Table 4.1. Based on a correction factor of 3.1, which is the average of the deposition ratios on May 9 and 10, the total deposition in the test zone from the squall line on May 10 is estimated to be 10.5×10^{12} pc. Water deposition was 5.42×10^{13} g.

A summary of estimated inputs and depositions is given in Table 4.3, which indicates that about 67% of the water which entered the storm was deposited as rain. Present evidence indicates that this is a bit high; a precipitation efficiency of 50% is perhaps more reasonable (Newton and Fankhauser, 1964). If both water and radioactivity inputs are adjusted upward by the same factor, such that water input is twice its deposition (50% efficiency), the radioactivity input is 11.9×10^{12} pc, which is slightly greater than the estimated deposition. In any case, it appears that input of radioactivity in the layer below 650 mb was sufficient to account for a large majority of the deposition of radioactivity in this storm.

TABLE 4.3

SUMMARY OF INPUT AND DEPOSITION OF WATER AND RADIOACTIVITY
MAY 10, 1964

	Input Below 650 mb	Deposition
Water (kg)	8.1×10^{10}	5.4×10^{10}
Total Beta Radioactivity (pc)	8.9×10^{12}	10.5×10^{12}

The problem of extending the conclusions reached in the case of one severe convective storm to other such storms is a very real one. In the following section a simplified method is described whereby the scavenging characteristics of this storm may be compared with others.

4.4 A SIMPLE METHOD FOR COMPARING DEPOSITION WITH LOW-LEVEL INPUT

The mass budget study described in the previous section is one way to compare deposition with low-altitude input. However, such studies can be done only for a very few cases because of the requirements for comprehensive and specialized data. There is a need for a method which can be applied more generally, using readily available data. There is, of course, the likelihood that a more general procedure may sacrifice accuracy, but we can compensate at least partially for this through the results of the mass budget study. That is, the result of the general procedure for the May 10 case, where input and deposition have been computed independently, and by a superior method, may be used as a guide to its validity in other instances.

The data required to use this method are (1) total rainfall and total deposition of any contaminant in the rain at a point, and (2) mixing ratios for water and the contaminant in air. The procedure is based on the following considerations. Knowledge of the humidity mixing ratio, m, allows one to compute the <u>minimum</u> mass of air, P, necessarily processed by a rain system in order to yield a mass of rain W over one square meter, or

$$P = \frac{W}{m} \tag{4-1}$$

This assumes that all the water vapor in P is deposited as rain, i.e., that the precipitation efficiency is 100%. The assumption of a more reasonable precipitation efficiency e, $0 < e < 1$, will increase the estimate of P to the more reasonable value P', where

$$P' = \frac{P}{e} \tag{4-2}$$

One may now test the hypothesis of a low-altitude contaminant input by comparing the mass of total deposited contaminant, M, with the mass M' of contaminant in P'. One obtains M from the relationship

$$M = CW \tag{4-3}$$

where C is the measured concentration of contaminant in rain, and M' is obtained from

$$M' = P'r \tag{4-4}$$

where r is the mixing ratio for radioactivity in air.

The data will support the hypothesis if the input at least equals the deposition, i.e., if

$$\frac{M'}{M} \geq 1 \tag{4-5}$$

Because e is not usually known, it is usually not possible to determine with certainty whether this condition holds in a particular case. One can, however, ask what e must be for input to equal or exceed deposition. By substitution of Equations (4-1) through (4-4) into (4-5), we find

$$e \leq \frac{r}{mC}$$

or

$$e_{max} = \frac{r}{mC}$$

Present indications are that e varies between about 0.10 for an average isolated thunderstorm (Braham, 1952) to about 0.50 or more for a squall line (Newton, 1963).

Although it is an obvious oversimplification of the combined relevant physical processes, this technique has the advantage of more general applicability than more rigorous ones might have. If it is found that the hypothesis of a low-altitude input can be generally supported, this technique or a modification of it may be useful as a means of estimating point deposition.

Most of the C data were collected by The University of Michigan group, in Michigan and Oklahoma. Total beta radioactivity was measured in a series of individual samples using a low background thin window flow counter and thallium-204 as a standard. Concentration averages for entire storms were computed by dividing total deposited activity by the total volume of rain collected. In most cases it is not possible accurately to fix the value of r which applies. Therefore probable maximum and minimum concentrations of total beta radioactivity in air were chosen from values measured on 24-hr filter samples at the nearest few stations in the U.S. Public Health Service Radiation Surveillance Network. Measured concentrations were converted to mixing ratios by dividing each sample by an air density of 1.2 kg/m^3. This represents

the density of dry air at 1000 mb pressure and a temperature of 17C. Because all samples were collected between May 1 and September 30, this estimate of air density is conservative with respect to the hypothesis, i.e., it tends to make a low estimate of the input. In each case the value of m used in the computation was an average humidity mixing ratio over the layer from the surface to about 670 mb (more precisely, the lowest 300 mb of the atmosphere), as determined from the nearest radiosonde ascent in the appropriate air mass. That is, if the rain occurred in a cold frontal situation, a sounding in the warm air was used. This same policy was followed in the choice of r_{max} and r_{min}.

The results are given in Table 4.4. The sources of the data and remarks regarding their selection are given in part (a). The data themselves and the values of e_{max} for r_{max} and r_{min} are given in part (b). It is to be emphasized that e_{max} represents the highest value of e which is consistent with the hypothesis of a low-level input, i.e., with Equation (4-5). Any value of $e < e_{max}$ is also consistent with that hypothesis. Cases 1 through 8 represent observations of radioactivity in rain sampled by The University of Michigan group. In each of these cases e_{max} is in the range of probable values of the precipitation efficiency (10-50%) or greater, so that the hypothesis is supported in each case. Case 6 is the storm of May 10, 1964, sampled at Chickasha. Comparison with results of the mass budget study performed on this storm

TABLE 4.4

DATA SOURCES

(a) Date, Time, and Location of Data (EST)

Case No.	Month, Year	C Day/Time[1]/Location	r Day/Time[2]/Length[3]/Location[4]	m Day/Time/Location	Remarks
1	9/61	1/1030/YIP	2/1000/25/IND (max) 5/ /120/AA (min)	1/0700/FNT	(A)
2	9/61	23/2020/YIP	24/0900/24/LAN (max) 24/0800/24/MSN (min)	23/1900/FNT	(B)
3	9/61	30/2100/YIP	30/0900/24/LAN (max) 2/1000/72/ AA (min)	30/1900/FNT	(C)
4	6/62	25/1900/YIP	25/0900/24/LAN (max) 25/0700/24/PVL (min)	25/0700/FNT	(D)
5	5/64	9/1940/CHA	9/0900/24/LIT (max) 9/1200/24/PNC (min)	9/1800/FSI	(E)
6	5/64	10/1815/CHA	10/1300/24/PNC (max) 11/1100/22/PNC (min)	10/1700/FSI	(F)
7	5/64	28/2315/CHA	29/1200/26/PNC (max) 29/1300/20/OKC (min)	28/1900/OKC	(G)
8	5/64	29/1600/CHA	29/1200/26/PNC (max) 31/1200/48/OKC (min)	29/0700/OKC	(G)
9	5/62	24/ /TOP	25/0800/24/TOP	24/1900/TOP	
10	5/62	24/ /JEF	25/0700/24/JEF	24/1900/CBI	

[1]Time rain began.
[2]Time sample ended.
[3]Length of sample (hr).
[4]U.S. Weather Bureau Station Identifiers, except CHA = Chickasha, Okla., JEF = Jefferson City, Mo., AA = Ann Arbor, Mich., PVL = Painesville, O.

TABLE 4.4 (Continued)

Remarks for Part (a)

(A) The two stations closest to Willow Run Airport (YIP) which took samples of the air which would have reached Michigan on Sept. 1 were Indianapolis, Ind., and Springfield, Ill. Indianapolis reported concentrations of < 0.10 pc/m^3 on 8/31, 9/1, and 9/2. Springfield reported < 0.10 in 96-hr samples ended 0800, 9/1, and 0800 9/5. Madison, Wisc., sampling the same air mass, reported a value of 0.10 in a 24-hr sample ended at 0800 on 9/1. Therefore it is likely that values at Indianapolis and Springfield were not a great deal less than 0.10. The minimum value was for Ann Arbor and represents a 5-day sample from 8/31 to 9/5.

(B) The USPHS RSN data show a very large gradient of activity across the cold front, the cold air being less active. The maximum and minimum concentrations among Lansing, Indianapolis, Springfield, and Madison for the sample ending on the morning of the 24th are shown.

(C) There was some difficulty in picking a likely maximum and minimum in this case because of missing data at Lansing and Columbus for the 24-hr ending on the morning of 10/1. On the 30th both Columbus and Lansing had values of almost 16. Indianapolis had 7.39 on the 30th and 3.2 on the 1st, but again the cold air was lower in activity, and we should choose samples representative of the warm air.

(D) Again a front is involved, and the values chosen are the extremes of samples taken in the warm air. The sounding was also chosen to represent the warm moist air.

(E) Ponca City and Oklahoma City are the two stations closest to Chickasha. Oklahoma City had motor failure on the 9th and 10th. The Ponca City sample ending on the 10th was 1.50 pc/m^3, a value intermediate between the maximum and minimum chosen, which represent conditions upwind on the previous day. The minimum value (Ponca City, 9th) is probably much too low in view of the value at Ponca City on the 10th.

(F) The range of possible concentrations in air on this day is apparently very small. The high and low were both from Ponca City, with the higher value representing the period of rain collection. The value upwind on the previous day (Little Rock sample ending on the morning of the 10th) is between the chosen limits.

(G) Ponca City and Oklahoma City are the two closest stations and the samples chosen represent the same air which must have entered the storms from low levels.

TABLE 4.4 (Concluded)

(b) Storm Data

Case No.	C (pc/kg)	m (g/kg)	r (pc/kg)	e_{max} (%)	Type of Storm
1	7.13	10.6	0.0843 (max) 0.038 (min)	111.5 50.7	Area of convective activity, associated with small cyclone, non-frontal.
2	141.6	9.30	1.36 0.958	103.2 72.7	Post-cold-frontal showers.
3	654.3	8.04	13.25 5.33	252 101.3	Weak pre-cold-frontal squall lines.
4	1,064	5.28	4.66 2.66	82.8 47.3	Cold frontal thunderstorm.
5	303.4	9.37	1.72 0.724	60.6 25.5	Severe squall line—transient cells.
6	317.0	11.2	1.35 1.25	38.1 35.2	Severe squall line—persistent cell.
7	457.9	6.97	2.54 2.12	79.5 66.3	Short heavy showers, imbedded in area of light, steady rain.
8	320.7	7.89	2.54 1.067	100.2 42.1	Showers of moderate intensity and steady rain.
9	59,000	8.73	6.41	1.24	Severe storms.
10	8,800	5.70	4.08	8.13	Severe storms.

above shows that the simplified "single-station" procedure made a low estimate of the greatest precipitation efficiency allowable if the hypothesis is to be supported. That is, the simplified procedures indicated that the low-level input hypothesis could be supported only for $e \leq 35\%$. The more reliable mass budget analysis revealed, however, that input could account for deposition even for $e \leq 50\%$. This comparison now serves as a basis for extending the conclusions of the mass budget study of one case to other convective storms. The simple procedure was a conservative one for the testing of the hypothesis in the case of May 10. If this is true in general, it strengthens the conclusion of support for the hypothesis, based on results of cases 1-8.

By comparison, cases 9 and 10 do not appear to support the hypothesis. The data on concentrations of radioactivity in both air and rain are from the U.S. Public Health Service Radiation Surveillance Network. These two cases are the only ones in which collection of rain of more than a trace amount was accomplished by the RSN in the Kansas-Missouri area during the May, 1962, period of high iodine-131 in milk (List, et al., 1964). In both of these cases, the low-level air concentration of radioactivity, as approximated by 24-hr filter samples, could not account for the concentrations found in the rain.

Martell (1965) has suggested that at least part of the high concentrations of iodine-131 observed in milk during May, 1962, could have originated from vented underground tests in Nevada. The iodine, if in gaseous form, would not have been detected in filter samples. Reiter (1965), after computation of isentropic trajectories, states that

"...the Nevada Paca shot [May 7, 1963 GMT] could not have been involved in the Wichita fallout for irrefutable meteorological reasons." This does not exclude with certainty the possibility that the Nevada Eel shot of May 19, from which some radioactivity was detected off-site (see Reiter, 1965, Table 3), contributed to the fallout in rain in cases 9 and 10. Similarities between these cases and the Wichita case provide a very strong argument for the same debris source, however.

Thus, it seems very likely that some of the debris from the high concentrations present aloft (List, et al., 1964) must have entered the rain. The question remains, "By what mechanism did this occur?" It should be pointed out that the observation that cloud tops reached or exceeded the level of the debris does not constitute proof that the entry of the debris to the cloud took place at the cloud top. Dingle (1965) has suggested an alternative, and others may be possible. Certainly, our knowledge of circulations associated with severe storm systems, both inside and outside the cloud, does not preclude the possibility that air from very high altitudes may reach low altitudes and subsequently enter the storm from below. Such occurrences would be very local and one would not expect that they would be detected by one of the 24-hr filter samples.

In summary, use of the simple procedure with air concentrations of radioactivity determined from 24-hr filter samples indicates in general that deposition of radioactivity in rain does not exceed that which it is reasonable to assume entered the storm at low altitudes.

Two cases were discussed where such a conclusion, based on the 24-hr sample, would not be justified. The input mechanism in these cases is still obscure, but even here a low-altitude mechanism is not untenable.

4.5 A QUANTITATIVE STUDY OF THE ROLE OF EVAPORATION IN DETERMINING CONCENTRATION IN RAIN ON MAY 9, 1964

It has frequently been suggested that temporal variations in raindrop evaporation could explain a significant portion of the observed temporal variability of concentrations of contaminants in rain at ground level (Bleichrodt, et al., 1959; Salter, Kruger, and Hosler, 1962). In qualitative terms, there is no doubt that evaporation of falling rain tends to concentrate residues carried by the drops and that variations of the amount of evaporation could produce variations of concentration. However, until now it has not been possible to evaluate quantitatively the magnitude of the effect and thus to assess its importance.

An approximate evaluation of the evaporation effect is possible from the present data owing to (1) observations of raindrop-size distributions at the ground, and (2) the existence of a computer program (Hardy, 1963) to compute changes of raindrop-size distribution with height due to evaporation and coalescence. Input to the computer program consists of a guess of the raindrop-size distribution at the cloud base; output is the subsequent size distribution at the ground. After a trial-and-error process in which the original guess for the drop-size distribution at the cloud-base is successively modified, one obtains a distribution at the cloud base from which the program computes a ground-

level distribution which agrees with that observed. By comparison of the respective liquid water concentrations at the cloud base and the ground, one obtains an approximation of the effect of evaporation during the fall between cloud base and ground. I.e., concentration is increased to the extent that water is lost in the height interval. The increase of concentration may be expressed by a concentration factor defined by

$$K = \frac{L_c}{L_g}$$

where L_c and L_g are the liquid water concentrations (g/m^3) of the rain at the cloud base and the ground, respectively. Application of this technique to a series of time intervals shows the effect of temporal variations of evaporation on concentration variations.

Because of the assumption of steady-state rain (i.e., constant flux at each height) used in the formulation of the program, its use is limited to situations of that type. In convective rain situations, its use would therefore be restricted to periods of light steady rain at the beginning and end of heavy showers. An ideal situation occurred before the first rain burst on May 9, 1964. At this time our station received light rain, slowly increasing in intensity, for about 1 hour.

Input data required for the computer program, in addition to the drop-size distribution at the cloud base, are (1) height of the cloud base, and (2) vertical profiles of temperature and relative humidity. A time-series of computations requires data on the local time changes

of (1) and (2). Such data are not available, and must be estimated. The variation of cloud height for our station was estimated from observations taken at FSI during the approach of a heavy shower earlier on May 9 as the squall line passed there. Temperature and humidity profiles are even less well-known. The temperature profile used was that observed at FSI at 1800. Computations were made for two humidity profile models, which represent (approximately) limiting conditions. Model A is taken as the 1800 sounding at FSI, invariant with time, and is inconsistent with the cloud base estimates in that relative humidity is not constrained to reach 100% at the cloud base. Model A represents conditions before the rain began, and therefore a drier atmosphere than probably prevailed during the light rain. In Model B the profiles are estimated by assuming a linear variation of relative humidity between that observed at the surface at meso-network station 11 and 100% at the cloud base. Model B is time-dependent. Because surface humidities were $\geq$ 90% during the period, Model B represents a nearly saturated lower atmosphere. The temperature profile and both humidity models are given in Table 4.5. The estimated ceiling height variations are implicit in humidity Model B of Table 4.5. That is, the ceiling remained at 1400 m until 2051 and decreased thereafter. Results of the computations are given in Figure 4.6.

The solid lines are "observed" concentration factors, K_o, for radioactivity computed for individual samples from the relationship

TALBE 4.5

TEMPERATURE AND RELATIVE HUMIDITY PROFILE MODELS USED IN EVAPORATION COMPUTATIONS

Height Interval (m):		0-200	200-400	400-600	600-800	800-1000	1000-1200	1200-1400
Temperature (C):		23.6	21.8	19.8	18.0	16.1	14.2	14.0
			Relative Humidity, Model A (%)					
		66	68	69	72	74	75	60
			Relative Humidity, Model B (%)					
Time:	2013-2026	92	93	94	95	97	98	99
	2026-2030	93	94	95	96	97	98	99
	2030-2033	93	94	95	96	97	99	99
	2033-2043	94	95	96	97	98	99	99
	2043-2048	94	95	96	97	98	99	99
	2048-2051	94	95	96	97	98	99	99
	2051-2053	95	96	97	98	99	99	--
	2053-2056	95	96	97	98	99	--	--
	2056-2059	96	97	98	99	99	--	--
	2059-2100	97	98	99	99	--	--	--

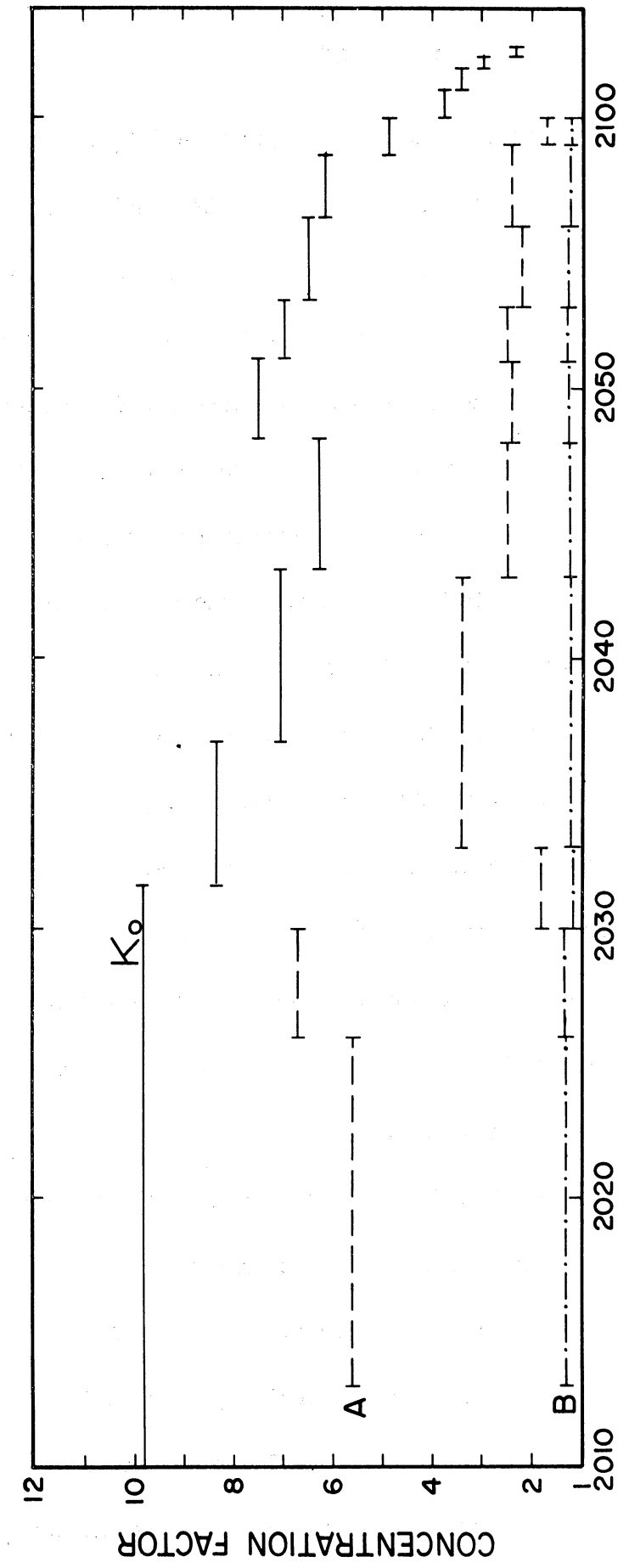

Figure 4.6. Results of evaporation computations for May 9, 1964. K_o is "observed" evaporation. A and B are computed from the respective humidity models.

$$K_o = \frac{C_g}{C_c} \qquad (4\text{-}6)$$

where C_g is observed concentration at the ground and C_c is the concentration in the liquid water of the cloud. The results of Figure 4.6 were obtained using a C_c equal to the minimum concentration observed during the first rain burst. Concentration factors computed from humidity profile Models A and B are shown as dashed and dash-dot lines, respectively. It is seen immediately that under conditions of Model B, evaporation could not account for the observations, even with any reasonable adjustment of the ceiling height used in the computation. The results with humidity Model A come closer to the K_o values, but still represent only about 1/3 to 1/2 of the concentration enhancement required to match them. It is of interest that the over-all slope of the Model A results is roughly the same as that of the K_o values. However, the increase in K_o at about 2048 is not seen in the results of either humidity profile model, and the perturbation in Model A results was not observed, probably because the required resolution was lost in the long collection periods during the light rain.

One is now justified in asking whether such a combination of ceiling height and temperature and humidity profiles can be found that the computed results would agree with observations. Model A represents as dry an atmosphere as one would want to consider, because it is based on a sounding made before the rain began. Computations for the first rain sample, using humidity Model A, show that raising the ceiling height

to 2000 m (6560 ft) has the effect of increasing the concentration factor to approximately 14, which is greater than the "observed" value shown in Figure 4.6.

However, comparison of computed and "observed" values must be done in view of several uncertainties. It appears that the best course to follow is the usual one of presenting the results of the simplified model, as in Figure 4.6, and then modifying the results by introducing additional physical considerations to approximate reality more closely. As the computation now stands, several effects are omitted. Two of these are concerned with limitations of the computation of K, while the other two relate to uncertainties in the value of C_c to be used in the computation of K_o. The computation of K is incomplete in that it omits (1) loss of radioactivity due to the complete evaporation of some drops, and (2) the effect of vertical motion on evaporation. Loss of radioactivity results in a computed concentration greater than that which actually prevailed. Upward air motion during the light rain has the effect of increasing evaporation through an increase of fall times of the drops. Of course, the increase in concentration thus effected is limited to some extent through the simultaneous increase of relative humidity aloft which is also the result of the vertical motion. The assessment of the magnitude of either of these effects is difficult; nevertheless, they tend to compensate for each other, so that if their magnitudes are comparable the computed K values will be realistic.

Use of the minimum observed concentration during a heavy shower as the value of C_c is also an oversimplification. Again, two opposing processes are ignored: (1) evaporation in the downdraft, and (2) dilution in the cloud. Evaporation tends to make the minimum observed concentration higher than the concentration in the cloud, and dilution may have the opposite effect. If so, the chosen value may not be far wrong. In this case, however, rough evaluations of the magnitudes involved are possible, and are performed in the following section. Suffice it to say here that the evaluations of Section 4.6 indicate that the effects of evaporation and dilution processes probably combined to yield a minimum concentration which is lower than the C_c which applies to the light rain portion of Figure 4.6. Therefore the "observed" K_o curve of Figure 4.6 probably overestimates the actual evaporation.

4.6 EVAPORATION AND DILUTION IN THE CORE OF A HEAVY RAIN SHOWER ON MAY 9, 1964: SOME SEMIQUANTITATIVE RELATIONSHIPS

Investigation of the possible effects of evaporation and dilution within the first heavy rain portion of the May 9 storm has revealed several interesting relationships, which are described in the following paragraphs.

4.6.1 Evaporation in the Downdraft

In Section 4.5 the process of evaporation was considered for the period of light rain beginning at 1940 on May 9, and ending with the onset of the heavy rain. The computation of K_o during that period was

dependent upon the assumption that the value of C_c, the concentration of radioactivity in cloud water, could be represented by the minimum concentration observed in the rain during the subsequent heavy rain shower. In actuality we know from the work of Fujita (1959) that evaporation from raindrops takes place during their descent, as evidenced by the cold air outflow from thunderstorms. It is the purpose of this subsection to examine the process of evaporation in thunderstorm downdrafts and to specify as best we can the magnitude of this effect upon concentrations in rain water for the particular case now under scrutiny, i.e., the first heavy rain shower on May 9.

In principle, the amount of evaporation which takes place in a thunderstorm downdraft is a function of the mass of the downdraft, its temperature and pressure at its point of origin aloft, and its temperature and pressure when it reaches the earth's surface (Braham, 1952).

Newton (1950) has employed wet-bulb potential temperature θ_w as a tracer for downdraft air, on the basis of its conservatism with respect to evaporation, condensation, and adiabatic processes. Newton examined a squall line situation and found that air with a θ_w characteristic of mid-tropospheric levels had penetrated to within 3000 ft of the ground in the thunderstorm downdraft. It appears that this technique should be a valid indication of the height of origin of the downdraft associated with severe, highly organized storm systems, such as those described by Browning (1964). Browning's severe storm model

includes a downdraft composed of air which enters the storm at middle levels. Less highly organized storms, a classification which applies to the heavy showers observed at our station on May 9, are less likely to utilize outside air in an organized manner for downdrafts. Rather, the downdraft air is likely to be a mixture of air which originated at many different levels, because of the greater importance of entrainment into downdrafts of small cross-section, such as the ones of the 9th evidently were. Therefore, one can have little confidence in the results of the θ_w technique for the May 9 storm. Nevertheless, the results may indicate an approximate range of likely heights, especially when viewed together with results from the storm of May 10 to which the θ_w technique is more confidently applied.

Table 4.6 shows that between 2100 and 2130 on May 9 the value of θ_w at WB11 never fell below 19.0 C. Comparison of this value against the vertical profile of θ_w computed from radiosonde data from FSI and OKC should reveal the height of origin of the downdraft. Using the FSI profile (Table 4.6), one concludes that the air must have originated between 850 and 700 mb, whereas the OKC profile indicates a lower origin, below 850 mb. Examination of the May 10 downdraft (Table 4.6) indicates that the values obtained for May 9, although rough, are of the right magnitude. Part (b) of Table 4.6 indicates that the height of downdraft origin on the 10th was between 700 and 500 mb. This is higher than computed for the 9th, as may be expected from the fact that a more

TABLE 4.6

HEIGHTS OF ORIGIN OF DOWNDRAFT USING θ_w

Observed at WB11				1800 CST Sounding				1700 CST Sounding	
				FSI		OKC		FSI	
Time (CST)	Temp. (C)	R.H. (%)	θ_w (C)	Pressure (mb)	θ_w (C)	Pressure (mb)	θ_w (C)	Pressure (mb)	θ_w (C)
				(a) May 9, 1964					
2100	21.1	96	21.7	970 (sfc)	21.8	969 (sfc)	20.8		
2105	20.0	94	20.4	889	20.4	850	17.9		
2110	18.9	91	19.0	850	20.4	824	16.0		
2115	18.9	92	19.1	700	15.8	700	13.9		
2120	18.3	99	19.4	633	16.5	696	13.1		
2125	18.3	100	19.4	592	14.2	628	15.6		
2130	18.3	100	19.4	517	15.3	538	15.2		
				500	15.8	500	15.3		
				(b) May 10, 1964					
1800	22.8	86	22.4					962 (sfc)	23.4
1805	21.1	76	19.7					900	21.9
1810	18.9	78	17.8					869	21.6
1815	18.3	82	17.9					850	21.8
1820	17.8	84	17.3					834	21.0
1825	17.2	92	17.9					750	19.7
1830	15.0	99	16.0					700	16.9
								650	16.6
								600	17.5
								550	16.4
								500	17.1
								430	19.0

organized storm occurred on the 10th. Thus, a height of origin of somewhere below 700 mb is reasonable for the storm of the 9th.

Using the results of Fujita (1959), reproduced in Figure 4.7, it is found that evaporation in a downdraft originating below 700 mb (10,000 ft) would result in a K between 1.0 and 2.3. (It can be shown that $K = R_e/R_g + 1.$) That is, it is possible that no concentration by evaporation occurred at all. If it did occur, the concentration would have been increased by a factor of no more than 2.3.

We now examine the observed minimum concentration, and the C_c expected on the basis of the idea of proportional mixing ratios (Section 4.4). Taking the ratio r/m (p. 120, Table 4.4(b)) and converting from g to kg, we find that C_c should be in the range 77-184 pc/kg. This range is perhaps excessively broad, owing to a desire to be conservative in appraising the usefulness of the proportional mixing ratio idea. It is more realistic to choose the value of r determined from the 24-hr sample taken at Ponca City, Oklahoma, ending at 1200 on May 10. The value of C_c thus determined is 116 pc/kg, almost exactly the value of the minimum concentration observed in the first heavy shower, 114 pc/kg. Lest the reader be overawed by this exceptional agreement, he is reminded that the process of dilution has yet to be considered. The seeming agreement will be remarkable only if dilution turns out to have a negligible effect in this case.

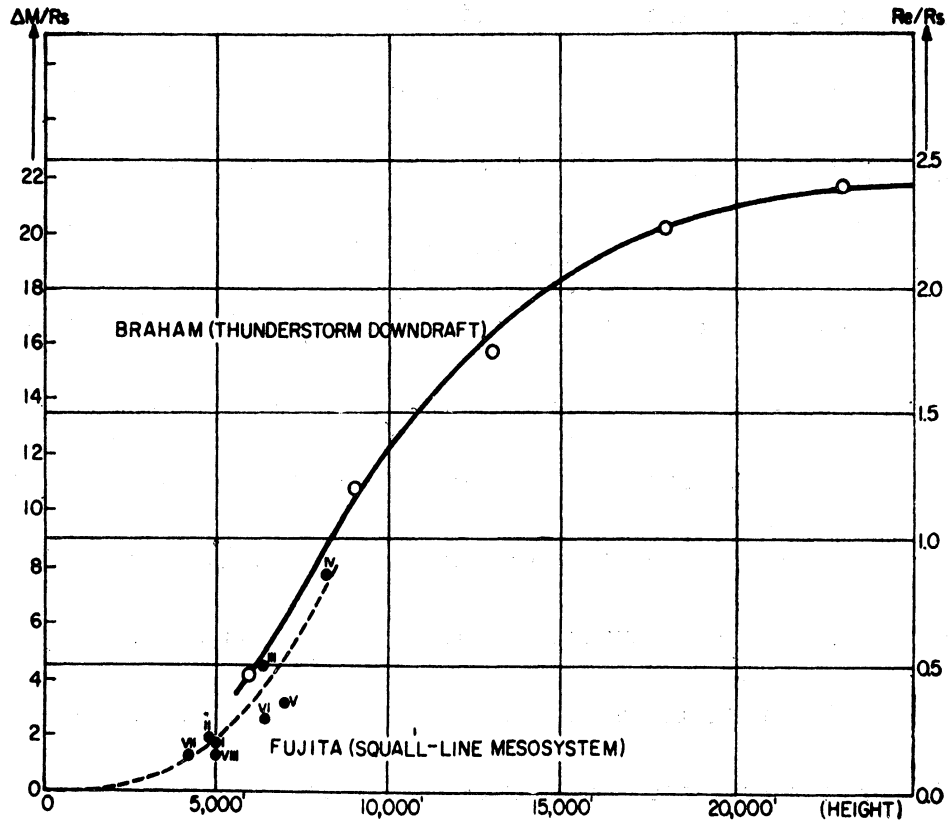

Figure 4.7. Evaporation of raindrops as a function of fall distance. Vertical scale at right is evaporated rain divided by rain which reaches the ground. To convert this scale to one of concentration factor, add 1.0 to the values shown. (From Fujita, 1959.)

4.6.2 Dilution

It is conceivable that dilution of the radioactivity in some samples could come about during lifting of the moist air, in the following way. Assume that the radioactive particles are attached to tropospheric aerosols which serve as condensation nuclei for cloud droplets. During the early stages of ascent in the convective updraft, condensation of water and attachment of radioactivity proceed at roughly the same rate. However, if lifting is extensive, a point may be reached at which all the radioactive condensation nuclei have become attached to liquid water. Any further lifting will condense additional water onto existing droplets or nonradioactive condensation nuclei. This will increase the liquid water content of the parcel, while the content of attached radioactive particles is not changed. Therefore concentration is decreased by dilution with excess water. It is expected that this mechanism would not affect all samples equally. Only those samples collected in heavy rain lifted to high altitudes would be so affected, and it is expected that within the heavy rain there would be sample-to-sample variations in the magnitude of the effect. It is not possible by any obvious procedure to estimate with confidence how this concentration varies with time, except that the greatest dilution should occur in the parcel lifted the highest.

To aid the discussion of dilution, it is convenient to introduce a new parameter, derived from rainfall and radioactivity measurements. The concentration of attached activity in air, C^*, is defined by the

relationship:

$$C^* = L \cdot C \qquad (4.7)$$

where L is the liquid water density of rain in air (g/m^3) and C is a concentration of contaminant in rain (pc/g). C* is the concentration in air of radioactivity which is attached to rain; it has units of pc/m^3 of air. However, just as the number density of raindrops is not to be construed strictly as so many drops of each size in a particular cubic meter of air, because of differing fall speeds of the different sized drops, so C* is not to be construed as representing any particular cubic meter of air, but rather a time- and space-averaged value. Thus a time series of C* values, one computed for each rain water sample, represents an upright chain of intersecting volumes, each defined by horizontal wind speed, sample duration, and the range of raindrop fall speeds. Thus, if the storm system may be characterized as a translating steady state circulation system, and if the height of origin of the respective rain samples is reflected in their rainfall rate, then each rain sample represents a rising parcel at a different stage of ascent. That is, the initial light rain comes from parcels which have been lifted only slightly, whereas samples of increasing rainfall rate correspond to parcels which have been lifted to increasing altitudes. The series of samples does not in fact represent one parcel at different stages of ascent, but can be considered to do so if the convection system can be considered to be steady state

for the time interval required for the storm to traverse a point on the ground. It is important to note that this is a less restrictive condition than that usually required of a storm in order to be considered "steady-state" (Browning, 1964).

In spite of the limited specificity of C*, if dilution occurs as described in Section 4.5, then a graph of L vs. C* for a given shower should behave as follows. Both L and C* should initially increase from zero, but at some point C* will reach a constant upper limit imposed by the supply of contaminant, while L continues to increase due to further condensation.

Results computed for both heavy showers on May 9 are given in Figure 4.8. L's were assigned to each sample, based on measured raindrop-size distributions. Plotted points are labeled with sample number and connected in order of collection. The two showers are distinguishable by different identification symbols. Although the curves are somewhat less than smooth, one important feature is clear in both rain bursts: during the course of the increase in L, C* reaches a maximum and then diminishes. A constant C* with increasing L would have signaled a dilution mechanism; a decreasing C* indicates that dilution, if active at all, is not the only mechanism at work.

Evidently, some mechanism exists which separates water and contaminant. This is not to be taken in an absolute sense, of course, because some water must always accompany contaminant particles if they are to reach the ground via wet processes. What is meant, therefore,

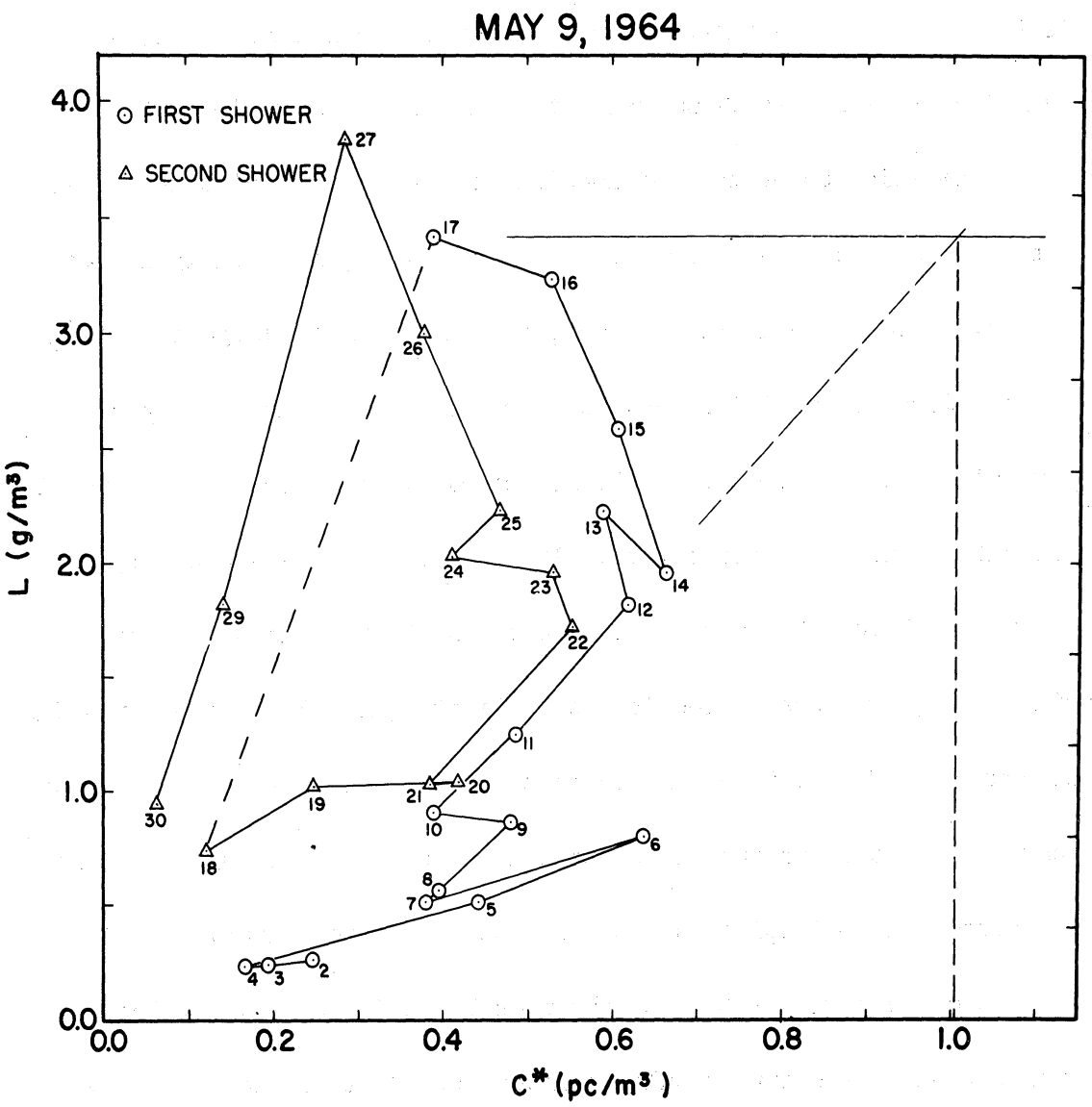

Figure 4.8. Variation of C* with L for both heavy showers on May 9, 1964. The dashed line between samples 17 and 18 connects the two showers. See text for discussion of lines at right of figure.

is that water with a higher concentration of contaminant is systematically separated from that with a lower concentration. One mechanism which comes to mind immediately is that in which the first water to be condensed falls out of a rising air parcel early in its ascent. Because nucleation takes place first on the largest particles and the largest particles tend to carry the most radioactivity per particle (Shalmon, 1964), the "first precipitation" should contain high concentrations of radioactivity. Thus, in a steady-state storm, as described above, the rain which reaches the ground first at a point will be highly concentrated in radioactivity (as well as gross residue, of course). The fact that heavy rain arrives slightly later indicates that condensation in the rising parcel proceeds fast enough to cause an increase in L despite the loss of the first precipitation.

To correct Figure 4.8 for the possible effects of water loss by evaporation, the points should be moved upward at constant C*. Evaporation would decrease both L and m of a sample, but would increase C proportionally. Therefore C*, the product of C and L (Equation (4-7)) would remain unaffected.

4.6.3 The First Precipitation of Condensed Water

Again it is possible to check the feasibility of the first-precipitation mechanism using the present data. Let us assume that the curves of Figure 4.7 come about as a result both of dilution and first precipitation. Our attention now is focused on a single sample—number 17—

which represents the maximum L as well as the minimum C attained during the first shower. The concentration expected in this sample by the dilution effect alone is evaluated first—neglecting any evaporative effect. If dilution were the exclusive mechanism, then in Figure 4.8 C* would have remained constant at a value of about 0.65 pc/m^3 after sample 14. Dividing 0.65 pc/m^3 by the L of sample 17 gives a hypothetical concentration of 191 pc/kg for sample 17. Now it is required to determine whether the first-precipitation mechanism could have accounted for the discrepancy between 191 pc/kg and the observed value of 114 pc/kg (see Figure 3.3).

The first-precipitation mechanism may be described mathematically as follows. Let C_H and C_O represent the hypothetical and observed concentrations, respectively. Similarly, let L_H and L_O represent the hypothetical and observed liquid water contents (g/m^3). L_H is unknown, and there are two other unknowns: the mass of water (per unit volume), L_F, and the contaminant concentration C_F, of the condensed water which fell out. Now, the observed concentration of attached activity in air, C^*_O, must equal the hypothetical value, C^*_H, minus that which fell out of the rising parcel (C^*_F). Thus,

$$C^*_O = C^*_H - C^*_F$$

or

$$C_O L_O = C_H L_H - C_F L_F$$

Because L_F is unknown, let it be expressed as a fraction of the known

L_0, i.e.,

$$L_F = \Lambda L_0$$

where Λ is the proportionality coefficient. It is required, of course, that

$$L_0 = L_H - L_F$$

so that

$$L_H = L_0 + \Lambda L_0$$

By substitution from above

$$C_0 L_0 = C_H(L_0 + \Lambda L_0) - C_F \Lambda L_0$$

or

$$C_F = \frac{C_H(1 + \Lambda) - C_0}{\Lambda}$$

Computations of C_F were performed for Λ = 0.1, 0.2,...1.0 for both heavy showers on May 9. The results are shown in Figure 4.9. As might be expected, when the mass of water which falls out is only a small fraction of L_0, the corresponding concentration of contaminant (C_F) in that water must be large. As Λ increases, C_F decreases, rapidly at first and then more slowly. In Figure 4.9 we look for the answer to the question, "Can the first-precipitation mechanism, superimposed on the dilution mechanism, yield C_0 with reasonable values of C_F and L_H?" Notice that scales of L_F and L_H for each shower are given at the bottom of the figure. Confining our attention to the first shower, and choosing a reasonable value of L_H, say 5.0 g/m^3, we find that C_F is required to be about 350 pc/kg. Referring to Figure 3.3, we see that

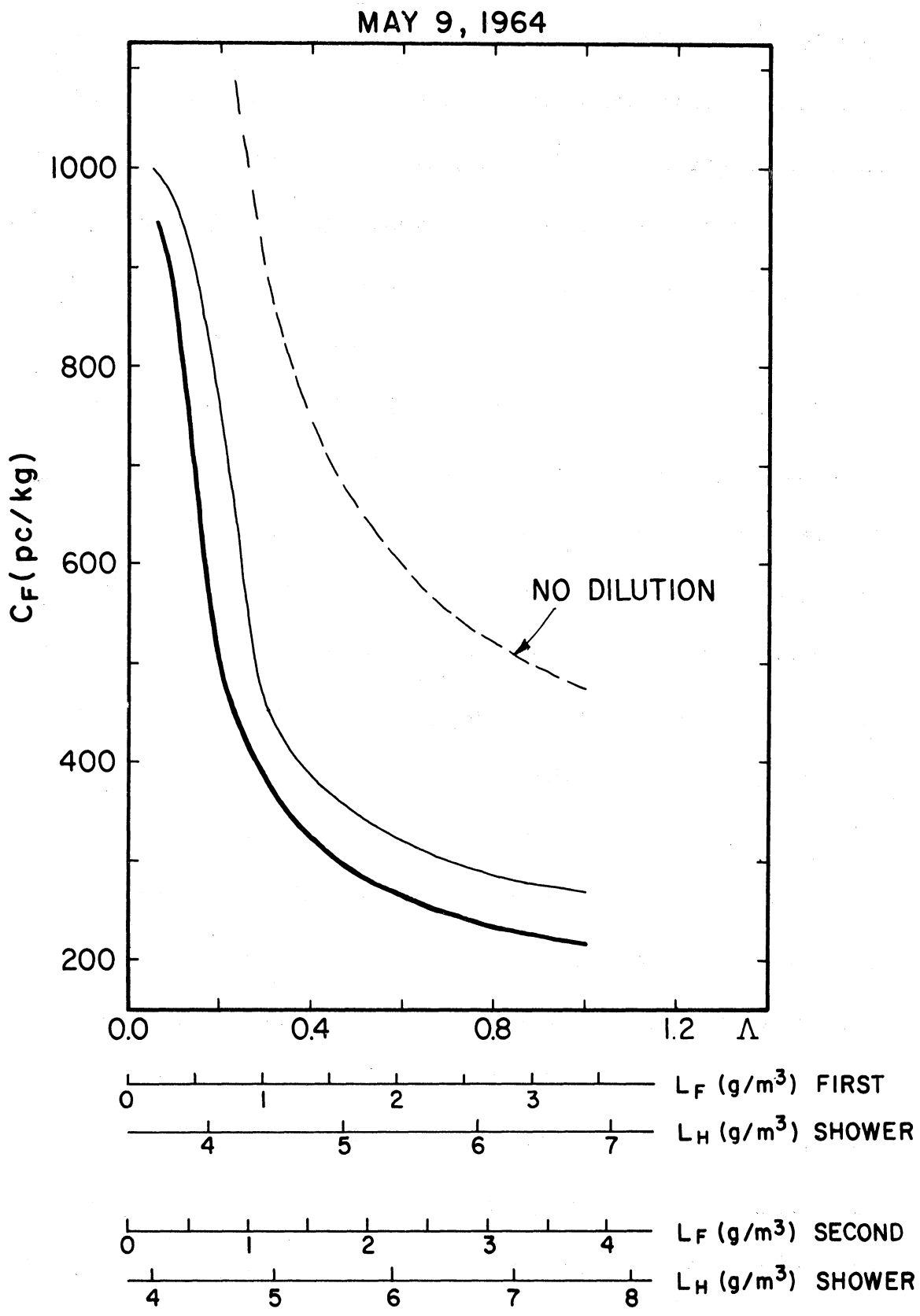

Figure 4.9. Variation of C_F as a function of Λ for both heavy showers on May 9, 1964. Thin line is first shower; heavy line is second shower.

this is a reasonable value. That is, such a value is roughly half-way between the maximum and minimum observed in the first shower. Shifting attention to the second shower, $L_H = 5.0$ requires $C_F = 365$, approximately the value of the concentration peak of 399 which was observed in association with the second shower.

Thus, it appears that the first-precipitation mechanism is a likely contributor to the high concentrations prevalent at the beginning of heavy showers, i.e., during the period of increasing rainfall rate. This mechanism is especially attractive in view of its ability to explain the second major concentration peak, which is not well explained by evaporation. The larger concentrations before the first shower compared to the second shower are easily explained by greater evaporation in the light rain before the first shower.

If we may now retreat for a moment, the question of whether first-precipitation could explain the observations without the need for dilution should be addressed. The proper method of choosing a C_H in this case is not entirely clear, but as a first approximation, let us assume that the nearly straight line (Figure 4.8) formed by samples 10, 11, 12, and 14 (and paralleled by the line 21-22 in the second shower) represents the relationship existing between C* and L in the absence of dilution. This extension is indicated by the dashed line in Figure 4.8. The line intersects $L = 3.4$ g/m^3 (maximum L of the first shower) at a value of $C^* = 1.0$ pc/m^3, which implies that C_H (= C*/L) = 294 pc/kg.

Computation of C_F as a function of Λ yields the dashed line in Figure 4.9. It appears unlikely that a reasonable combination of Λ and C_F can be found without dilution coming into play to some extent.

Comparison of the figure 294 pc/kg, which is really an estimate of C_c unaffected by dilution or first precipitation, with the minimum observed concentration of 114 pc/kg indicates that too low a value of C_c was used for the computation of K_o in Section 4.5. The effect of evaporation tends to limit the amount of the underestimation, but only to a certain extent. Evaporation could have increased C_c by a factor not greater than 2.3 (cf. Section 4.6.1). Comparison of 294 pc/kg with 114 pc/kg indicates that dilution and first precipitation could have decreased C_c by a factor of about 2.6. Therefore the use of C_c = 114 pc/kg in Section 4.5 implies that the K_o curve of Figure 4.6 is probably a little high.

Computations of C* were also made for the May 10 rain, and are plotted vs. L in Figure 4.10, showing a completely different curve than that obtained for May 9 (Figure 4.8). What we see is a rather good approximation to a straight line, both before (open circles) and after (solid circles) the maximum L. This is just the result expected for the case of no dilution. However, comparison of the characteristics of the respective storms gives cause for concern. If dilution and first precipitation took place in the showers of the 9th, these processes would also be expected from such a vigorous storm as that of the 10th. Let us not forget the possible influence of evaporation in the downdraft,

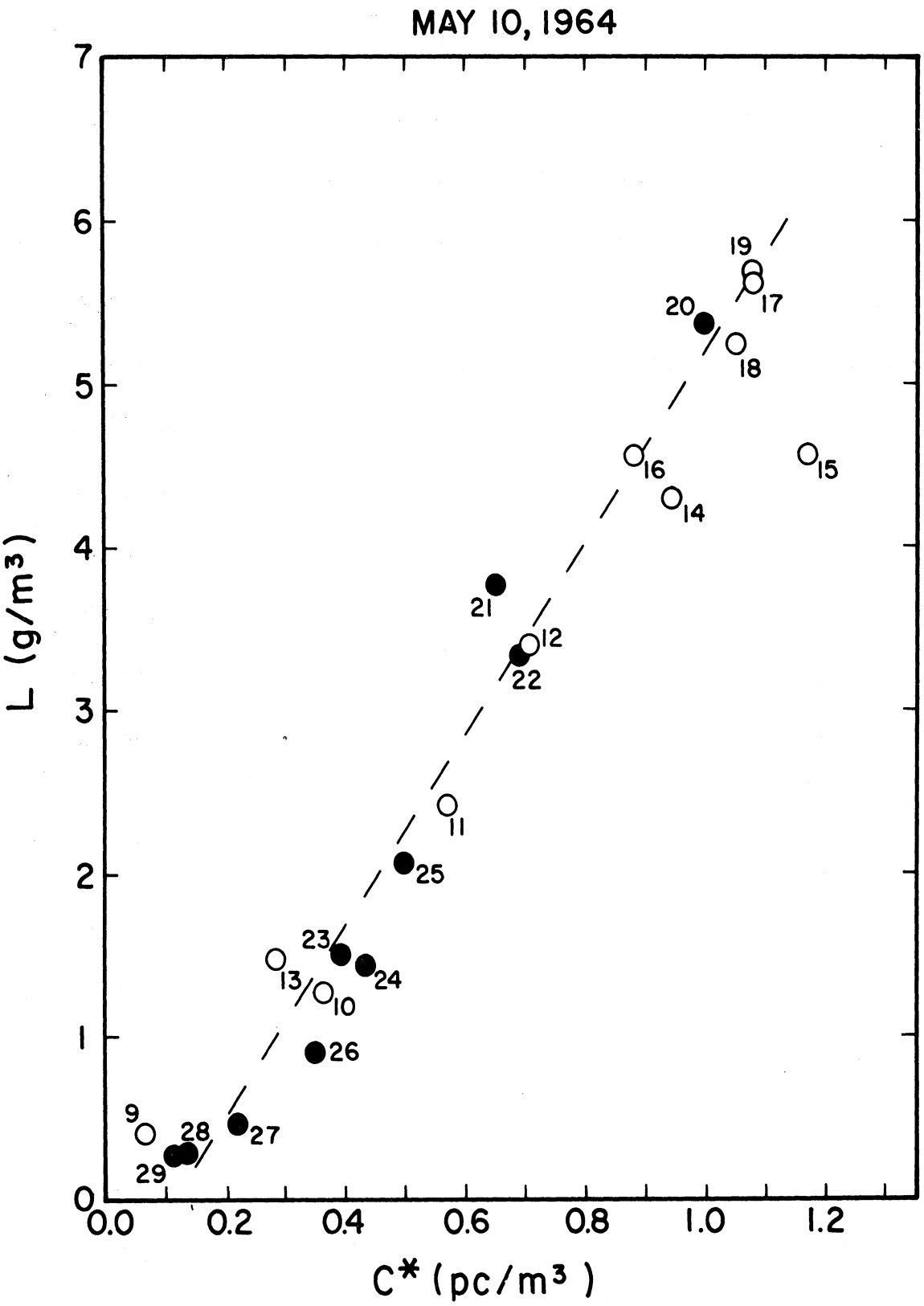

Figure 4.10. Variation of C* with L for the storm of May 10, 1964. Open circles represent samples collected before maximum L; solid circles were after maximum L.

however. The storm of May 10, as evidenced by its persistence on radar and rainfall rate maps, can be classified with the severe storms described by Browning (1964). Browning's model for such storms includes an influx of air at middle levels, which upon entering the storm, forms the downdraft. The analysis of the height of origin of the downdraft, using Θ_w as a tracer, indicated that the downdraft in this storm originated between 700 and 500 mb, (10,000-18,000 ft) in agreement with Browning's "middle levels." Thus, one should expect that considerable evaporation of rain in the downdraft would occur; in any case, more than on the 9th. Use of Figure 4.7 shows that a K of between 2.3 and 3.2 should be expected within the heavy rain in the downdraft. Thus it appears that the results of Figure 4.10 suffer from the effects of evaporation. It will be recalled that evaporation tends to decrease L without affecting C*. In this case it appears that dilution and first precipitation of condensed water were compensated by evaporation to the extent that C* vs. L is a straight line.

The above discussion points to significant differences between the storms of May 9 and 10. The following paragraph describes these differences in terms of the physical processes treated in this section.

In at least three important ways, the storm of May 9 is different from that of the 10th. First, the degree of organization of the two storms, especially as reflected in the character of the downdrafts, is dissimilar. Differences were thus produced in the amount of evaporation in the downdraft, and therefore in (1) the amplitudes of concen-

tration, and (2) the shapes of the C* vs. L curves. In each of these cases, the differences are consistent with the conclusion that the storm of the 10th exhibited more evaporation into the downdraft than that of the 9th. This conclusion is of no little significance from the viewpoint of water budget and precipitation efficiency. It indicates that the most severe and best organized storms may have a built-in mechanism (evaporation in the downdraft) which limits precipitation efficiency.

4.7 SUMMARY

This chapter contains several results of basic importance to the processes of contaminant deposition by convective storms. The mass-budget analysis of Section 4.3 indicates that all or nearly all of the radioactivity deposited in the test zone on May 10 can be accounted for by input of radioactivity in air below 650 mb.

The results of Section 4.4 indicate that the low-level input mechanism is plausible for some, but possibly not all storms. In a case (List, et al., 1964) where high concentrations of airborne bomb debris were present at 50,000 ft and convective storms were known to penetrate to this level, some of the debris from aloft was deposited in rain, as shown by the presence of fresh fission products. The route of debris into the storm is not entirely clear, but it is definitely possible that it was first brought down to the surface and thence entered via the convective updraft.

Several obvious differences in the character of the two storms examined suggest that evaporation of rain in the downdraft of the 10th was greater than that in either downdraft on the 9th. Conversely, evaporation in the initial light rain on the 9th could have contributed significantly to high contaminant concentrations observed at that time.

The mechanism of first precipitation of condensed water from a rising parcel is also a plausible contributor to observed variations of concentration. It is especially useful in explaining high concentrations preceding second or third showers, when evaporation should be small.

CHAPTER 5

DISCUSSION

5.1 PRESENT RESULTS

Chapter 4 contains several results of basic importance to the processes of contaminant deposition by severe storms and to processes of severe storms themselves. The mass-budget analysis of Section 4.3 shows that for the case of May 10, 1964, the input of radioactivity below 650 mb was sufficient to account for deposition when both input and deposition are computed with respect to an area of 582 sq n mi. Although there is no proof that the deposited activity entered at low levels, there are strong indications that such was the case. Temporal variations of radioactivity were largely parallel to those of plant pollens, a tracer for low-level air. It is a remote possibility that this circumstance could arise if the respective contaminants entered the storm in greatly different ways. It is more reasonable to conclude that the radioactivity came into the storm from low altitude with the pollens and the water vapor. The radioactive particles are thus in a most favorable position to be associated with condensation nuclei and so to become attached to the liquid water. Thus there is ample evidence for a low-altitude input to the storm of May 10, 1964, but can this conclusion be extended with confidence to other storms? The evidence in Section 4.4 indicates that it can in many cases. In the majority of the cases examined, low-altitude input was shown to be feasible

with a reasonable precipitation efficiency, based on the idea of proportional mixing ratios of water and radioactivity in both air and rain. In a case (List, et al., 1964) where high concentrations of airborne bomb debris were present at 50,000 ft and convective storms were known to penetrate to this level, some of the debris from aloft was deposited in rain, as shown by the presence of fresh fission products (iodine-131). The route of the debris into the storm is not clear, but it is not impossible that it was first brought near the surface and thence entered via the convective updraft. In the event that entry of the deposited activity took place at high levels, it is possible that the special propensity of iodine-131 for attachment to particles (Reiter, 1965) was mainly responsible for its deposition. The same mechanisms may not work in the case of other nuclides or older debris.

The case for low-altitude input is strengthened by the success of certain mechanisms in explaining temporal variations of concentration. These mechanisms, namely evaporation, dilution, and first precipitation of condensed water, are based on the hypothesis of a low-altitude input. Several obvious differences in the character of the two storms examined support the conclusion that evaporation of rain in the downdraft was significant on the 10th but almost negligible on the 9th. For this reason, and because of much evaporation in the initial light rain on the 9th, evaporation appears to be a contributor to the large concentration variations observed in association with rainfall

rate variations on that date. While data deficiencies do not permit a definite conclusion regarding the magnitude of the evaporation effect, it can be said that such an occurrence was possible. Evaporation could be a significant factor in the following hypothetical but realistic situation: A moderately high cloud base, of the order of 5000 ft, having little variation during an intial period of light rain, but going rapidly to zero soon after the start of a heavy rain burst; a fairly dry lower atmosphere even in the light rain, but going to 100% relative humidity soon after the heavy rain begins. An additional bit of evidence that evaporation could cause observed variations is found in the results of Booker, et al. (1964). They found concentrations of strontium-90 in rain to be higher than those of hail collected within a "few blocks" by factors of 2 to 6. Hail could be considered representative of in-cloud concentrations because any melted liquid water and a proportional fraction of radioactivity probably would be swept off the falling stone. Hence, little concentration enhancement would occur, as it does when water evaporates from raindrops. If the concentration in the hail represents that in the cloud, then observed concentrations in the rain indicate that a true concentration factor of between 2 and 6 affected the rain as it fell.

Although it now seems possible, even probable, that evaporation contributes significantly to the concentration decrease at the beginning of the first shower, one may ask whether the same can be true of the

second shower. In particular, could it cause the increase which took place between showers on the 9th, for example, when the maximum before the second shower was higher than the minimum in the first shower by a factor of 3.5? In view of the lack of organization of the showers on the 9th and the evidently shallow downdrafts, such an event is unlikely. It is more reasonable to suppose that other effects, such as first precipitation of condensed water, must contribute to the concentration peak associated with the second shower.

First precipitation of condensed water bearing high concentrations of contaminants is especially attractive because it explains concentration peaks associated with showers which occur some time after the beginning of the rain. At such times the low-altitude air must be nearly saturated, and evaporation would be retarded.

The several results reached in Chapter 4, while perhaps not conclusive individually, are mutually consistent in support of a low-altitude contaminant input and permit that conclusion in the majority of cases.

Several additional features brought out in Chapter 4 are worthy of further note. First, the idea that the ratio of water and contaminant mixing ratios in air is about equal to that in rain is evidently reasonable if one is careful to specify which samples he is talking about. This circumstance is rather fortuitous owing to the fact that the effects of evaporation on the one hand, and dilution and first precipitation on the other, tend to compensate for each other in the case

of the minimum concentration in a shower. The idea of proportional mixing ratios may be more generally applied to cloud liquid water than to rain at the ground. If this relationship could be established, it would be a powerful tool for studying evaporation in storm downdrafts, an aspect of a storm's mass budget. Evidence presented in Chapter 4 indicates that evaporation in the downdraft may serve to limit the efficiency of precipitation in organized storms. Another by-product of the investigation of scavenging processes is the potential use of the concept of first precipitation of condensed water to study the structure of showers and water storage aloft.

5.2 RESULTS OF OTHERS

From the literature review given in Chapter 1, it is clear that conclusions drawn from some of the earlier sampling programs differ markedly from those presented here. As pointed out earlier, this may stem in part from the lack of adequate data. Nevertheless, it is important to reexamine those earlier papers which report results different from those presented here.

Kruger and Hosler (1963) expected that concentration of radioactivity in rain would be a reflection of the environmental concentration of radioactivity at the height of rain formation. Because concentrations of radioactivity in the atmosphere generally increase upward, the rain which formed at the highest altitude was expected to have the highest concentration of radioactivity. In other words, heavy

rain, associated with deeply penetrating cloud tops, should contain the highest concentrations. Figures 3.3 and 3.13 show that exactly the opposite occurred in the storms of May 9 and 10, 1964. The first rain to fall from an individual shower contained the higher concentrations of radioactivity, and the heaviest rain contained the lower. Therefore the present data are not consistent with the concentration variations predicted on the basis of a high-altitude input mechanism. However, several papers and reports were published in which the data were interpreted as supporting the above hypothesis. It is important to examine these data carefully to see whether they support the conclusions drawn from them.

5.2.1 Pennsylvania Data

Kruger and Hosler (1963), based upon data summarized in Figure 1.1 (above), concluded,

> "...we have been able to relate the peak Sr^{90} concentration to the highest development of the precipitating cloud and to its position relative to the tropopause and jet axis."

Examination of Figure 1.1 reveals that the highest concentrations actually are found nearest the tropopause and/or jet stream. But how were these numbers and positions determined? The number represents the maximum concentration of strontium-90 observed during an entire sampling period, which in some cases represented several individual showers. The horizontal position of the numbers was determined by the location of the collection site with respect to the jet stream. The vertical position

was determined by the maximum observed 3-cm radar echo height during the entire collection period. In other words, the plotted numbers and positions represent the artificial pairing of two events which could have occurred several hours apart. It is not possible to tell what the time intervals were in the different cases, because the times of the echo top maxima were not reported. Nevertheless, use of the reported rainfall rates for the individual samples allows some judgment of whether high concentrations were actually associated physically with high echo tops.

Consider for example the concentration maxima of 51.0, 9.9 and 6.7 dpm/ℓ. (Although differences between the group of three highest and the group of four lowest concentrations appear to be significant, it is questionable whether significant differences exist among the four lowest individual concentrations.) The concentration of 51.0 dpm/ℓ occurred in the last sample collected from a shower ending at 1740 on March 8, 1962. The sample was collected over a period of 1.5 hr, during which time the average rainfall rate was less than 0.5 mm/hr. In view of the maximum rainfall rate of 10.9 mm/hr observed between 1517 and 1529, it does not appear proper to associate this concentration with the maximum echo top of the shower. In any case, proper or not, no evidence has been presented that high concentrations are found in rain which is formed at high altitudes.

Similarly, the association of a concentration of 6.7 dpm/ℓ with the maximum echo top does not appear to be valid. This concentration

was observed during the first (16 min) sample (10.5 mm/hr) from a shower which reached a peak rainfall rate of 21.4 mm/hr during the following sample (10 min). The remaining high concentration (9.9 dpm/ℓ) occurred in a sample of high rainfall rate (54.4 mm/hr), which suggests an association with higher echo tops in this case.

Thus, in two of the three highest concentrations in Figure 1.1, it appears that mechanisms other than the penetration of high echo tops into high concentrations of radioactivity are equally likely causes of the high concentrations. Because the two suspect samples were collected at the beginning and end of showers, evaporation probably operated to elevate the sample concentrations, especially in the case of the 1.5-hr collection period.

Additional work was reported by the same group in 1963 and 1964 (Kruger, et al., 1963; Kruger, et al., 1964) in which a vertically-pointing radar was used to obtain echo tops over the station. The conclusion (Kruger, et al., 1964) drawn for the seven convective rains sampled during 1962 and 1963 was:

> "The peak concentration has been shown to occur during the period of peak cloud development as revealed by radar echo tops."

The data do not support this conclusion. As revealed by Table 1.1, in only three of seven cases did the echo peak occur during the collection of the sample of maximum concentration. On the other hand, this conclusion in itself is evidence against the original proposition that the highest concentrations should occur in the rain which formed

at the highest altitude, because the rain in the observed echo top certainly could not have contributed to the concentration observed at the same time. In fact, consideration of times of echo peaks and concentration peaks reveals that in only one of the seven cases could the rain which allegedly originated in the echo peak have contributed to the sample of maximum concentration. (This collection period was 45 min long.) Furthermore, the implication that the water observed at heights of 15,000-44,000 ft directly above the collector would fall vertically downward, so as to be sampled near the radar site is highly doubtful. In reality, it is difficult to see why radar-observed phenomena at such heights above the collector should have any direct influence upon events occurring at the ground at the same time. Assuming a precipitation fall speed of 8 m/sec (3.0 mm diameter drop in still air), and a mean horizontal wind speed of 10 m/sec, drops would have to start falling from the 20,000 ft level at a distance of 25,000 ft (4.7 mi) upwind in order to impact at the collection site. This is, moreover, a conservative estimate, considering that during a good part of its fall, the precipitation element supposedly containing the large amount of radioactivity would be a snowflake and thus fall much more slowly than 8 m/sec.

In the final analysis, it must be concluded that the data presented in Figure 1.1 and Table 1.1 support neither the conclusions drawn from them nor the original hypothesis of Kruger and Hosler (1963). It is natural then to inquire whether these data support the conclusions

reached for the cases examined in this dissertation. Owing to their limited resolution and the absence of a tracer for low-level air such as pollen, the usefulness of a comparison of these data with those reported in Chapter 3 is perhaps questionable. Yet it is interesting to examine them regarding the relationship between concentration variations and rainfall rate variations. It must be kept in mind that there is a great discrepancy between the resolution of the Pennsylvania data and The University of Michigan data from the Oklahoma field station. Even with such limitations, one sees repeatedly in the Pennsylvania data the same familiar sequence: the maximum concentration occurs slightly before (usually the sample prior to) the rainfall rate peak; a rapid decrease in concentration is in progress at the rainfall rate peak; and the concentration minimum occurs soon after the rate peak (usually within 5 min). This pattern is found in at least 8 individual showers on March 8 and July 24, 1961, June 24, August 20, and September 10, 1962, and April 22, May 10, and May 21, 1963. Based on this indication of similar behavior in the two sets of observations there appears to be a possibility that the scavenging characteristics of the Pennsylvania storms are the same as a majority of those sampled in the midwest. The storms discussed by List, et al., (1964) may be an exception because of unevenly mixed tropospheric contamination as discussed in Chapter 4.

5.2.2 Illinois Data

The conclusions of Huff and Stout (1964) regarding their Type A and Type C (Figure 1.3) radioactivity concentration profiles infer high-level inputs of activity to convective storms. They concluded, "Type A distributions appear to be representative of distributions in mature convective systems in which any high-level source of radioactivity has been diluted somewhat by earlier penetrations of convective storms." All of the rainfall rate and concentration variations examined for the storms of May 9 and 10, 1964, fall into Type A. The data for these storms are consistent with the hypothesis that a low-altitude input mechanism is dominant for Type A distributions. Moreover, consideration of the dimensions of, and the particle velocity within, a radioactivity source region relative to the dimensions and velocity of a penetrating thunderstorm shows that the conclusion of Huff and Stout for Type A is only remotely probable. That is, the repeated penetration of the same volume of the source (even assuming it would still exist after the first penetration) is very unlikely. Type C, in which maxima of concentration and rainfall rate appear in the same sample, was interpreted as arising from initial penetrations of high concentrations of radioactivity (aloft). It is a curious thing that not one Type C distribution has ever been observed during our high-resolution sampling of both rainfall rate and concentration. Indeed it appears likely that the second rain burst of May 9 would have been classified as a Type C situation if rainfall rate were computed from weighing rain gauge data, and if sampling

resolution were poorer. It is strongly suggested that many Type C distributions should really be called Type A. If a true Type C exists, it is probably better and more quantitatively explained by a combination of evaporative and first-precipitation effects.

In view of (1) the high resolution and quantitative results of the present data, and (2) a reevaluation of some of the data upon which conflicting conclusions were based, there appear to be very few cases of deposition of contaminants by convective rains in which the low-altitude input model suggested here may not apply. This model is restated below.

5.3 A SCAVENGING MODEL FOR CONVECTIVE STORMS

Careful interpretation of the evidence to date leads to the proposition that the scavenging processes of most convective storms may be described as follows. The source of the radioactivity is air from near the surface of the earth—the same air which supplies moisture to the storm. The radioactivity present in this air has its ultimate origin in the stratosphere, where the individual particles which contain the radioactivity are much smaller. The distribution of radioactivity on particles in the lower troposphere is derived from that of the stratosphere by the processes of agglomeration, condensation-evaporation, and reflotation of surface particles by wind.

The great majority of the radioactive particles become attached to liquid water by virtue of their association with nuclei of condensa-

tion. Probably only a very small fraction of the total radioactivity in the air immediately affected by rain scavenging is attached to particles which are large enough to be collected by impaction, or small enough to be collected diffusively.

As the buoyant air rises, condensation proceeds until a time is reached when all radioactive particles have been nucleated. Any further lifting causes dilution of the radioactivity by excess water. Some of the condensed water and radioactivity falls out of the rising parcel. This water reaches the ground at the beginning of the heavy shower and, with evaporation of raindrops and impaction collection of large particles in the relatively dry uncleaned air near the surface, contributes to the initially high concentrations of all types of contaminants observed then. Concentrations decrease rapidly during the heaviest rain owing to the effects of dilution and first precipitation aloft. In well-organized downdrafts these effects may be counteracted by evaporation of raindrops into the adiabatically-warming air of the downdraft. After the heavy shower is over and rain falls from layer clouds to the rear of the storm, evaporation is again a factor. Ceilings rise and advection of drier air at low altitudes causes increasing evaporation and, consequently, increasing concentrations.

CHAPTER 6

SUMMARY AND CONCLUSIONS

A field observational program was established near Chickasha, Oklahoma, during May, 1964, to obtain rain scavenging data of high resolution under convective storm conditions. The field site was chosen to take advantage of the data collection facilities of the National Severe Storms Laboratory at Norman, Oklahoma, the Agricultural Research Service rain gauge network centered at Chickasha, and the University of Oklahoma network of automatic rain samplers, which was located within the ARS network.

At the Chickasha field site, sequential samples of rain were collected at frequent intervals for later analysis of their content of artificial radioactivity, plant pollens, and gross residue. Observations were also made of raindrop-size spectra, total rainfall, wind direction and speed, and atmospheric pollen concentrations. From these data were prepared time profiles of concentrations of the three contaminants, rainfall rate, and deposition rates of radioactivity and pollens, for the severe storms which occurred on May 9 and 10.

Data obtained from the ARS and NSSL permitted the reconstruction of the storm in terms of time sequences of radar echo distributions, rainfall rate distributions, and mesoscale pressure and wind analyses.

Conventional synoptic weather data were used to depict large scale flow conditions aloft and at the surface and to prepare local

synoptic charts of the south-central U.S. and vertical cross-sections of the atmosphere.

Quantitative investigations regarding the source of input of radioactivity and causes for observed temporal variations of contaminant concentrations in rain water were carried out.

A mass-budget analysis of the severe storm of May 10 was undertaken to test the hypothesis that low-altitude input of radioactivity could account for that deposited by the storm. Input of air was computed using wind velocity profiles at FSI. Water input was computed from the moisture profiles of the same soundings. Input of radioactivity was calculated by use of concentrations in air determined from 24-hr filter samples at several sites in Oklahoma and adjacent states, and the assumption of uniform mixing ratios in time and space. Deposition of water was computed from ARS network data, and radioactivity deposition was based on measurements of the University of Oklahoma network.

A simplified analysis, using the concept of proportional mixing ratios of contaminants and water, both in air and in rain, was used to extend the results of the mass-budget analysis to other storms.

Computations of the influence of evaporation during the initial light rain portion of the May 9 storm were made to test the hypothesis that differential evaporation of raindrops can contribute to observed concentration variations. The computations were based on observations of surface drop-size spectra and a computer program which computes

changes in size spectra with distance fallen under specified conditions of temperature and humidity.

The effects of dilution and first precipitation in the rising air and evaporation in the downdraft were examined for their effects upon concentration at ground level.

Conclusions drawn from results of the above analyses are summarized in the following paragraphs.

The single main conclusion which follows from the work described here is that input of air from low altitudes into convective storms supplies most of the particulate matter, as well as the water, which is deposited by the storms. Such an input mechanism is to be expected qualitatively for several reasons. Attachment of contaminant particles to rain elements is favored by the intimate association of the particles with large amounts of water, and this is provided simply and directly by input via the well-known convective updraft. Secondly, the basic similarity between concentration variations of radioactivity and plant pollens is most simply explained by a common source; namely, low-altitude air. The low-altitude input mechanism is the dominant one, but perhaps not the only one, both in storms which are well organized and those which are not.

The above conclusion is supported by studies which show quantitatively that observed concentration variations can be explained by various physical mechanisms based on a low-altitude input. It is observed repeatedly that concentration in individual showers varies with

rainfall rate in a consistent manner. Concentrations reach a maximum during the early stages of a shower, decrease rapidly as the rainfall rate peak is approached, and reach a minimum soon after the rainfall rate maximum.

This behavior can be explained in terms of three physical mechanisms. The most important of these is the first precipitation of condensed water from the rising parcel of air. This provides high concentrations early in the shower and low concentrations in the heavy rain are a logical sequel. Dilution of the supply of contaminants by condensation of excess water in the rising air further contributes to the low concentrations in the heavy rain. Evaporation of water from raindrops, both in the initial light rain and in penetrative downdrafts serves as a mechanism to concentrate residue between the cloud and the ground.

Characteristics of individual showers determine which mechanism is dominant at a given time and thus determine concentration variations at a given point. During an individual shower, the mechanism which is dominant may vary as a function of both time and space.

Additional research is needed in several areas. Mass-budget analyses of additional cases should be carried out. This should be done for the pollen contaminant as well as for radioactivity by instituting a collection network to obtain pollen deposition. Additional data on evaporation during light rain, in the form of frequent temperature and humidity profiles and cloud bases, are needed to improve these com-

putations. Further investigation of the structure of the May 10 storm and its relation to scavenging is possible through the use of the FPS-6 radar data, and should be undertaken. Experiments involving the injection of different chemical or radioactive tracers into storms at different heights (i.e., at low and middle levels and at the top) and observation of their respective temporal variations of concentration and deposition rate in rain at the surface are needed. Such experiments could establish characteristic patterns of deposition for high- and low-altitude input against which to compare the corresponding patterns of environmental contaminants.

APPENDIX A

OBSERVATIONAL PROGRAM

A.1 LOCATION OF THE FIELD STATION

The field station was located 2 miles northwest of Chickasha, Oklahoma, and 0.25 mile south of station 11 of the NSSL mesonetwork. Station 11 was also the site of station 5 in a network of automatic rain samplers operated by the University of Oklahoma. The location is shown in Figure A.1. This site was centrally located with respect to the NSSL mesonetwork and the network of recording rain gauges maintained by the U.S. Department of Agriculture, Agricultural Research Service, Southern Plains Branch. The rain gauge network is shown in detail in Figure A.1; its position within the mesonetwork is shown in Figure A.9.

A.2 SITE DESCRIPTION

Figure A.2 shows the distribution of instruments and the sampling station at the field site. The station was located in a wheat field bordered on the west by a dirt road and on the south by railroad tracks. The station was approximately 70 meters from both the dirt road and the railroad tracks. U.S. Highway 62 (State Highway 9) runs along and just south of the railroad tracks. Fields of wheat or alfalfa stretched almost unbroken for a mile or more in all quadrants. The field site was in a region of little relief and few trees and buildings;

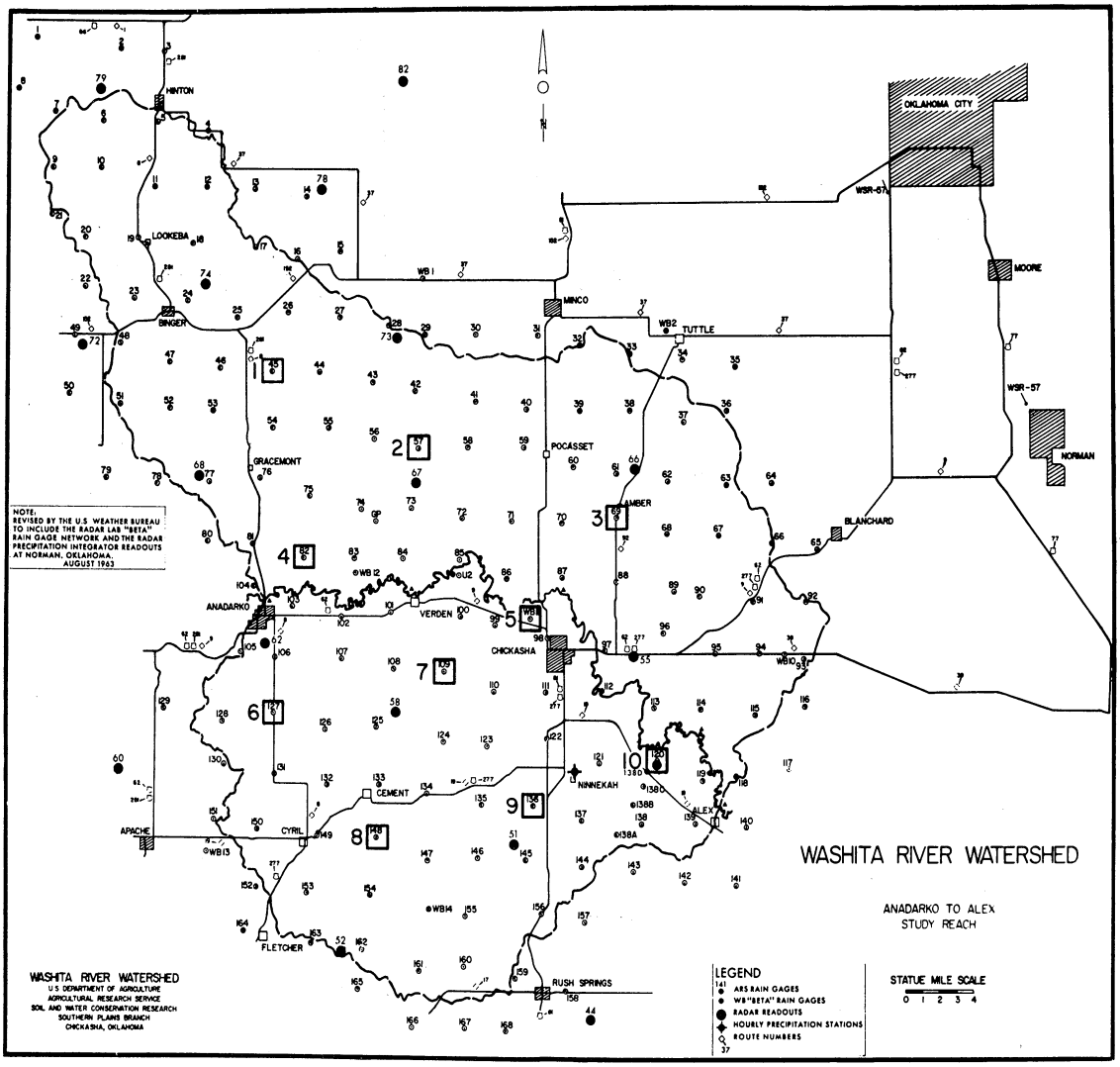

Figure A.1. U.S. Department of Agriculture, Agricultural Research Service rain-gauge network. Stations enclosed by squares indicate locations of University of Oklahoma automatic rain samplers. The University of Michigan field site was 0.25 mile south of automatic sampler station number 5, 2 miles northwest of Chickasha. (From Hall and Nelson, 1964.)

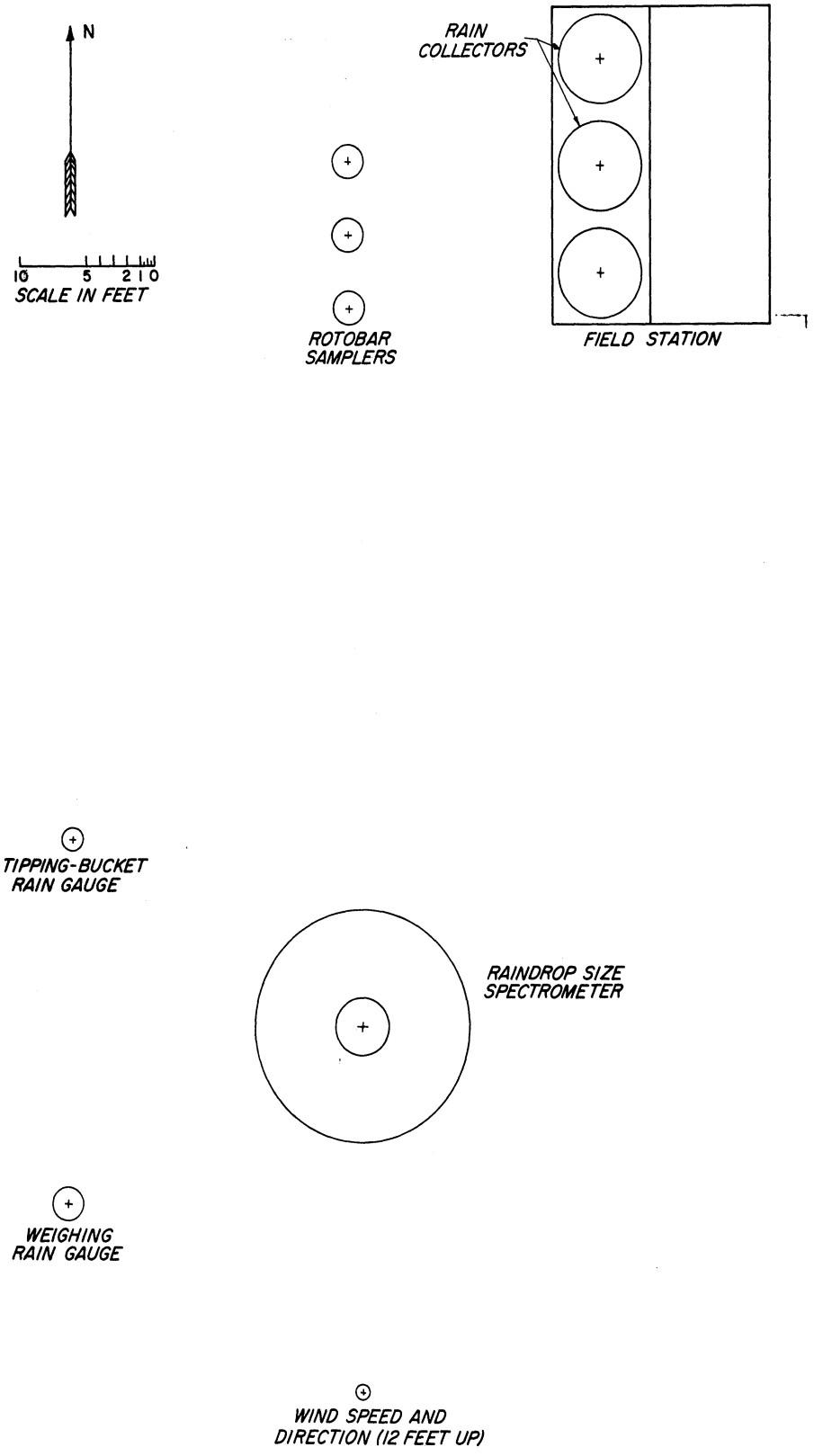

Figure A.2. Plan of field site, showing distribution of instruments about the field station. The location was chosen so that the southwest corner of the field station was about 70 m from the roadway to the west and an equal distance from the railroad right-of-way to the south.

thus the flow of air as it approached the station was relatively undisturbed by surface obstructions. Figure A.3 is a view looking southwestward from the field station, showing the location of rain gauges, wind instruments, and the raindrop spectrometer tent at the site and a general view of the landscape.

A.3 SITE INSTRUMENTATION

A.3.1 Rain Collectors

Three specially constructed fiberglass funnels were used to collect samples of rain. Each funnel has a horizontal sampling area of 2.5 m^2, giving a total area of 7.5 m^2. The slope of the funnel sides is 45° to insure rapid drainage and to minimize splash losses. An 8-in. vertical lip extends upward from the top of the conical section. A 4-in. diameter exit tube is provided at the bottom. Figure A.4 shows the funnels mounted on the roof of the field station with the exit tubes extending through the roof to the inside of the station. Easy access to the funnels from the bottom is provided in case they became clogged with giant hail. Flexible plastic tubing is used to carry the rainwater to the bottling station, located under the center funnel. Figure A.5 shows the outlet from the rain collecting funnels and a flexible plastic tube leading to the bottling station.

The use of three moderately sized collectors instead of a single large one offers several important advantages. Most important, it is possible to take samples of equal size in comparable periods of time,

Figure A.3. View from roof of field station, looking southwestward, May 1965. The height of the wheat in May 1964 was approximately 1/3 of that shown here. Note the flat landscape and few buildings or trees.

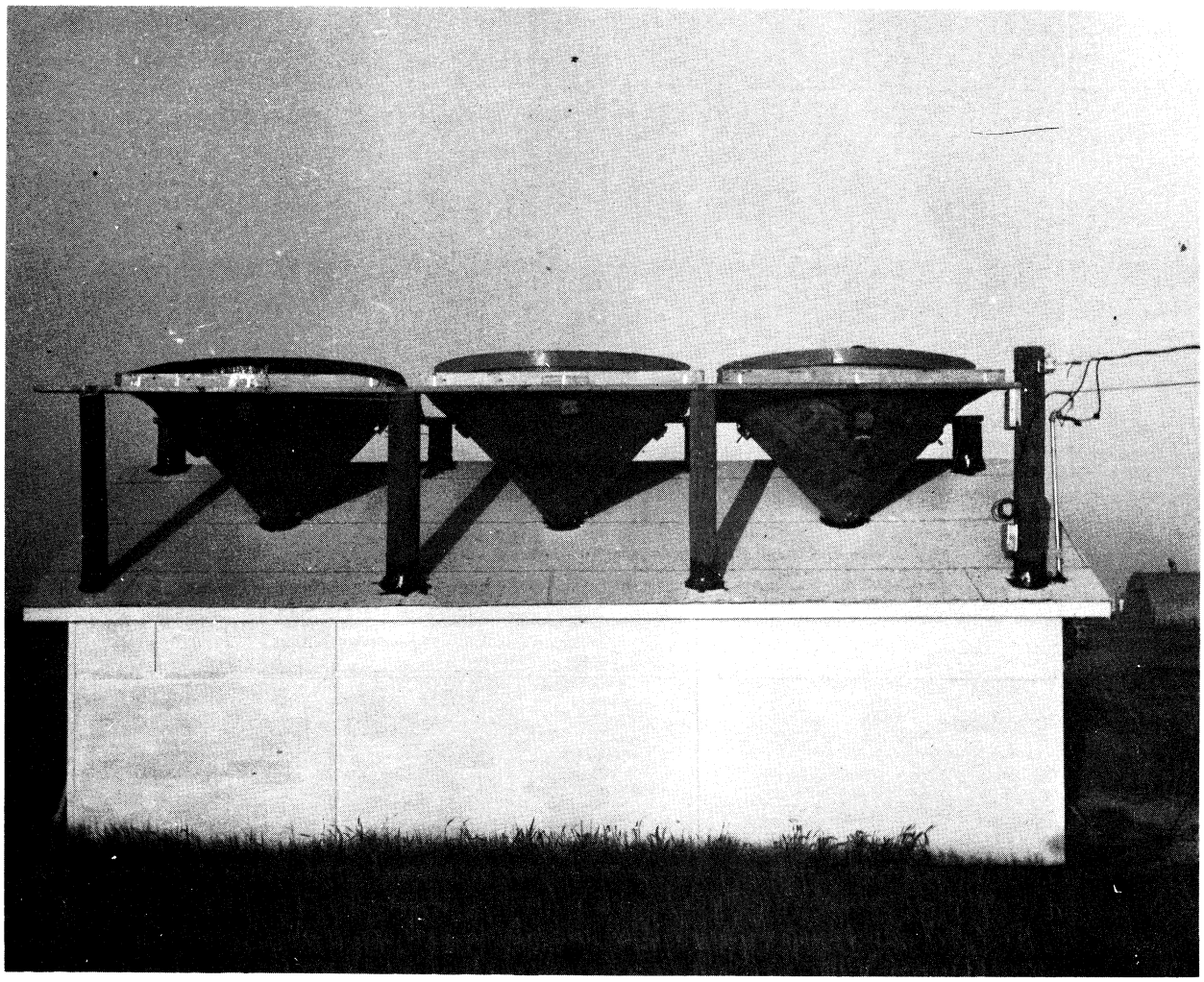

Figure A.4. West elevation of the field station, showing the three rain-sampling funnels and the eight power-line poles which served both to support the funnels and to anchor the field station under severe storm conditions.

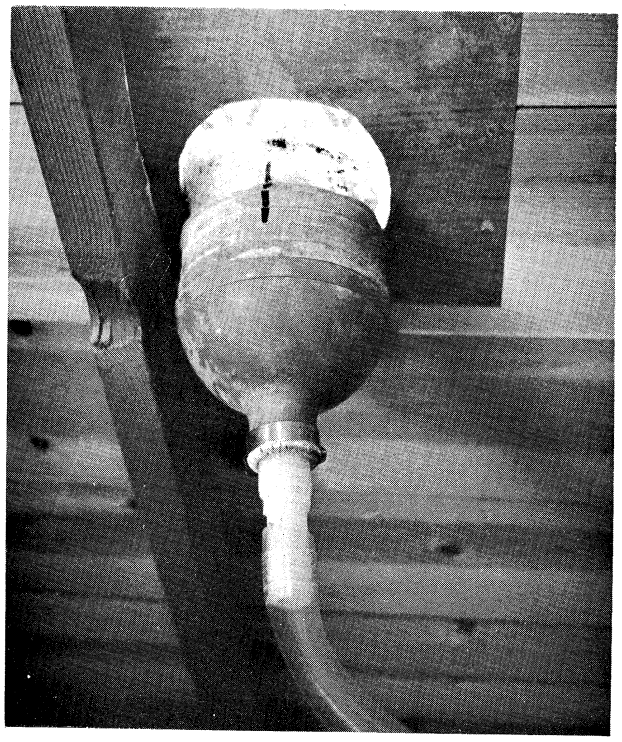

Figure A.5(a). Outlet from rain-sampling funnel and connection to plastic tube.

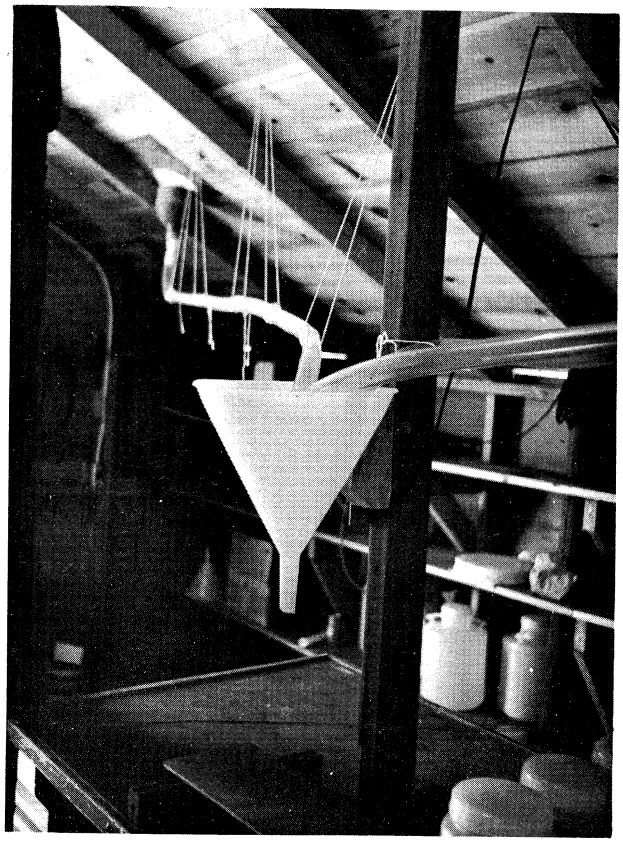

Figure A.5(b). Bottling station and plastic tubes.

even if the rainfall rate changes, by diverting water from one or two funnels as the rainfall rate increases. Figure A.6 shows the relationship between rainfall rate and the time required to collect 4 liters of water. For example, with all three funnels it requires 0.32 min (approximately 19 sec) to collect 4 liters of water at a rainfall rate of 100 mm hr^{-1}.

Convenience of cleaning, transporation, and handling are other advantages of the use of three units.

A.3.2 The Photoelectric Raindrop-Size Spectrometer

The photoelectric raindrop-size spectrometer has been described by Dingle and Schulte (1962). The basic principle of operation is that a raindrop falling through that portion of a thin beam of light observed by a photocell will scatter light to the photocell in proportion to the square of the drop diameter. The instrument used during May, 1964, was an improved version of the one described in the reference given above.

To provide a uniform dark background for the sensitive field of the spectrometer, the instrument is surrounded by a special black canvas tent, shown in Figure A.3. Figure A.7 shows the spectrometer and some of its associated electronic apparatus with the tent partially removed.

The output from the spectrometer is recorded on an oscillograph where two or more channels may be used to expand the useful dynamic range of the record.

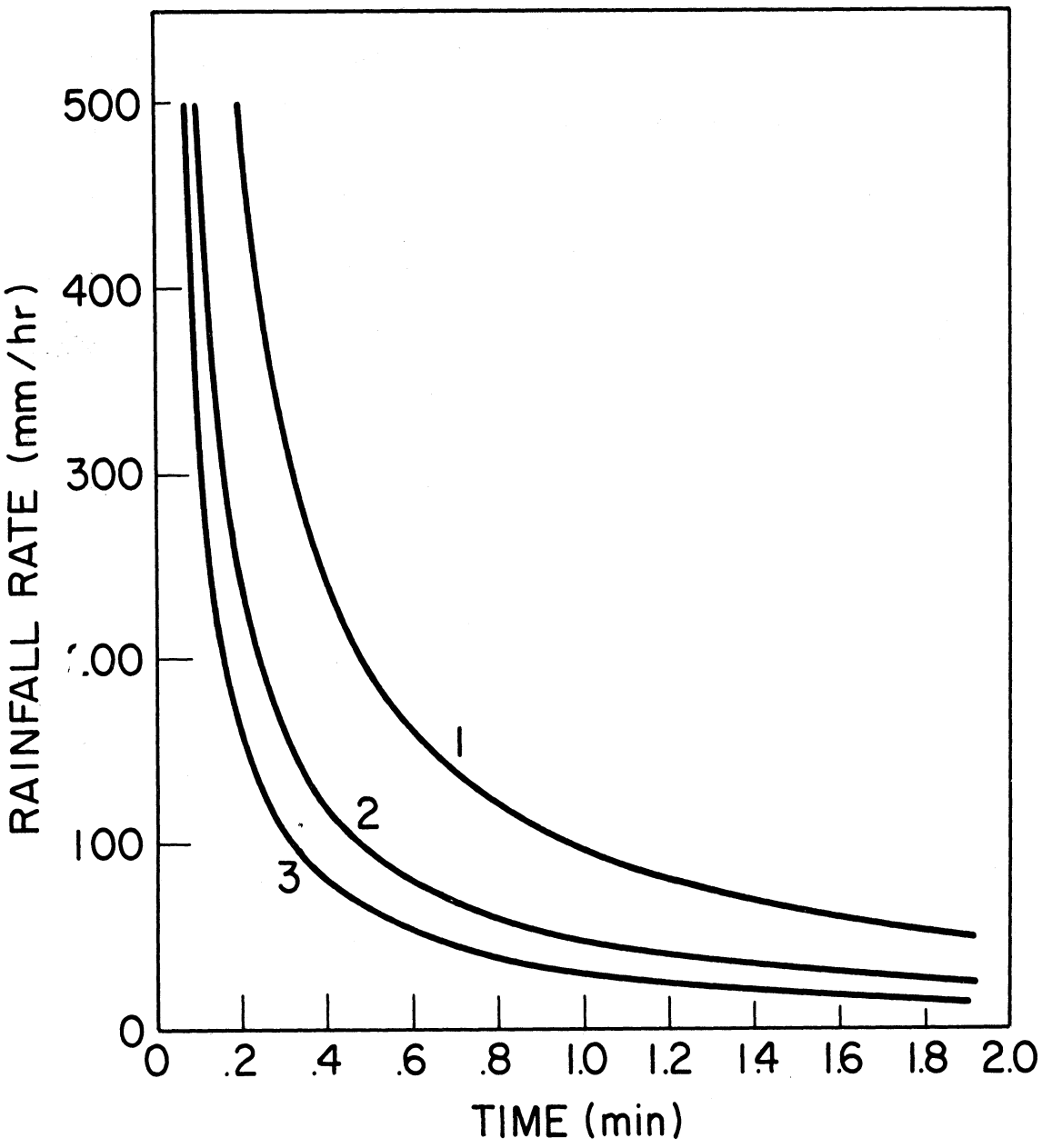

Figure A.6. The relationship between rainfall rate and the time required to collect 4 liters of water, for sampling areas of (1) 2.5 m^2, (2) 5.0 m^2, and (3) 7.5 m^2.

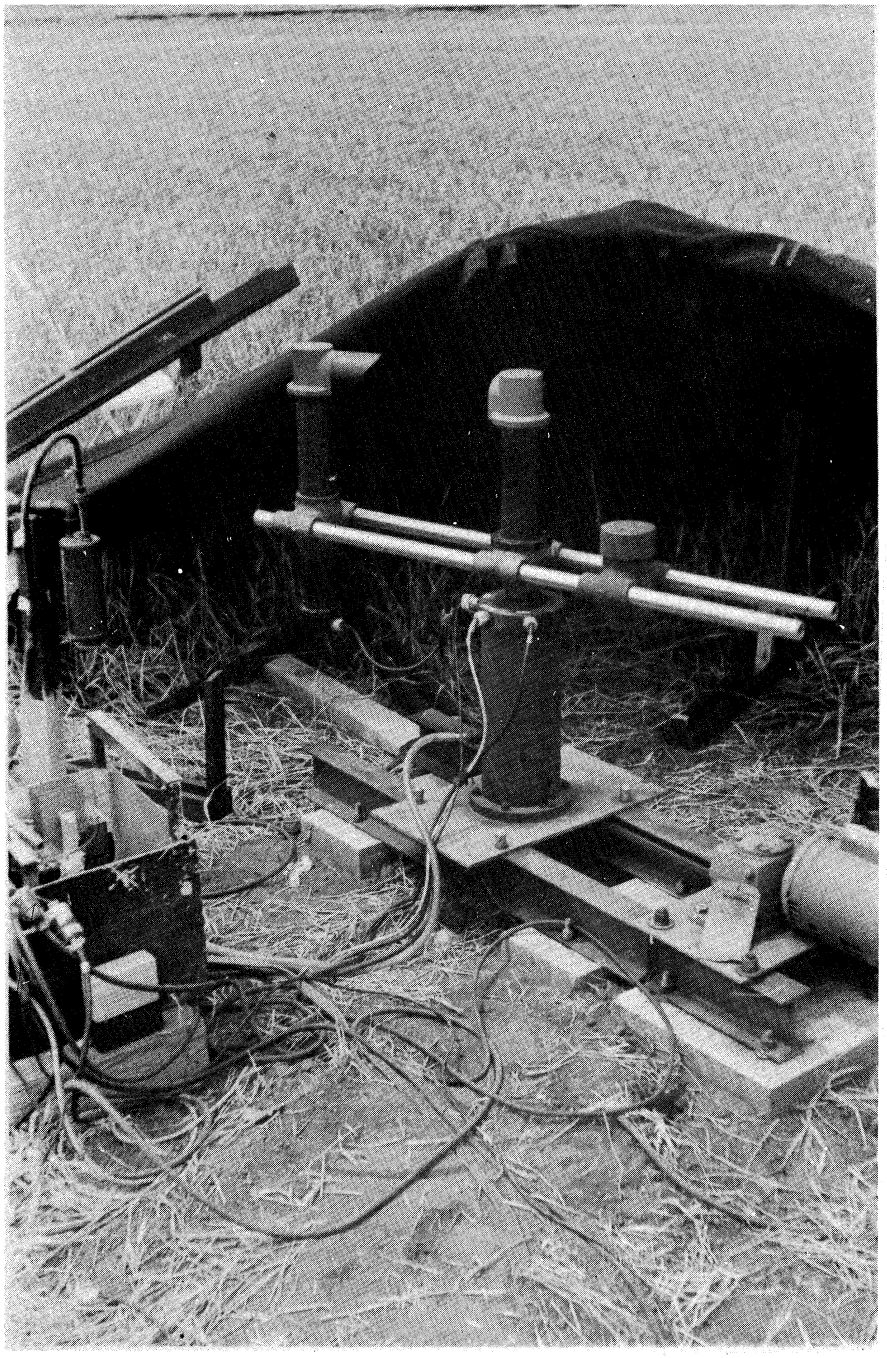

Figure A.7. The raindrop-size spectrometer and associated equipment with the tent folded back.

A.3.3 Rain Gauges

Rainfall was monitored by two recording rain gauges. The field positions of the rain gauges are shown schematically in Figure A.2, and the gauges are shown in Figure A.3 as well.

A 12-in. Belfort Instrument Co. tipping-bucket rain gauge was used to collect detailed data on variations in rainfall rate. This instrument records an event mark on an Esterline Angus (EA) recorder for every 0.01 in. of accumulated rain.

An 8-in. diameter weighing rain gauge equipped with a tenfold magnifying funnel collector was also used to record accumulated rain continuously on a 6-hr chart.

A.3.4 Wind Speed and Direction

The wind instruments were placed on a pole at a height of 12 ft above the ground. Their position is shown in Figure A.3.

Wind speed was measured by a Bendix-Friez 3-cup anemometer. The passage of every 1/60 mile, 1/6 mile, 1/67 mile, and 16.7 miles of air past the anemometer was recorded as an event mark by respective event pens on the EA recorder.

Wind direction was measured by a standard wind vane and recorded continuously by the analog pen of the EA recorder.

A.3.5 Sampler for Airborne Pollens

Concentrations of pollens in air were measured by the rotobar sampler (Harrington, Gill, and Warr, 1959). The sampler is shown in

Figure A.8. This device rotates a thin bar through the air at a constant speed. Particles impinge on the leading edge of the bar because of their inertia and are collected by a thin coating of dilute rubber cement which serves as an adhesive. The instrument samples a volume of approximately 1 m^3 in an hour. It has a collection efficiency of about 70% for a ragweed pollen grain 20μ in diameter. The efficiencies for other pollen grains can be approximated from their physical properties.

A tape recorder was also used to record pertinent observations of weather conditions. The taped comments were later played back and recorded in written form at a convenient time.

A.4 OPERATIONAL PROCEDURES

A.4.1 Rain Collectors

When rain appeared imminent, the three collectors were uncovered and, if several days had passed without rain, their sampling surfaces were scrubbed with tap water. At the beginning of the rain, water was collected from all of the three collectors. As the rainfall rate increased, water was collected from only two collectors or a single one, in order to collect at a rate of one sample per minute. During periods of very low rainfall rate, three collectors were always used.

When sample bottles were changed, an event mark was made on the EA chart by means of a button located near the bottling station. Thus, information on the time of collection of each sample was recorded on

Figure A.8(a). Rotobar pollen sampler, showing rain shield and rotating-bar apparatus, in position at the field site.

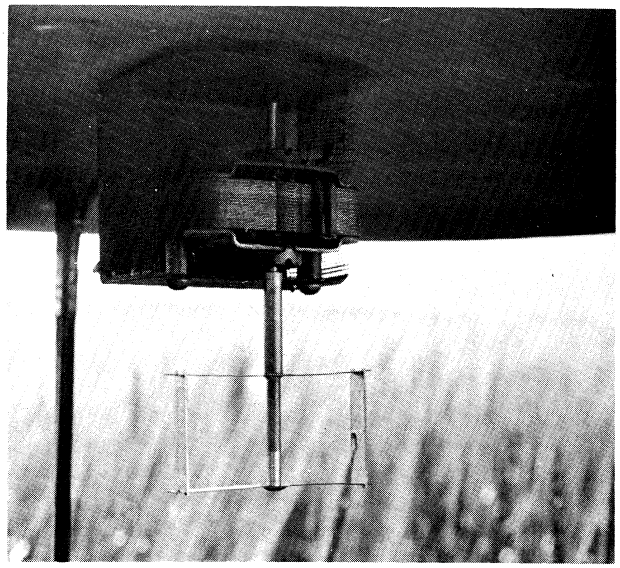

Figure A.8(b). Close-up of rotating-bar apparatus.

the same chart as the wind record and the data from the tipping-bucket rain gauge. Information on the sequence of numbered sample bottles was transcribed on the tape recorder, and also, from time to time, bottle numbers were written on the EA chart.

A.4.2 Raindrop-Size Spectrometer

The electronic circuits of the spectrometer were switched on immediately upon arriving at the field station during a rain alert. About 15 min of warm-up time was necessary. Shortly before the rain began, the source lamp in the spectrometer was turned on and a balancing adjustment was made on the amplifiers at the spectrometer.

Before and after each rain, and during occasional lulls in the rain, the output from a standard glass bead, placed in a standard position in the sensitive field of the spectrometer, was recorded on the oscillograph. These data provided a reference to the spectrometer calibration.

During periods of rainfall, the spectrometer required a nominal amount of attention to keep the galvanometer traces properly positioned on the oscillograph chart, and to maintain a chart speed rapid enough for proper resolution of the pulses. During periods of heavy rain, a faster chart speed was required to resolve pulses from closely spaced drops.

Occasional changes of chart rolls were also required. Upon removal from the oscillograph each roll of light-sensitive paper was

wrapped in black paper and returned to its original box to prevent undue exposure of the paper to light.

A.4.3 Rotobar Samplers

Whenever radar observations showed the presence of rain within 100 n mi of the WSR-57 radar at Norman, sampling was begun as soon as practicable. The usual practice was to expose two bars for a period of an hour. This was done for several hours before the rain. On some occasions, samples were also taken during and after periods of rain.

APPENDIX B

RAINWATER ANALYSIS PROCEDURES

This appendix describes the radiochemical and palynological procedures used in the analysis of the rain samples. To obtain the most information from the rain samples, it was desirable to determine both radionuclides and plant pollens in each sample. Such a procedure insures the maximum resolution of temporal variations of contaminant concentrations consistent with the number of samples collected, and also makes possible the comparison of concentrations of the respective contaminants during the same time interval. Such a capability is desirable so that the temporal variations of the two diverse kinds of contaminants can be compared. There can then be no ambiguity concerning precise times of maxima or minima of one entity with respect to the other, as would be possible, for example, if alternate samples were analyzed for the different entities. Consequently, a procedure was devised which makes possible the determination of both radionuclides and plant pollens in the same sample of rainwater.

As an aid to subsequent analysis, approximately 2.5 ml of a solution of 5 mg of zirconium ion per ml of glacial acetic acid were added for each liter of rainwater in a sample. The zirconium carrier was used to prevent significant adsorption of any of the radionuclides on the walls of the sample bottles. The glacial acetic acid likewise acted to reduce adhesion of suspended particulate matter to the walls

of the containers. To prevent bacterial destruction of pollen grains, 10 ml of formalin were added per liter of rainwater.

The rain samples were transported by truck from the field site to the laboratories of the National Sanitation Foundation, School of Public Health, The University of Michigan, for analysis.

B.1 DETERMINATION OF RADIONUCLIDE CONCENTRATION

The analysis procedure described below provides for the determination of concentrations of six individual gamma-ray-emitting radionuclides, or groups of radionuclides, as well as concentrations of gross beta radioactivity and total solids. These quantities were determined in each sample; however, only total beta radioactivity is reported here.

Sample volume was determined by measurement of the liquid contents of each sample bottle in a graduated cylinder. The rain was then transferred to a 4-liter beaker. The graduated cylinder was washed three times with distilled water, each wash being added to the large beaker. Loose sediment was transferred from the sample bottle to the beaker with a little distilled water. The sides of the sample bottle were scrubbed with a rubber spatula and a solution of distilled water and ethanol. (For convenience, only wide-mouth sample bottles were used.) This wash and a following distilled water wash were added to the large beaker.

The volume of each sample was reduced by evaporation on a hot plate to approximately 50 ml, and then transferred to a 150-ml beaker. The walls of the large beaker were scrubbed with distilled water and a rubber spatula, and the washes were added to the small beaker. Care was taken to insure that no sample evaporated to dryness on the hot plate to avoid charring the pollen grains and other residue in the sample. The remaining solution was transferred to a stainless steel planchet. The last of the solid material in the beaker was washed into the planchet with a stream of distilled water. The solution was evaporated to dryness in the planchet under a heat lamp, again with care to avoid charring the solid sample. Subsequent examination of the residue by microscope showed no evidence that pollen had been charred during the sample analysis procedure.

The mass of the solid residue was found by subtracting the predetermined mass of the empty planchet from the combined mass of residue plus planchet. Both measurements were made with an analytical balance. Due to incomplete dissolution of the ZrOCl salt used as a source of zirconium ions, or formation of another insoluble salt, a crystalline precipitate was present at the bottom of the storage jug. It is likely that some of this solid matter was transferred to some of the sample bottles along with the carrier solution. Because the total mass of salts added to each sample is unknown, it was impossible to correct the residue concentrations for this error; consequently one must use

caution in interpreting residue concentrations. A look at Figures 3.3 and 3.13 shows that general trends are probably significant, particularly at the beginning of showers, when natural residue is abundant in the rain, but high frequency variations are almost certainly caused by the error discussed above.

Gross beta radioactivity was measured with a low-background (1 cpm) flow-type beta counter which had been calibrated with a thallium-204 source. The total count was corrected for internal absorption of beta particles within the sample.

No correction for radioactive decay was made. Such a procedure was justified owing to the long period of time between the last known atmospheric detonation, in December, 1962, and the date of collection. The samples were all counted within two months of each other and within four months of collection. Since such periods are short relative to the half-lives of the bulk of the beta-emitting radionuclides remaining in the atmosphere in May, 1964, no correction for radioactive decay was deemed necessary. Concentrations of both beta- and gamma-emitting radionuclides are shown as a function of time for May 9 in Figure 3.1. The parallel variation of the beta curve with respect to the decay-corrected total gamma curve is ample evidence that decay-correction was unnecessary in this case. The same conclusion follows from comparison of the gamma and beta concentrations for the other rains sampled.

Determination of the amount of radioactivity or mass of residue in a sample and the volume of that sample makes it possible to compute the

concentration of radioactivity or residue. From the sampling area, the sample volume, and the time required to collect a sample, one may compute a rainfall rate for a sample; when this is multiplied by a concentration, the result is a deposition rate. For each sample collected, the following quantities were computed: the concentration of gross beta radioactivity, the concentration of non-volatile residue, and the deposition rate of total beta radioactivity. Tabulations of these quantities are given in Appendix D for May 9 and 10, 1964.

It is essential to state the magnitude of the error to be associated with these parameters. The magnitude of the standard deviation σ_D to be applied to any derived result D, such as concentration or deposition rate, is computed from the equation

$$\sigma_D = (K_1^2 + K_2^2 + \ldots + K_n^2)^{\frac{1}{2}}$$

where

$$K_j = \frac{\partial D}{\partial j} \sigma_j$$

and σ_j is the standard deviation of any component j of the derived result. For example, the derived result for concentration is

$$C = \frac{A}{V}$$

and is composed of components A (total radioactivity) and V (sample volume). Thus

$$\sigma_C = \left(\left(\frac{\partial C}{\partial A}\right) \sigma^2_A + \left(\frac{\partial C}{\partial V}\right)^2 \sigma^2_V\right)^{\frac{1}{2}}$$

which reduces to

$$\sigma_C = \left(\left(\frac{C}{A}\right)^2 \sigma^2_A + \left(\frac{C}{V}\right)^2 \sigma^2_V\right)^{\frac{1}{2}} \qquad \text{(B.1)}$$

Sample volume was usually determined to the nearest 10 ml. This implies a possible error of ±5 ml, which is negligibly small compared to the volume of a typical sample, i.e., $\geq$ 2000 ml. The second term of Equation (B.1) can therefore be neglected. Using a standard deviation due to counting $\sigma_A = 0.05 \cdot A$ (see Chapter 3) and typical values of C and A, (which may be obtained from Tables C.1 and C.2) one may verify that σ_C amounts to about 5% of C on May 9 and 10. This implies two standard error limits of ±10% for the concentration of radioactivity. Similar computations for the deposition rate, using a standard deviation σ_T of sample collection time T of 1 sec, lead to two standard error limits of ±14%. These limits are very acceptable, especially in view of the magnitude of the variations of the parameters involved.

B.2 DETERMINATION OF POLLEN CONCENTRATIONS

The pollen analysis was performed directly on the residue in the stainless steel planchets, after all counting for radioactivity had been done and checked. Pollen grains in the original sample were counted by the "additive pollen" technique of Benninghoff (1962; also see Stoutamire and Benninghoff, 1964). A known number of grains of an exotic genus (one which would not appear naturally in the samples under analysis) was added to each sample in the planchet before the pollen analysis procedure began. After treatment of the sample and preparation of microscope slides, both the exotic grains and the native

grains of interest were counted. Only a fraction of the entire sample was examined under the microscope. The total number of each native type was computed by multiplying the number of that type counted by the fraction (exotic grains added/exotic grains counted).

The exotic pollen used was eucalyptus. Non-defatted eucalyptus pollen was suspended in tertiary-butyl alcohol (TBA). The concentration of eucalyptus in TBA was determined by the method of Davis (1965). Results of counting three slides showed that 12,024 (standard error = 223) grains of eucalyptus pollen were contained in 0.20 ml alcohol, the volume added to each sample.

The samples were acetolyzed using a procedure adapted from Erdtman (1943), and six microscope slides were prepared from each sample. Glycerine jelly was used as the mounting medium. The cover slips were ringed with cement to prevent dessication.

After examination of several slides from each rain, several pollen types were chosen for identification. The same types were chosen for both rains. Criteria for the choice of the types to be counted were that the pollens selected should be abundant, and that they should provide a large range of diameters between types. It was, of course, necessary for a chosen type to be present in a large fraction of the samples.

The pollen types chosen for counting are listed in Table B.1, together with pertinent characteristics of size and shape. In addition to the types listed, a separate total of all other pollens present,

TABLE B.1

POLLEN TYPES DETERMINED IN RAIN WATER SAMPLES, 1964

Type	Taxon	Shape	Diameter (μ)	
			Measured[1]	Literature[2]
Willow (*Salix*)	genus	spheroidal or oblate	18 x 16	17-18
Oak (*Quercus*)	genus	spheroidal (flattened and angular when moist)	25 (3)	range: 30 x 25 to 30 x 26 (expanded)
Black walnut (*Juglans nigra*)	species	oblately flattened	34[3]	31-34
Hickory (*Carya*)	genus	spheroidal or oblate	44[3]	40-52
Pine (*Pinus*)	genus	ellipsoidal body, two spheroidal air bladders	67 x 44 (1)	46-65[3]
Chenopods/ Amaranths	families	spheroidal	25 (1)	19-13 (moist and expanded)
Grass (*Gramineae*)	family	spheroidal, ovoidal, or ellipsoidal	25-59[3]	22-100
Composites (*Compositae*)	family	spheroidal	20	19-40
Sorrel (*Rumex*)	genus	spheroidal or ellipsoidal	19	18-32

[1]Average of measurements (parentheses indicate number measured if <10) of non-acetolysed pollen in glycerine jelly.
[2]Wodehouse (1935).
[3]Largest diameter.

representing a wide range of sizes, was tabulated. Note that literature values of grain sizes are given in the form of a range. The range accounts primarily for systematic differences in size between species in a particular genus or family. Reference is sometimes made to the condition of the grain when measured (e.g., "moist and expanded"). This specification is necessary because grains collapse and fold to some extent upon partial dessication. Inference of the size of a grain suspended in the atmosphere from measurements made upon expanded grains is not straight-forward, but a rough estimate is that the maximum dimension might be reduced by 10%. Grain shape is probably more severely affected than the maximum diameter. Photomicrographs of representative grains of most of the types are shown in Figure B.1. For a more complete description and additional photographs of each type, see Wodehouse (1935).

As in the case of the radionuclides, both concentrations and deposition rates of individual genera and total pollens were computed. These are tabulated for each storm, together with the radioactivity data, in Appendix D.

The following error analysis of the total pollen determinations was made from counts of two or more replicate slides from each sample. This analysis neglects error introduced from measurement of sample volumes, which has been shown earlier to be negligibly small. Let $x_1, x_2, \ldots, x_k$ be the total (native) pollen concentration of the sample, computed from each of k slides, and $n_1, n_2, \ldots, n_k$ be the number of exotic

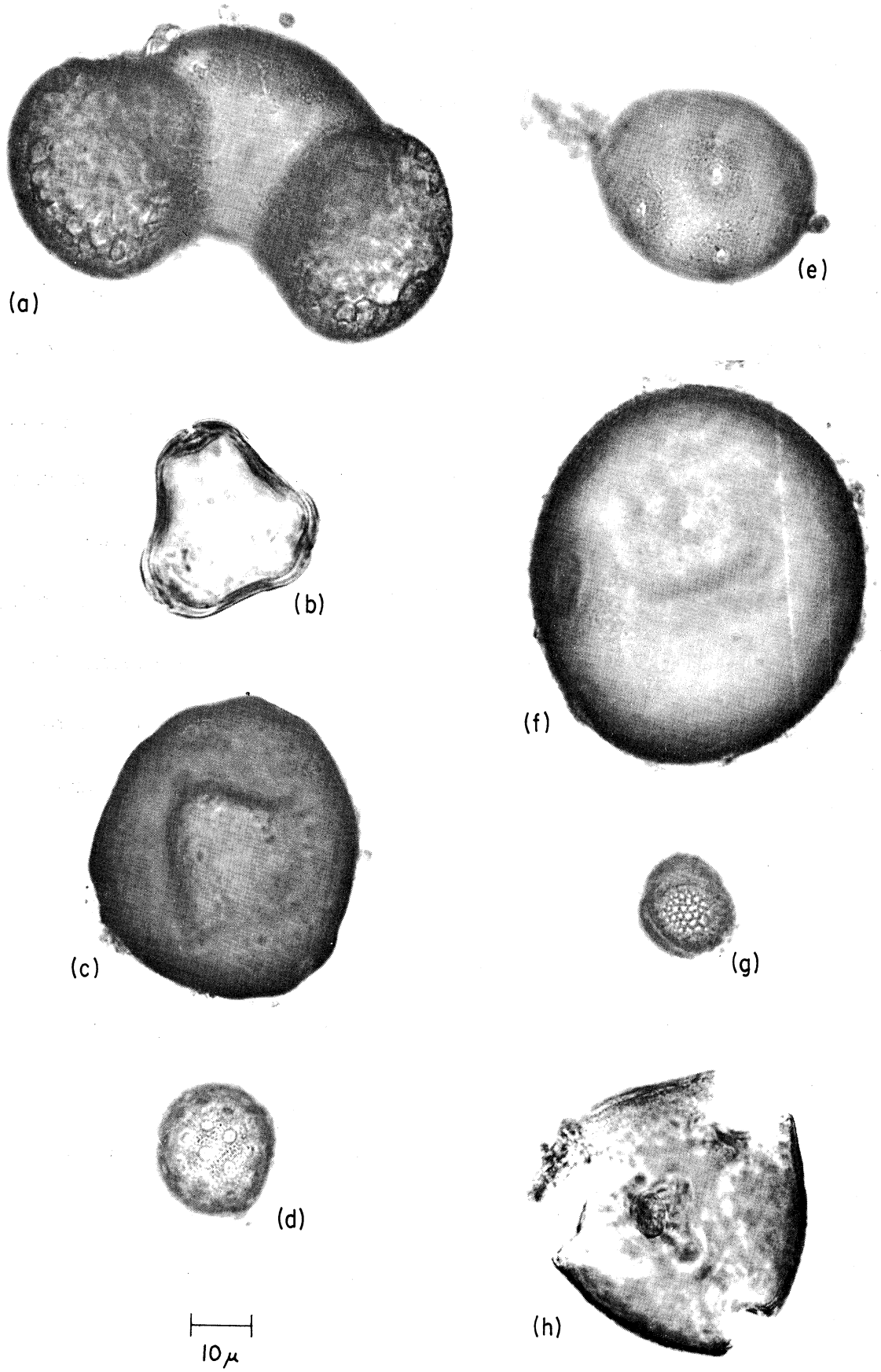

Figure B.1. Photographs of some pollens determined in rain samples. (a) pine (b) eucalyptus (added) (c) hickory (d) chenopod/amaranth (e) black walnut (f) grass (g) willow (h) oak.

pollen counted on each slide. Then the concentration of total pollen T, computed from the sums of total native and exotic pollen on all slides counted is given by

$$T = \frac{\sum_{i=1}^{k} n_i x_i}{\sum_{i=1}^{k} n_i}$$

and the standard error σ_T of T is given by

$$\left\{\left[\left[\frac{1}{\left(\sum_{i=1}^{k} n_i\right)^2}\right]\left[\sum_{i=1}^{k} (n_i^2)\right]\right]S^2\right\}^{1/2}$$

where

$$S^2 = \frac{\sum_{i=1}^{k} n_i (x_i - T)^2}{\sum_{i=1}^{k} n_i}$$

Because of the low number of slides counted, three standard error limits have been applied to concentrations of total pollen. These limits correspond to a confidence interval of at least 90%, from Chebyshev's Inequality, a very conservative measure. They are shown graphically in Figures 3.3 and 3.13 and are tabulated in Appendix D.

Three standard error limits for pollen deposition rate are shown in Figures 3.4 and 3.14 and are tabulated in Appendix D. These errors were computed by assuming that the error of sample timing was negligible

compared to the statistical error of counting, which was discussed above. Thus, the error applied to the pollen deposition rate and that of the pollen concentration amount to equal percentages of their respective parameters.

APPENDIX C

ANALYSIS PROCEDURES FOR OTHER DATA

C.1 DATA COLLECTED AT THE CHICKASHA FIELD SITE

C.1.1 Tipping-Bucket Rain-Gauge Data

The operation of the tipping-bucket rain gauge is such that a series of event marks, each indicating the accumulation of approximately 0.01 in. of rain, is recorded on the EA strip chart. The strip chart is driven at a constant known speed; thus it is possible to determine the time interval required to collect each increment of rain, and thence to compute the rainfall rate for that interval. Such rainfall rate estimates are properly plotted as functions of time in the form of bar graphs, the area under every bar being equal and representing the accumulation of 0.01 in. of rain. In heavy rain, however, the bars become long spikes which are difficult to resolve. Therefore it was convenient in some of the present cases to draw line graphs, connecting points of rainfall rate which were plotted at the midpoints of their respective time intervals. Such a curve is extremely useful in delineating fine structure in the rain field, but one must realize that individual points on the curve are not averages over equal time periods. Individual points may represent averages over periods ranging from several seconds to an hour or more.

The gauge was calibrated, after proper leveling, by carefully dripping a measurable amount of water from a buret into one side of the bucket until it tipped. At least 15 tips of each side were made.

Calibration revealed several interesting things. It required on the average 0.0113 in. of rain to make the bucket tip; furthermore, there was a significant difference (significant at the 5% level) between the rainfall required to tip the respective sides of the bucket. In addition, the amount of rainfall required to tip a given side was not constant. On the assumption that the individual amounts of rainfall required to tip a particular side of the bucket was normally distributed, the 95% confidence interval of the mean was computed for each bucket. Because in practice it was not possible to associate a particular bucket with an event mark indicating a tip, the lowest and highest values from the respective confidence intervals were used to compute the 95% confidence interval of the rain fall rate, shown as a function of the rate in Figure C.1. The figure shows, for example, that one may have 95% confidence that the true value of an indicated rainfall rate (i.e., in Figures 3.3, 3.4, 3.13, or 3.14) of 100 mm/hr lies between 90.8 and 109.2 mm/hr.

C.1.2 Airborne Pollen Data

Preparation of microscope slides was facilitated by applying the dilute rubber cement adhesive over a layer of double coated (both sides) cellophane tape which had been previously applied to the metal bars.

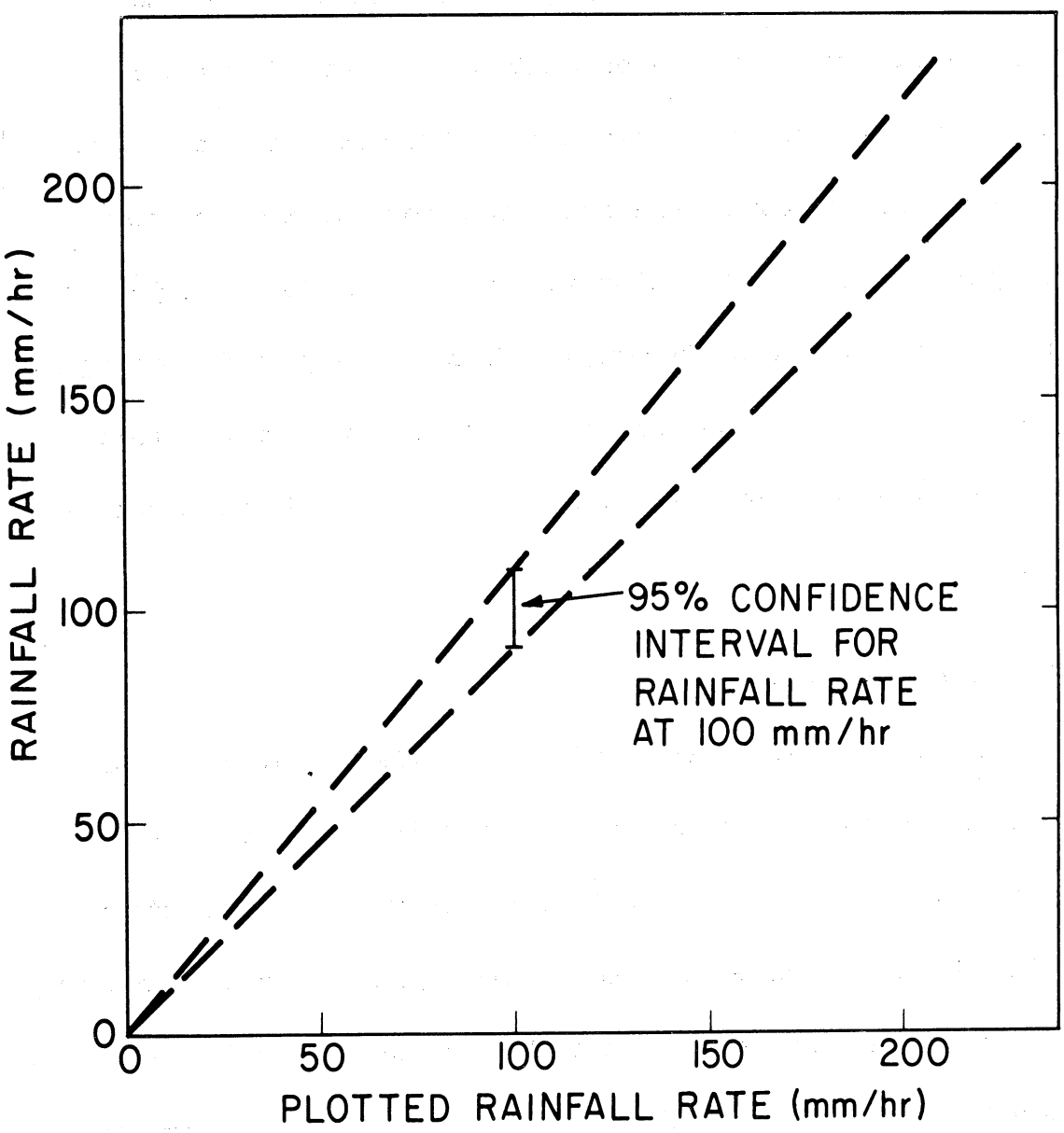

Figure C.1. Reliability of rainfall rates computed from tipping bucket rain-gauge data, 1964.

In preparing a slide of the sample, the tape was carefully removed from the bar and placed flat on a slide, sample up. A streak of melted glycerine jelly, containing a small amount of saturated aqueous basic fuchsin was placed on a cover slip, which was then inverted and placed on the sample. After warming the slide for about 5 min and removing air bubbles by applying slight pressure on the cover glass, the sample was stored for about a week to allow the stain to darken the pollen grains. Numbers of grains were determined using a microscope.

C.2 DATA FROM OTHER GROUPS

The location of the field site and the time period of the observations were chosen to coincide with data collection programs of several other research groups. Thus we were able to concentrate on collecting very detailed data on rain scavenging at a particular point, knowing that specialized meso-scale data on the precipitation system, as well as scavenging data from the surrounding area, would be available. Several kinds of supporting data have been made available to use by other groups. This section describes the data acquired from other sources, the circumstances of their collection, and our preparation procedures.

C.2.1 Rain Gauge Network

The Agricultural Research Service (ARS) maintains a network of 175 recording rain gauges in the Washita River watershed between

Anadarko and Alex, Oklahoma. The watershed and the rain-gauge network are shown in Figure A.1. The rain gauges are of the weighing type, and they record accumulated rainfall on 12-hr charts. The gauges are spaced at intervals of 3 to 4 miles; the entire network covered an area of about 1200 square miles.

Accumulated time and rainfall were read from the rain gauge charts and punched on cards by the ARS. Readings were made at inflection points on the curve of accumulated rainfall. Because of the time scale on the charts, the data were ordinarily read at intervals of 5 min or longer. Accumulated time was read to the nearest minute, and rainfall to the nearest hundredth of an inch.

From punched data on accumulated rainfall and elapsed time, a series of rainfall rates was computed for the intervals between chart readings. The intervals were of varying length; in practice, however, readings were taken such that rainfall rates were relatively constant in each interval. This made possible a valid comparison of rates at different gauges.

It was desired to reconstruct the rainfall rate pattern over the watershed at 10-minute intervals. For example, on May 9, maps were drawn representing conditions at 2030, 2040,...,2130. The value of rainfall rate at a particular gauge at 2030, say, was taken as the value corresponding to the time interval spanning 2030. In cases where the map time coincided with a gauge reading, an arithmetic mean of the rates associated with the time intervals adjacent to the map time was used.

Rainfall rates were machine-plotted at the locations of the respective gauges. Contours of the rainfall rate field were drawn by hand, using the original rate computations at individual stations as a guide. A time series of such maps (e.g., Figure 3.10) shows the motion of rain systems in more detail than is possible from radar data. Moreover, the rain-gauge data represent conditions at the surface, whereas radar, even at 0° elevation, must necessarily integrate over a layer above the surface.

Maps of total squall line rainfall were similarly prepared by machine for both days of interest (Figures 3.11 and 3.21).

C.2.2 Radar Observations

Radar surveillance of the study area was provided by four radar sets. The WSR-57 radars at Norman (NRO) and Will Rogers Field, Oklahoma City (OKC), scanned horizontally (PPI). Two vertically scanning (RHI) radars, an MPS-4 at NRO, and an FPS-6 at Tinker Air Force Base (TIK) were also in operation. The latter was operated by the Weather Radar Branch of the Air Force Cambridge Research Laboratory. The radar sites are shown on the map in Figure C.2. Except for the WSR-57 radar at OKC, these radars were operated exclusively for the purpose of collecting research data on severe storms.

The available physical characteristics of the radars are listed in Table C.1. Processing of the radar data was limited to PPI data from the WSR-57 radar at NRO. Echo outlines were traced for a series

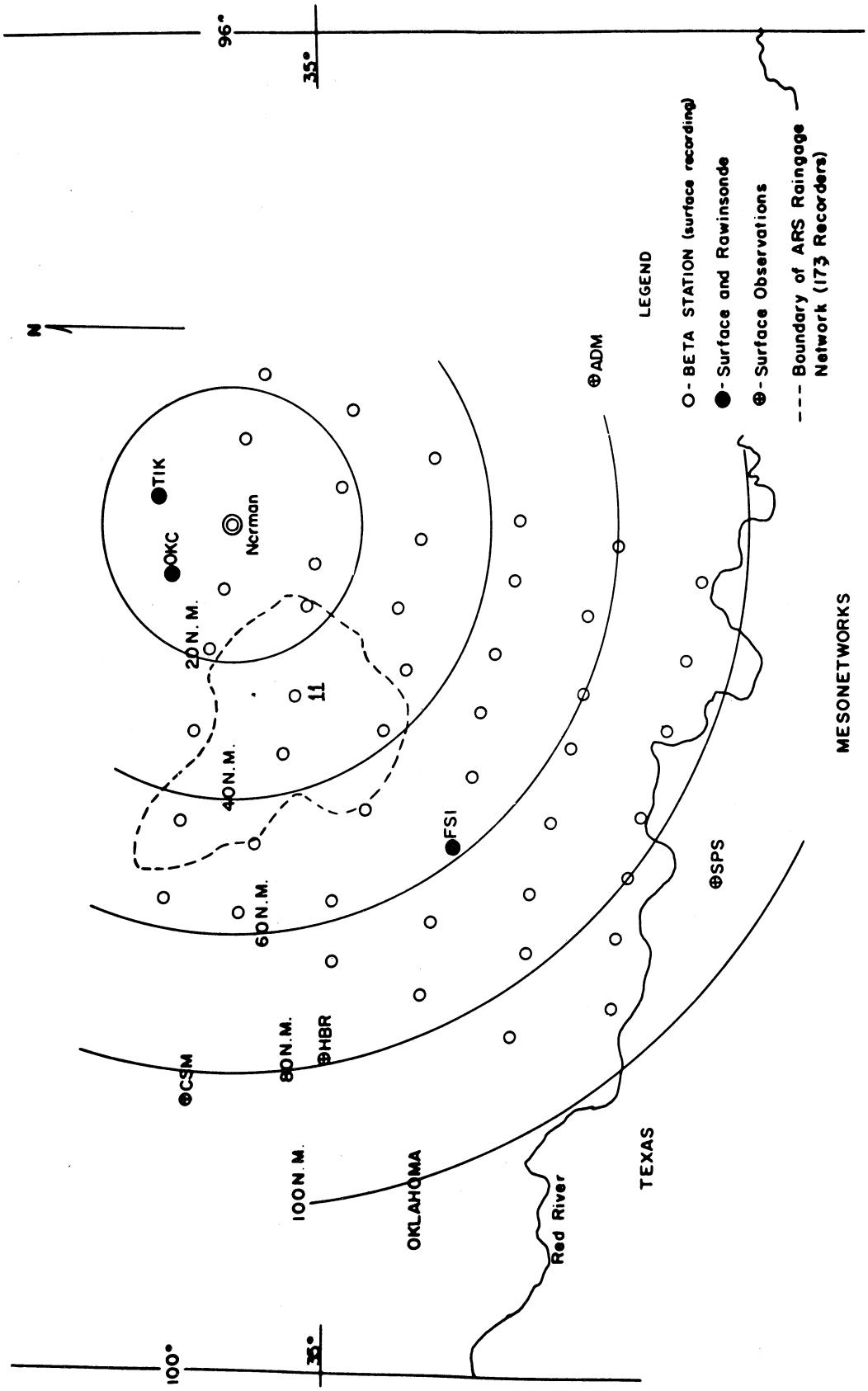

Figure C.2. Map of study area, showing radar sites at Norman, OKC, and TIK. The NSSL mesonetwork stations are shown as open circles; station 11 is indicated. The dashed line outlines the ARS raingauge network.

TABLE C.1

CHARACTERISTICS OF RADAR

Name	Location	Wave Length	Peak Power (megawatts)	Pulse Repetition Frequency (pulses/sec)	Pulse Width (μsec)	Beam Width (half power) (degrees)		Scan Rate (scans/min)
						Vertical	Horizontal	
WSR-57	NRO	10.4	0.50	---	4	2	2	3.3
WSR-57	OKC	10	--	---	--	--	-	--
MPS-4	NRO	4.67	0.14	---	1.37	0.8	4	60
FPS-6	TIK	10	5.2	360	2	0.86	3.5	20

of stepped-gain reductions below maximum sensitivity to show the distribution of echo intensity. A time series of such maps was prepared to show the movement of echo centers with respect to the rain collection site on the days of interest. (Figures 3.8 and 3.18.) Contours represent reductions below maximum sensitivity in units of decibels (db). Corresponding values of radar reflectivity Z_e are given in Table C.2.

TABLE C.2

RADAR REFLECTIVITY

Contour No.	Attenuation (db)	Z_e (min) ($mm^6\ m^{-3}$)
1	-100	17.7
2	- 94	70.2
3	- 88	2.80×10^2
4	- 82	1.11×10^3
5	- 76	4.44×10^3
6	- 70	1.77×10^4
7	- 64	7.02×10^4
8	- 58	2.80×10^5
9	- 52	1.11×10^6
10	- 46	4.44×10^6

C.2.3 The University of Oklahoma Network of Automatic Rain-Sampling Stations

The Atmospheric Research Laboratory, University of Oklahoma, operated a network of ten automatic rain-sampling stations in the ARS rain gauge network. The locations of the stations are shown in Figure C.2. The samplers were designed to collect 12 sequential 4-liter samples without attention. One sample was collected for every 0.05 in. of rain, depending on wind conditions. Further details of the sampling network are given by Saucier, et al., (1965). Data for May 9 and 10 have been made available to us. These data have been discussed by Hall (1965).

C.2.4 Surface Network

Temperature, pressure, relative humidity, rainfall, and wind speed and direction were recorded continuously at 47 mesonetwork stations in south central Oklahoma. Locations of these stations are shown in Figure C.2. Temporal variations of temperature, pressure and relative humidity were traced in composite (Figures 3.12 and 3.22) from microfilm records of original charts from station 11. Errors in chart times were corrected.

Mesoanalyses of the pressure field were made following the method described by Williams (1963). The method consists of analysing values of altimeter setting, i.e., equivalent sea level pressure. The procedure eliminates the effects of small inaccuracies in barograph settings and imprecise knowledge of station elevation. Corrections to be applied

to individual barograph readings to obtain altimeter setting values are determined by comparison of barograph readings with smooth fields of altimeter setting, analyzed from nearby synoptic stations, at times before and after the events of interest. The average of the corrections so determined is applied to the barograph reading at each mesonetwork station to obtain the values of altimeter setting used in the analysis.

C.2.5 Local Rawinsonde Ascents

Rawinsonde ascents were made from three sites in the area: OKC, TIK, and Fort Sill, Oklahoma (FSI). FSI is located about 60 n mi southwest of OKC. (See Figure C.2.) Regular ascents were made at OKC at 0000 and 1200 GMT (0600 and 1800 CST). Special ascents were made at FSI in connection with the severe storms observation program and at TIK in connection with the Federal Aviation Administration's sonic boom testing program. On May 10, for example, ascents were made at FSI at 0900, 1200, 1500, 1700, 1900, and 2100 CST.

C.2.6 Conventional Synoptic Data

Surface weather maps and 500 mb isobaric analyses were reproduced from the U.S. Weather Bureau series of daily weather maps. Upper air charts were prepared for approximately the jet stream level using checked radiosonde and rawinsonde data from the U.S. Weather Bureau (1964). These analyses are presented in Chapter 3.

Cross-sections were prepared from checked U.S. Weather Bureau (1964) data. Lines of constant potential temperature were drawn at intervals of 2K from the 700 mb level to roughly the tropopause, above which the interval is 5K. Isotachs were drawn at intervals of 10 m/sec. The cross sections for May 9 and 10 are presented in Chapter 3.

APPENDIX D

TABULATIONS OF TOTAL BETA RADIOACTIVITY DATA AND TOTAL POLLEN DATA FROM RAIN SAMPLES COLLECTED MAY 9, AND MAY 10, 1964

Tabulations of measured and derived parameters associated with the rain samples are presented below. Data from May 9 are given in Table D.1. Sample 33 was sacrificed after beta counting to check for possible charring of pollen grains. Therefore, no pollen or gamma radioactivity data are available. Information concerning size and shape characteristics of the various pollen types included in the total is given in Appendix B.

Data for May 10 are given in Table D.2.

TABLE D.1

RAIN SAMPLE DATA FOR MAY 9, 1964

Sample No.	Time, CST			Volume (ml)	Rainfall Rate (mm/hr)	Residue Concentration[1] (g/ℓ)	Total Beta Concentration[1] (pc/ℓ)	Total Pollen Concentration (grains/ml)	Total Beta Deposition Rate[1] ($pc/m^2/hr$)	Total Pollen Deposition Rate[1] ($grains/m^2/hr$)
	Start	End	Mid							
1	1941.00	2031.64	2006.32	1880	.36	5.76 -1	1.12 +3	287 ±18	4.03 +2	1.03 +5 ±0.065 +5
2	2031.64	2037.14	2034.39	2060	2.59	3.38 -1	9.50 +2	182 ±18	2.46 +3	4.71 +5 ±0.467 +5
3	2037.14	2043.34	2040.24	2000	2.58	1.43 -1	8.04 +2	114 ±10	2.07 +3	2.94 +5 ±0.258 +5
4	2043.34	2048.20	2045.77	2150	3.54	1.39 -1	7.14 +2	69.2 ± 3.9	2.53 +3	2.45 +5 ±0.099 +5
5	2048.20	2051.06	2049.63	2140	5.99	1.86 -1	8.53 +2	52.9 ± 9.5	5.11 +3	3.17 +5 ±0.570 +5
6	2051.06	2053.15	2052.11	2000	7.65	1.05 -1	7.95 +2	36.4 ± 4.8	6.08 +3	2.81 +5 ±0.367 +5
7	2053.15	2056.32	2054.74	1920	4.85	7.66 -2	7.39 +2	24.8 ± 7.8	3.58 +3	1.20 +5 ±0.378 +5
8	2056.32	2058.64	2057.48	2095	7.24	9.02 -2	7.00 +2	43.5 ±10.5	5.07 +3	3.14 +5 ±0.761 +5
9	2058.64	2100.02	2059.33	2030	11.80	1.05 -1	5.55 +2	36.5 ± 4.3	6.55 +3	4.31 +5 ±0.508 +5
10	2100.02	2101.07	2100.55	2150	16.40	8.88 -2	4.28 +2	23.3 ±13.1	7.02 +3	3.82 +5 ±2.15 +5
11	2101.07	2101.81	2101.44	2010	21.80	7.51 -2	3.89 +2	15.0 ± 3.8	8.48 +3	3.27 +5 ±0.829 +5
12	2101.81	2102.27	2102.04	2050	35.60	8.49 -2	3.39 +2	16.2 ± 4.8	1.21 +4	5.73 +5 ±1.71 +5
13	2102.27	2102.62	2102.45	1800	50.00	1.41 -1	2.64 +2	9.79 ± 2.79	1.32 +4	4.89 +5 ±1.395 +5
14	2102.62	2103.74	2103.18	3935	42.20	3.94 -2	3.38 +2	8.34 ± 1.13	1.43 +4	3.52 +5 ±0.477 +5
15	2103.74	2104.52	2104.13	4040	62.10	2.55 -2	2.34 +2	5.12 ± 2.03	1.45 +4	3.17 +5 ±1.26 +5
16	2104.52	2105.57	2105.05	4020	92.00	1.92 -2	1.63 +2	4.01 ± 1.03	1.50 +4	3.72 +5 ±0.948 +5
17	2105.57	2107.81	2106.69	3540	38.00	1.42 -2	1.14 +2	1.73 ± .30	4.30 +3	6.57 +4 ±1.14 +4
18	2107.81	2112.44	2110.13	3670	8.57	3.81 -2	2.27 +2	8.66 ± 1.10	1.94 +3	7.43 +4 ±0.943 +4
19	2112.44	2113.50	2112.57	3740	28.20	4.71 -2	2.42 +2	18.4 ± .3	6.82 +3	5.19 +5 ±0.085 +5
20	2113.50	2114.58	2114.04	3670	27.20	4.93 -2	3.99 +2	18.0 ± 4.7	1.08 +4	5.20 +5 ±1.28 +5
21	2114.58	2115.85	2115.22	3780	23.80	5.11 -2	3.74 +2	15.0 ± 5.1	8.90 +3	3.59 +5 ±1.21 +5
22	2115.85	2116.56	2116.21	3960	44.60	4.29 -2	3.21 +2	8.34 ± 2.60	1.43 +4	3.71 +5 ±1.16 +5
23	2116.56	2117.42	2116.99	3960	55.30	1.92 -2	2.70 +2	3.80 ± 1.38	1.49 +4	2.10 +5 ±0.765 +5
24	2117.42	2118.02	2117.72	3780	75.60	2.35 -2	2.02 +2	1.06 ± .27	1.53 +4	8.09 +4 ±2.04 +4
25	2118.02	2118.52	2118.27	3660	87.90	2.76 -2	1.71 +2	1.05 ± .45	1.50 +4	9.23 +4 ±3.95 +4
26	2118.52	2119.13	2118.84	3770	78.30	2.81 -2	1.26 +2	.973 ± .461	9.87 +3	7.74 +4 ±3.01 +4
27	2119.13	2120.43	2119.78	3980	73.60	1.26 -2	7.48 +1	.272 ± .078	5.50 +3	2.00 +4 ±0.573 +4
28	2120.43	2122.28	2121.36	3840	49.80	2.33 -2	8.43 +1	.438 ± .290	4.20 +3	2.18 +4 ±1.44 +4
29	2122.28	2125.22	2123.75	4060	33.20	1.45 -2	7.72 +1	.548 ± .097	2.56 +3	1.82 +4 ±0.322 +4
30	2125.22	2129.20	2127.21	3660	22.10	1.35 -2	6.61 +1	.624 ± .163	1.46 +3	1.38 +4 ±0.36 +4
31	2129.20	2133.33	2131.27	3865	11.20	2.05 -2	7.77 +1	1.14 ± .54	8.70 +2	1.25 +4 ±0.605 +4
32	2133.33	2142.96	2138.15	2930	3.28	2.48 -2	9.88 +1	.841 ± .488	3.24 +2	2.76 +3 ±1.6 +3
33	2142.96	2157.33	2150.14	3575	1.99	3.86 -2	1.31 +2	—	2.61 +2	—
34	2157.33	2203.22	2200.49	3760	5.11	1.96 -2	1.03 +2	2.33 ± .58	5.26 +2	1.19 +4 ±0.296 +4
35	2203.22	2216.59	2210.12	3900	2.34	2.31 -2	1.61 +2	2.90 ± .94	3.77 +2	6.79 +3 ±2.20 +4
36	2216.59	2242.05	2229.32	1790	.56	4.50 -2	3.10 +2	5.27 ± 1.54	1.74 +2	2.13 +3 ±0.863 +3
37	2320.00	2332.74	2326.37	1950	1.22	8.15 -2	1.12 +3	21.4 ± 2.8	1.37 +3	2.62 +4 ±0.342 +4
38	2332.74	2337.92	2335.33	1970	3.04	5.74 -2	6.50 +2	17.4 ± 3.6	1.98 +3	5.26 +4 ±1.094 +4
39	2337.92	2350.81	2344.37	630	.39	1.34 -2	5.40 +2	16.8 ± 3.2	2.11 +2	6.59 +3 ±1.25 +3

[1]Digits at right are powers of 10 by which remainder of number is multiplied. Example: Beta Concentration (Sample 1) = $1.12 \times 10^{+3}$ pc/ℓ.

TABLE D.2

RAIN SAMPLE DATA FOR MAY 10, 1964

Sample No.	Time, CST			Volume (ml)	Rainfall Rate (mm/hr)	Residue Concentration[1] (g/ℓ)	Total Beta Concentration[1] (pc/ℓ)	Total Pollen Concentration (grains/ml)	Total Beta Deposition Rate[1] ($pc/m^2/hr$)	Total Pollen Deposition Rate[1] ($grains/m^2/hr$)
	Start	End	Mid							
1	1004.00	1018.19	1011.09	2020	1.14	9.50 -2	1.16 +3	83.2 ±40.2	1.32 +3	9.49 +4 ±4.58 +4
2	1018.18	1023.38	1020.78	2080	3.20	7.21 -2	8.29 +2	76.5 ± 3.4	2.65 +3	2.45 +5 ±0.109 +5
3	1023.38	1027.89	1025.64	2030	3.60	7.19 -2	4.85 +2	30.4 ± .5	1.75 +3	1.09 +5 ±0.018 +5
4	1027.89	1041.12	1034.51	1440	.87	6.10 -2	4.05 +2	16.4 ± 1.4	3.52 +2	1.43 +4 ±0.122 +4
5	1159.00	1200.00	1159.50	1380	11.00	1.07 -1	7.55 +2	37.8 ± 7.7	8.30 +3	4.22 +5 ±0.847 +5
6	1200.00	1201.65	1200.82	2070	10.00	7.44 -2	5.90 +2	45.4 ±32.0	5.90 +3	4.54 +5 ±3.20 +5
7	1201.65	1209.94	1205.79	1600	1.54	5.10 -2	5.10 +2	37.6 ± 3.3	7.85 +2	5.81 +4 ±0.508 +4
8	1325.00	1350.00	1337.50	480	.15	6.58 -2	4.22 +2	90.7 ± 4.2	6.33 +1	4.08 +4 ±0.063 +4
9	1816.00	1824.06	1820.03	2060	3.07	1.07 -1	3.26 +2	49.6 ±17.3	1.00 +3	1.52 +5 ±0.532 +5
10	1824.06	1824.99	1824.53	2000	25.80	4.05 -2	2.85 +2	15.7 ± 1.9	7.35 +3	4.05 +5 ±0.49 +5
11	1824.99	1825.41	1825.20	1930	55.00	3.15 -2	2.33 +2	9.41± 3.42	1.28 +4	5.18 +5 ±1.88 +5
12	1825.41	1825.72	1825.57	2100	81.30	3.07 -2	2.07 +2	9.05± 1.16	1.68 +4	7.36 +5 ±0.944 +5
13	1825.72	1826.06	1825.89	2000	70.60	2.76 -2	1.94 +2	6.85± 1.20	1.37 +4	4.84 +5 ±0.847 +5
14	1826.06	1826.54	1826.30	2100	105.00	2.53 -2	2.20 +2	6.41± 1.40	2.31 +4	6.73 +5 ±1.47 +5
15	1826.54	1826.96	1826.75	1980	113.20	2.84 -2	2.56 +2	8.38± 2.00	2.90 +4	9.45 +5 ±2.26 +5
16	1826.96	1827.39	1827.18	2020	112.90	3.35 -2	1.93 +2	4.79± .56	2.18 +4	5.41 +5 ±0.633 +5
17	1827.39	1827.72	1827.56	2000	145.60	6.72 -2	1.89 +2	8.12± 2.26	2.75 +4	1.18 +6 ±0.329 +6
18	1827.72	1828.43	1828.08	3920	132.50	2.91 -2	2.01 +2	7.30± 1.56	2.66 +4	9.65 +5 ±2.06 +5
19	1828.43	1828.97	1828.70	3250	144.20	2.86 -2	1.93 +2	5.48± .53	2.78 +4	7.90 +5 ±0.764 +5
20	1828.97	1829.64	1829.31	3800	136.00	2.49 -2	1.86 +2	5.09± 1.08	2.53 +4	6.90 +5 ±1.47 +5
21	1829.64	1830.64	1830.14	3830	91.90	2.06 -2	1.73 +2	4.28± .94	1.59 +4	3.94 +5 ±0.863 +5
22	1830.64	1831.78	1831.21	3760	79.20	3.12 -2	2.07 +2	6.20± 2.12	1.64 +4	4.93 +5 ±1.68 +5
23	1831.78	1834.85	1833.32	3980	31.10	3.04 -2	2.62 +2	4.67± 2.23	8.15 +3	1.46 +5 ±0.694 +5
24	1834.85	1836.40	1835.63	3960	29.40	4.39 -2	3.03 +2	12.8 ± 3.7	8.91 +3	3.76 +5 ±1.08 +5
25	1836.40	1837.41	1836.91	3850	45.70	3.51 -2	2.42 +2	3.78± 1.68	1.11 +4	1.73 +5 ±0.768 +5
26	1837.41	1839.97	1838.69	3650	17.10	3.92 -2	3.88 +2	8.42± 2.20	6.64 +3	1.42 +5 ±0.376 +5
27	1839.97	1844.84	1842.41	3830	7.92	4.10 -2	4.81 +2	7.44± 1.38	3.81 +3	5.89 +4 ±1.09 +4
28	1844.84	1857.89	1851.37	7360	4.51	5.20 -2	4.77 +2	20.1 ± 3.4	2.15 +3	9.07 +4 ±1.53 +4
29	1857.89	1911.00	1904.45	6700	4.09	6.31 -2	4.25 +2	13.9 ± 3.1	1.74 +3	5.69 +4 ±1.27 +4
30	1946.00	1950.34	1948.17	1980	3.65	2.51 -1	7.14 +2	60.0 ±17.8	2.61 +3	2.17 +5 ±0.65 +5
31	1950.34	1952.15	1951.25	2040	9.02	2.48 -1	5.86 +2	52.3 ±25.9	5.29 +3	4.72 +5 ±2.33 +5
32	1952.15	2014.50	2003.33	1620	.58	1.64 -1	4.91 +2	47.8 ±10.2	2.85 +2	2.77 +4 ±0.592 +4

[1]Digits at right are powers of 10 by which remainder of number is multiplied. Example: Beta Concentration (Sample 1) = $1.16 \times 10^{+3}$ pc/ℓ.

BIBLIOGRAPHY

Benninghoff, W. S., 1962. Calculation of pollen and spore density in sediments by addition of exotic pollen in known quantities (abstract). Pollen et Spores (Paris), 4 (2), 332-333.

Bleichrodt, J. F., J. Blok, R. H. Dekker, and G. J. H. Lock, 1959. The dependence of artificial radioactivity in rain on the rainfall rate. Tellus, 11, 404.

Booker, D. R., G. Hamada, and P. Kruger, 1964. Radioactive fallout from two severe storms in Oklahoma during May, 1963, Progress Report, Contract AT(04-3)-457, U.S. Atomic Energy Commission, Hazleton-Nuclear Science Corp., Palo Alto, California, HNS-58.

Braham, R. R., 1952. The water and energy budgets of the thunderstorm and their relation to thunderstorm development. J. Meteorol., 9, 227-242.

Browning, K. A., 1964. Airflow and precipitation trajectories within severe local storms which travel to the right of the winds. J. Atm. Sci. 21, 634-639.

Brun, R. J., and H. W. Mergler, 1953. Impingement of water droplets on a cylinder in an incompressible flow field and evaluation of rotating multicylinder method for measurement of droplet size distribution, volume-median droplet size, and liquid-water content in clouds. Technical Note 2904, National Advisory Committee for Aeronautics, Washington, D.C.

Chamberlain, A. C., 1959. Deposition of iodine-131 in northern England in October, 1957. Quart. J. Roy. Meteorol. Soc., 85, 350.

Danielsen, E. F., 1964. Project Springfield report, Contract No. DA-49-146-XZ-079, Defense Atomic Support Agency, Isotopes, Inc., Westwood, N.J.

Danielsen, E. F., 1965. Remarks made at special class on isentropic analysis, Washington, D.C., March, 1965.

Davis, M. B., 1965. A method for determination of absolute pollen frequency. in G. Kummel and D. Raup, editors, Handbook of Paleontological Techniques, pp. 674-686, Freeman and Co., San Francisco, in press.

BIBLIOGRAPHY (Continued)

Dingle, A. N. and H. F. Schulte, 1962. A research instrument for the study of raindrop-size spectra. J. Appl. Meteorol., 1, 48-59.

Dingle, A. N., 1965. Stratospheric tapping by intense convective storms: implications for public health in the United States, Science, 148 (3667), 227-229.

Dingle, A. N., and D. F. Gatz, 1963. Rain scavenging of particulate matter from the atmosphere, Final Report, Contract No. AT(11-1)-739, U.S. Atomic Energy Commission, The University of Michigan, Office of Research Administration, Ann Arbor.

Engelmann, R. J., 1963. Rain scavenging of particulates, U. S. Atomic Energy Commission Research and Development Report, Hanford Atomic Products Operation, Richland, Washington.

Erdtman, G., 1943. An Introduction to Pollen Analysis. Chronica Botanica Co., Waltham, Mass.

Fitzgerald, D. R. and F. R. Valovcin, 1964. High altitude observations of the development of a tornado producing thunderstorm (preliminary draft), Paper presented at the Conf. on Physics and Dynamics of Clouds, Chicago, March, 1964.

Fletcher, N. H., 1962, The Physics of Rainclouds, University Press, Cambridge, 386 pp.

Fujita, T., 1959. Precipitation and cold air production in mesoscale thunderstorm systems. J. Meteorol., 16, 454-466.

Gatz, D. F., and A. N. Dingle, 1965. Air cleansing by convective storms, in: Klement, A. W., Ed., Fallout from Nuclear Weapons Tests, Proc. of Conf., Germantown, Md., Nov. 3-6, 1964, TID-7701.

Giles, K. C., 1961. Distribution of radioactivity with respect to tropopauses and jet streams. U.S. Atomic Energy Commission, Health and Safety Laboratory, Report HASL-115, 184-252.

Goldsmith, P., H. J. Delafield, and L. C. Cox, 1963. The role of diffusiophoresis in the scavenging of radioactive particles from the atmosphere, Quart. J. Roy. Meteorol. Soc., 89 (379), 43-61.

Greenfield, S. M., 1957. Rain scavenging of radioactive particulate matter from the atmosphere. J. Meteorol., 14, 115-125.

BIBLIOGRAPHY (Continued)

Hall, S. J., 1965. Radioactivity in precipitation: case studies from 1964 spring season, in: Klement, A. W. Ed., Radioactive Fallout from Nuclear Weapons Tests, Proc. of Conf., Germantown, Md., Nov. 3-6, 1964.

Hall, S. J., and E. H. Klehr, 1963. Severe convective storms and the stratospheric scavenging of radioactive particles. First Progress Report, Contract No. AT(40-1)-3083, U.S. Atomic Energy Commission, The University of Oklahoma, Norman, ARL-1402-1.

Hall, S. J., and R. Y. Nelson, 1964. Severe convective storms and the stratospheric scavenging of radioactive particles, Second Progress Report, Contract No. AT(40-1)-3083, U.S. Atomic Energy Commission, University of Oklahoma, Research Institute, Atmospheric Research Laboratory, ARL-1402-2.

Hardy, K. R., 1963. The development of raindrop size distributions and implications related to the physics of precipitation. J. Atm. Sci., 20, 299-312.

Harrington, J. B., G. C. Gill, and B. R. Warr, 1959. High-efficiency pollen samplers for use in clinical allergy. Jour. of Allergy, 30 (4), 357-375.

Holland, J. Z., 1959. Statement in: Fallout from Nuclear Weapons Tests (Hearings before Special Subcommittee on Radiation of the Joint Committee on Atomic Energy, May 5-8, 1959), Vol. 1, p. 275.

Huff, F. A., 1963. Study of rainout of radioactivity in Illinois, First Progress Report, Contract No. AT(11-1)-1199, U.S. Atomic Energy Commission, Illinois State Water Survey, Urbana.

Huff, F. A., 1964. Study of rainout of radioactivity in Illinois. 2nd. Prog. Report, Contract No. AT(11-1)-1199, U.S. Atomic Commission, Illinois State Water Survey, Urbana.

Huff, F. A., 1965. Study of rainout of radioactivity in Illinois, Third Progress Report, Contract No. AT(11-1)-1199, U.S. Atomic Energy Commission, Illinois State Water Survey, Urbana.

Huff, F. A., and G. E. Stout, 1964. Distribution of radioactive rainout in convective rainfall, J. Appl. Meteorol., 3 (6), 707-717.

BIBLIOGRAPHY (Continued)

Itagaki, K., and S. Koenuma, 1962. Altitude distribution of fallout contained in rain and snow. J. Geophys. Res., 67, 3927.

Jacobi, W., 1962. Die natürliche Radioaktivität der Atmosphare und ihre Bedeutung für die Strahlenbelastung des Menschen. Report, Hahn-Meitner-Institut für Kernforschung, Berlin, HMI-B21, March, 1962.

Junge, C. E., 1958. Atmospheric chemistry, Advances in Geophys., 4, 1-108.

Junge, C. E., 1963. Air Chemistry and Radioactivity, Academic Press, N.Y., pp. 245-247.

Kessler, E., 1964. Purposes and programs of the National Severe Storms Laboratory. Preprinted Report No. 23, U.S. Weather Bureau, National Severe Storms Laboratory.

Kruger, P., and C. L. Hosler, 1963. Sr^{90} concentration in precipitation from convective showers, J. Appl. Meteorol., 2 (3), 379-389.

Kruger, P., D. R. Booker, L. G. Davis, and C. L. Hosler, 1963. Radioactive fallout in convective shower precipitation. Progress Report, Contract No. AT(04-3)-457, U.S. Atomic Energy Commission, Hazleton-Nuclear Science Corp., Palo Alto, California, HNS-24.

Kruger, P., L. G. Davis, and C. L. Hosler, 1964. Sr^{90} concentration in convective shower precipitation, spring, 1963. Progress Report, Contract No. AT(04-3)-457, U.S. Atomic Energy Commission, Hazleton-Nuclear Science Corp., Palo Alto, California, HNS-50.

Langmuir, I., 1948. Production of rain by a chain reaction in cumulus clouds at temperatures above freezing. J. Meteorol., 5, 175-192.

List, R. J., K. Telegadas, and G. J. Ferber, 1964. Meteorological evaluation of the sources of iodine-131 in pasteurized milk. Science, 146, (3640), 59-64.

Lockhart, L. B., R. L. Patterson, and A. W. Saunders, 1965. The size distribution of radioactive atmospheric aerosols, J. Geophys. Res., 70, 6033-6041.

Machta, L., 1963. Meteorological processes in the transport of weapon radioiodine, Health Physics, 9, 1123.

BIBLIOGRAPHY (Continued)

Malkowski, G., 1965. Bermerkungen zum Mechanismus des Rain-out und Wash-out radioaktiver Partikel in der Atmosphäre. Atomkernenergie, 10, 151-152.

Martell, E. A., 1965. Iodine-131 fallout from underground tests II. Science, 148, 1576-1577.

May, F. G., 1958. The washout of Lycopodium spores by rain. Quart. J. Roy. Meteorol. Soc. 84, 451.

McDonald, J. E., 1963. Rain washout of partially wettable insoluble particles. J. Geophys. Res. 68 (17) 4993-5003.

McDonald J. E., 1964. Pollen wettability as a factor in washout by raindrops. Science, 143, 1180-1181.

Mordy, W. A., 1959. Computations of the growth by condensation of a population of cloud droplets, Tellus, 11, 16-44.

Neiburger, M., and C. W. Chien, 1960. Computations of the growth of cloud drops by condensation using an electronic digital computer, Amer. Geophys. Union, Monograph No. 5, pp. 191-209.

Newton, C. W., 1950. Structure and mechanism of the prefrontal squall line. J. Meteorol., 1, 210-222.

Newton, C. W., 1963. Dynamics of severe convective storms, Meteorological Monographs, 5 (27), 33-58.

Newton, C. W., and J. C. Fankhauser, 1964. On the movements of convective storms, with emphasis on size descrimination in relation to water-budget requirements, J. Appl. Meteorol., 3, 651-668.

Pasquill, F., 1962. Atmospheric diffusion, D. Van Nostrand Co., New York, p. 10ff.

Penn, S., and E. A. Martell, 1963. An analysis of the radioactive fallout over North America in late September, 1961, J. Geophys. Res., 68 (14), 4195-4207.

Reiter, E. R., 1965. Further studies on radioactive fallout. Progress Report No. 2, Contract No. AT(11-1)-1340, U.S. Atomic Energy Commission, Colorado State University.

BIBLIOGRAPHY (Continued)

Reiter, R., 1961. Investigations on the washout effect in the lower atmosphere, Atomkernenergie, 6, 68-74. (In German)

Rigby, M., and E. Z. Sinha, 1961. Annotated bibliography on precipitation chemistry, Meteorological and Geoastrophysical Abstracts, 12 (7).

Salter, L. P., P. Kruger, and C. L. Hosler, 1962. Sr^{90} concentration in precipitation resulting from large-scale uplift. J. Appl. Meteor., 1, 357-365.

Saucier, W. J., S. J. Hall, and R. Y. Nelson, 1965. The Oklahoma program for studies of convective storms and scavenging of radioactive particles, in A. W. Klement, editor, Radioactive Fallout from Nuclear Weapons Tests, Proc. of Conf., Germantown, Md., Nov. 3-6, 1964, TID-7701.

Shalmon, E., 1964. Deposition of some radionuclides on tropospheric aerosols. Doctoral Dissertation, The University of Michigan, School of Public Health.

Shleien, B., T. P. Galvin, and A. G. Friend, 1965. Particle size fractionation of airborne gamma-emitting radionuclides by graded filters. Science, 147, 290-292.

Shleien, B., D. Oakes, N. A. Gaeta, G. I. Coats, and A. G. Friend, 1965. Atmospheric radioactivity analysis and instrumentation, Status Report, Northeastern Radiological Health Laboratory, Division of Radiological Health, U.S. Public Health Service, Winchester, Mass., NERHL-65-2.

Small, S. H., 1960. Wet and dry deposition of fallout materials at Kjeller, Tellus, 12, 308.

Squires, P., 1958. Penetrative downdrafts in cumuli, Tellus, 10, 381.

Stoutamire, W. P., and W. S. Benninghoff, 1964. Biotic assemblage associated with a mastodon skull from Oakland Country, Michigan. Papers of the Mich. Acad. Sci., Arts, and Letters, Vol. XLIX, 1964.

U. S. Public Health Service, 1964. Tabulation of findings for May 1 - May 31, 1964, Public Health Service Radiation Surveillance Network, Washington, D.C. 20201.

U.S. Weather Bureau, 1964. Northern Hemisphere Data Tabulations, Daily Bulletin, May 9, 10, 1964. Separate copies available from Superintendent of Documents, Government Printing Office, Washington 25, D.C. 20402, at $ .25 each.

BIBLIOGRAPHY (Concluded)

U.S. Weather Bureau and Public Health Service, 1963. Mid-May iodine-131 fallout in the midwest, in: Fallout, Radiation Standards and Countermeasures (Hearings of the Subcommittee on Research, Development, and Radiation of the Joint Committee on Atomic Energy, June 3-6, (1963) pt. 1, pp. 109-121.

Vaughan, L. M., and W. A. Perkins, 1961. The washout of aerosol particles and gases by rain. Tech. Rept. No. 88, U.S. Army Chemical Corps Res. and Dev. Contract DA-48-007-403-CML 448, Aerosol Lab., Stanford University, Stanford, California.

Viemeister, P. E., 1960. Lightning and the origin of nitrates found in precipitation., J. Meteorol., 17 (6), 681-683.

Williams, D. T., 1963. Analysis methods for small-scale surface network data. Preprinted Report No. 17, U.S. Weather Bureau, National Severe Storms Laboratory.

Wodehouse, R. P., 1935. Pollen Grains, McGraw-Hill, New York.